eCOMMONS

Loyola University Chicago
Loyola eCommons

Dissertations | Theses and Dissertations

2014

Investigation of Chicago Air Pollution and Meteorological Influence on Pollution Development: Physical Measurements and Multivariate Statistical Analyses

Katrina Lyn Binaku
Loyola University Chicago

Recommended Citation

Binaku, Katrina Lyn, "Investigation of Chicago Air Pollution and Meteorological Influence on Pollution Development: Physical Measurements and Multivariate Statistical Analyses" (2014). *Dissertations.* Paper 1251.
http://ecommons.luc.edu/luc_diss/1251

This Dissertation is brought to you for free and open access by the Theses and Dissertations at Loyola eCommons. It has been accepted for inclusion in Dissertations by an authorized administrator of Loyola eCommons. For more information, please contact ecommons@luc.edu.

This work is licensed under a Creative Commons Attribution-Noncommercial-No Derivative Works 3.0 License.
Copyright © 2014 Katrina Lyn Binaku

LOYOLA UNIVERSITY CHICAGO

INVESTIGATION OF CHICAGO AIR POLLUTION AND METEOROLOGICAL INFLUENCE ON POLLUTION DEVELOPMENT: PHYSICAL MEASUREMENTS AND MULTIVARIATE STATISTICAL ANALYSES

A DISSERTATION SUBMITTED TO

THE FACULTY OF THE GRADUATE SCHOOL

IN CANDIDACY FOR THE DEGREE OF

DOCTOR OF PHILOSOPHY

PROGRAM IN CHEMISTRY

BY

KATRINA LYN BINAKU

CHICAGO, ILLINOIS

AUGUST 2014

Copyright by Katrina Lyn Binaku, 2014
All rights reserved.

ACKNOWLEDGMENTS

I would like to thank my research advisor, Dr. Martina Schmeling. Thank you for your guidance, advice, and assistance in the development of my project. With us being a research group of two for so long, our relationship helped me gain an enhanced appreciation for independent lab work. Thank you for having me as a member of your research lab and for your encouragement & faith in me. I am very grateful to Dr. David Crumrine, Dr. Nancy Tuchman, and Dr. Daniel Graham, whose valuable advice and suggestions helped me mature not only as a chemist but also as a person. You pushed me through some difficult times. Thank you for believing in me. I must also thank Dr. Timothy O'Brien for his mentorship. The knowledge he shared with me on the use of multivariate statistical methods helped me develop invaluable statistical skills that I will continue to use in the future. I must note a special thank you to Dr. Salim Diab, Dr. James Houlihan, and Br. Pierre St. Raymond. Without your mentorship during my undergraduate education, I would not have taken a forensic science course nor realized my interest in science could coincide with my path of studying criminal justice. Thank you for exhausting my brain and pushing me to my intellectual limits. Dr. D., Doc Houlihan, and Br. Pierre, I probably would not have thought about graduate school if it were not for each of you seeing intelligence and exceptional hard work in me. Thank you all so very much for your dedication to my education and growth.

I sincerely must thank my family and friends, especially my parents Hazir and Sharon Binaku, who worked hard and made many sacrifices to ensure that I received the best education and had unlimited opportunity to thrive in life. I will forever be grateful for the guidance, wisdom, and life lessons you shared. My younger self did not always appreciate that but I now understand it all. Thank you for letting me pursue my dreams and for the everlasting encouragement to be the best that I can be. I would not have been this successful in my life thus far if it were not for your love and support. You are the best parents in the world. To my brother, Adam, although you were thousands of miles away during most of my journey and think that I am a "science nerd" you too have helped me through this. A graduate student rarely enjoys hearing the question, "so, when are you going to finish" but in sibling rivalry fashion you really liked asking me that. Thanks little brother. To my friends, thank you for your support and encouragement in the best of times and the worst of times. It has been a long road and I am grateful that you have stuck with me throughout it all. I truly cannot thank you enough for your support.

It is essential that I also acknowledge the Department of Chemistry & Biochemistry and Loyola University Chicago as a whole. The Teaching Assistantship that I was awarded during my graduate studies is the reason I was able to attend graduate school. I cannot express enough appreciation that I have for the financial support given. Furthermore, I would have never realized the joy and passion I have for teaching if it was not for the experiences I have had as teaching assistant.

To my parents, Hazir and Sharon Binaku
and my brother, Adam Binaku

TABLE OF CONTENTS

LIST OF TABLES

LIST OF FIGURES

LIST OF ABBREVIATIONS

AGL	Above ground level
CAA	Clean air act
Ca^{2+}	Calcium
CAIR	Clean air interstate rule
CCA	Canonical correlation analysis
CH_3COOH	Acetic acid
CH_3COO^-	Acetate
$C_7H_4O_2^-$	Benzoate
Cl^-	Chloride
CM	Centimeters
CO	Carbon monoxide
CO_2	Carbon dioxide
CO_3^{2-}	Carbonate
CSAPR	Cross-state air pollution rule
EPA	Environmental protection agency
F^-	Fluoride
FA	Factor analysis
HCOOH	Formic acid
$HCOO^-$	Formate

HCO_3^-	Bicarbonate
HDPE	High-density polyethylene
HNO_3	Nitric acid
$HO_2\cdot$	Hydroperoxyl radical
HO·	Hydroxyl radical
HOOCCOOH	Oxalic acid
$C_2O_4^{2-}$	Oxalate
H_2SO_4	Sulfuric acid
HYSPLIT	Hybrid single-particle lagrangian integrated trajectory
IC	Ion chromatography, Ion chromatograph
K^+	Potassium
KM	Kilometers
LT	Local time
M	Meter
MEGAN	Model of emissions of gases and aerosols from nature
Mg^{2+}	Magnesium
ML	Milliliters
MM	Millimeters
mM	Millimolar
Mo	Molybdenum
MOSAIC	Model for simulating aerosol interactions with chemistry
MOZART	Model for ozone and related chemical tracers
MPa	Megapascal

NCAR	National center for atmospheric research
NEI	National emissions inventory
NH_3	Ammonia
NH_4^+	Ammonium
NH_4NO_3	Ammonium nitrate
NO_3^-	Nitrate
NM	Nanometers
NO	Nitric oxide
NO_2	Nitrogen dioxide
NO_2^*	Nitrogen dioxide, excited state
NO_x	Nitrogen oxides
O_3	Ozone
PC	Principal component
PCA	Principal component analysis
PEEK	Polyetheretherketone
PM	Particulate matter
PMT	Photomultiplier tube
PO_4^{3-}	Phosphate
PPB	Parts per billion
PPM	Parts per million
PVDF	Polyvinylidene fluoride
$RO_2\cdot$	Peroxyl radical
RPM	Rotations per minute

RT	Retention time
SOA	Secondary organic aerosol
SO_2	Sulfur dioxide
SO_4^{2-}	Sulfate
UTC	Coordinated universal time
UV	Ultraviolet
USEPA	United States environmental protection agency
USGS	United States geological survey
VOCs	Volatile organic compounds
WPS	WRF pre-processing system
WRF-Chem	Weather research and forecasting-chemistry model

ABSTRACT

The goal of this project was to evaluate air pollutants and meteorology in Chicago, Illinois during the summer months of 2010, 2011, and 2012 in order to determine whether a local lake breeze significantly increased the concentrations of secondary pollutant species. A total of 66-collection days of pollutant and meteorological data was completed in this study. Trace gases, nitrogen oxides and ozone, as well as the water-soluble fraction of aerosol material were the air pollutants of focus in this study. Data analysis of all 66-collection days showed that chloride, nitrate, sulfate, and oxalate were the most frequently quantified water-soluble ions in aerosol samples, followed by acetate, formate, potassium, phosphate, calcium, and magnesium ions. Ionic ratios showed that stationary sources, vehicular emissions, and secondary production in the atmosphere contributed to nitrate, sulfate, acetate, formate, and oxalate ions' presence in the local atmosphere, however, each summer had a different combination of these sources. Each summer had a different dominant wind direction profile, which contributed to the variability in ion and trace gas concentrations in the local atmosphere. Temperature, wind speed, and humidity averages each summer also contributed to the variability in air pollutant concentrations.

Collection days in this study were classified based on wind direction to segregate non-lake breeze (reference) and lake breeze days as well as variable days having sporadic changes in wind direction. The onset of a lake breeze varied from roughly 0900 local

time (LT) to 1245 LT and onset time was significantly affected by morning wind speed and temperature. Evaluating categorized days' air pollution data revealed that the majority of air pollutants were not significantly effected (Student *t* test) by the onset of a lake breeze when compared to reference day pollutant averages. However, ozone, sulfate, nitrate, and chloride concentrations were significantly different at 95% confidence level on lake breeze days compared to non-lake breeze (reference) days.

Another aspect of the project focused on comparing summer 2010–2012 data to earlier air pollutant and meteorological data collected at the same sampling location during summers 2002–2004. Nitrogen oxides and sulfate concentrations decreased, however, ozone and many water-soluble ions increased in concentration since the earlier study. Comparing these data to Illinois statewide reported emissions showed a similar trend in decreased nitrogen oxides and increased ozone observed during the same years our studies were completed. Identifying point-sources of air pollution and calculating backward air parcel trajectories proved valuable in understanding pollution variability.

The remainder of the project focused on the application of multivariate statistical methods to two sets of data containing multi-summer study results. Canonical correlation analysis (CCA) and principal component analysis (PCA) were both independently applied to summer 2002–2004 and summer 2010–2012 sets of air pollution and meteorological data generated by air pollution studies completed at the Loyola University Chicago air sampling station atop Mertz Hall. Both methods uncovered a variety of multivariate relationships between pollutant-pollutant and pollutant-meteorological variables. With this information, a better understanding of the complex nature of pollutants and their dependence on meteorology was achieved.

CHAPTER I

INTRODUCTION

Overview

When the United States Congress established the United States Environmental Protection Agency (USEPA), enacted the Clean Air Act (CAA) in 1970, and added amendments to CAA in 1977 and 1990, the nation moved towards stricter regulation, enforcement, and accountability with respect to air pollution.[1,2] As a result, air pollution levels in the United States have been on an overall decline the last several decades. Air quality standards for six criteria air pollutants [ozone – O_3, nitrogen dioxide – NO_2, particulate matter – PM_{10} and $PM_{2.5}$, carbon monoxide – CO, sulfur dioxide – SO_2, and lead – Pb] were instituted because of the CAA. Both national and state agencies continue to enforce and revise regulations to reduce emissions of harmful pollutants into the atmosphere.[2]

The importance of studying air pollution, both composition and concentration, worldwide over an extended period is due to findings of a negative impact that air pollution has on human health and the Earth's climate. Schlesinger (2007) reviewed a plethora of studies linking short and long-term respiratory ailments to the inorganic particulate portion of $PM_{2.5}$. The author pointed out that constituents in aerosols vary regionally and as a result, health studies differ in conclusions of whether or not certain pollutants have detrimental effects on health.[3] Kampa and Castanas (2008) briefly

reviewed studies bearing evidence that various constituents of particulate matter could negatively affect both nervous and urinary systems. A study by Balmes et al. (1987) showed sulfur dioxide could induce inflammation in the lungs, throat, and nose as well as cause bronchoconstriction in non-smoker human subjects with a history of asthma. Other studies involving controlled ozone exposure found ozone caused inflammation of lung tissue and temporary lung function reduction in humans.[6]

There are both direct and indirect impacts on Earth's climate that are associated with aerosol presence in the atmosphere.[7] Aerosols directly affect climate by absorbing and scattering incoming solar radiation, which results in a lesser amount of radiation reaching the Earth's surface, thus, cooling the area where aerosols are present.[7] In addition, some species that absorb incoming solar radiation, such as black carbon, warm the immediate atmospheric layer they reside in. The combination of a warming atmospheric layer and the cooling of Earth's surface alters the planet's radiative budget and ultimately affects the extent of evaporation at the surface of the Earth and formation of clouds in the atmosphere.[8-10] Both are considered an indirect aerosol effect.[8-10] These changes in balance between the amount of solar radiation (visible range) reaching the Earth's surface and the amount of thermal radiation (infrared) being emitted from Earth's surface results in a temperature alteration of Earth's system.[7,8-10]

The lifetime of air pollutants in the atmosphere ranges from hours to several days, thus transport of pollutants from emission sources can impact regions far away from the original source. Variability of air pollution composition due to differences in sources and the influence of meteorology and geography within a region was the subject of many

studies investigating the composition of air pollution worldwide.[11-16] Assessing air pollution within a region, by identifying and quantifying pollutant species while also determining sources, evolution, and fate, not only aids in disclosing impacts of air pollution but also assists in evaluating effectiveness of pollution reduction and control strategies.

The purpose of this project was to collect aerosol, trace gas, and meteorological data over three consecutive summer periods to complete the following: 1) evaluate the variability of chemical species' concentrations on non-lake breeze and lake breeze days, 2) determine statistical significance of lake breeze influence on specific pollutants' concentrations, 3) uncover significant relationships between air pollutants and local meteorology, and 4) analyze pollution trends over time by comparing summer 2010–2012 studies with summer 2002–2004 data collected at the same sampling location.

Nitrogen Oxides and Tropospheric Ozone: Gas-phase Chemistry

The atmosphere is an oxidizing medium and a plethora of chemical species contributes to the vast number of chemical reactions occurring in it. The presence of tropospheric ozone (O_3), particulate matter (PM), and reactive oxidative species such as hydroxyl ($HO\cdot$), hydroperoxyl ($HO_2\cdot$), and peroxyl ($RO_2\cdot$) radicals are attributed to anthropogenic and natural release of precursor species, with volatile organic compounds (VOCs), nitrogen oxides (NO_x), and sulfur compounds being the most important precursors.[17] Measurement of NO_x and O_3 mixing ratios are good indicators for the oxidative capacity of the local atmosphere and both species were recorded simultaneously during our study.

Nitrogen oxides, defined as the sum of nitric oxide (NO) and nitrogen dioxide (NO_2), play a major role in the chemistry of the troposphere.[8,17] Both have natural and anthropogenic sources with NO being the major form emitted. Significant anthropogenic emission sources include fossil fuel combustion through vehicular, electrical generation sources and other industrial activity.[8] NO_x directly contributes to photochemical smog as well as the production of tropospheric ozone.[8,17]

Tropospheric O_3 is a secondary pollutant, formed via chemical reactions of precursor species. Photolysis of nitrogen dioxide, producing nitric oxide and a ground state oxygen atom, is the most important reaction (reaction 1) in the process of tropospheric ozone production. An oxygen molecule reacts with a ground state oxygen atom to form ozone (reaction 2). One of several pathways of ozone destruction in the troposphere is shown in reaction 3. Nitric oxide rapidly reacts with ozone re-forming nitrogen dioxide and oxygen.[8,17]

$$NO_2 + h\nu\ (< 424\ nm) \rightarrow NO + O(^3P) \qquad (1)$$

$$O(^3P) + O_2 + M \rightarrow O_3 + M \qquad (2)$$

$$NO + O_3 \rightarrow NO_2 + O_2 \qquad (3)$$

$$HO_2\cdot + NO \rightarrow HO\cdot + NO_2 \qquad (4)$$

$$RO_2\cdot + NO \rightarrow RO\cdot + NO_2 \qquad (5)$$

The described three-reaction sequence (1–3) is in photoequilibrium; thus, no net ozone is produced. The presence of volatile organic compounds (VOCs) in the atmosphere leads to the formation of two important radicals that disrupt the NO, NO_2, O_3 photoequilibrium. Hydroperoxyl ($HO_2\cdot$) and peroxyl ($RO_2\cdot$) radicals rapidly convert NO to NO_2 (reactions 4–5), producing additional NO_2 available for photolysis, which results in net formation of

O_3.[8,17] If low concentrations of NO in the atmosphere are present, a net loss of O_3 results due to radicals ($HO_2\cdot$ and $RO_2\cdot$) reacting with and destroying O_3. Therefore, the concentration of O_3 in the troposphere is dependent upon the mixing ratio of NO and the presence of radical species.[8,17]

An additional pathway of ozone destruction in the troposphere is photolysis (reactions 6–7). Photolysis of ozone produces one of the most important radicals found in the troposphere, the hydroxyl radical ($HO\cdot$).[17]

$$O_3 + h\nu\,(319nm) \rightarrow O_2 + O(^1D) \qquad (6)$$

$$O(^1D) + H_2O \rightarrow 2HO\cdot \qquad (7)$$

Hydroxyl radicals are the main oxidative species in the troposphere, reacting with nearly all other species present in the atmosphere.[17] Furthermore, hydroxyl radicals are produced only during the daytime hours from photolysis with reactions 6–7 as their main source.[17]

Tropospheric Aerosols

Aerosols are particles of liquid or solid phase that are suspended in a gas.[8,18] The terms aerosol and particulate matter or particles are used interchangeably herein. The presence of aerosols in the tropospheric layer of the atmosphere is a result of both natural and anthropogenic sources.[8,19,20] Natural sources include forest fires, volcanoes, wind-driven suspension of material from deserts and soil, vegetation, and sea salt from oceans. The anthropogenic portion is mainly a result of burning biomass, farming activity, road dust suspended by vehicles, and combustion of fossil fuels via industrial and automobile use.[19,20]

Primary aerosols are directly emitted into the atmosphere whereas secondary aerosols form through various pathways in the gaseous or aqueous phase.[8,20] Aerosols have a range of sizes and shapes, which vary based on geography, meteorology, and atmospheric processing. While aerosol diameter ranges from sub-micron to about 100 micrometers (μm), regulated particles are less than 10 μm in diameter. The U.S. Environmental Protection Agency has two defined classifications: inhalable coarse particles – PM_{10} and fine particles – $PM_{2.5}$.[8,21]

The lifetime of aerosols varies, from hours to weeks, depending on meteorological conditions and particle characteristics. Larger aerosols have shorter lifetimes than smaller aerosols.[8,20] Aerosols are removed from the atmosphere either by wet or dry deposition. Wet deposition includes transport to ground level via dissolving in precipitation (rain, snow, fog, clouds, ice) while dry deposition is defined as aerosol adhesion to ground level surfaces through diffusion and convective transport.[8,20]

Although the composition of aerosols is location specific, there are several consistent components contributing to the bulk of quantifiable particulate matter: crustal material mainly consisting of silicon, aluminum, iron, and calcium oxides, organic and elemental (black) carbon, nitrates, and sulfates.[20,22] It is the composition, size, and lifetime of aerosols that directly contributes to their influence on human health and the Earth's climate.

Water-soluble inorganic ions and low molecular weight organic acid anions were targeted for analysis in this study. Secondary inorganic anions such as nitrate (NO_3^-) and sulfate (SO_4^{2-}) contribute to acidity of precipitation. Nitrate ions are primarily a result of

daytime gas-phase reactions of hydroxyl radicals and nitrogen dioxide, forming gaseous nitric acid, HNO_3 (reaction 8). Due to the low water solubility of both nitric oxide and nitrogen dioxide, production of nitric acid in the gas-phase is the most significant pathway. Gaseous nitric acid can undergo dry deposition or uptake into clouds and then be removed from the atmosphere via wet deposition. The high vapor pressure of nitric acid results in its primary existence in the gas phase. Reactions 4 and 5, described earlier, contribute as the main source of nitrogen dioxide consumed in reaction 8. Neutralization of nitric acid by gaseous ammonia, $NH_{3\,(g)}$, forming ammonium nitrate, $NH_4NO_{3\,(s,\,aq)}$, is a pathway of formation of nitrate aerosol in both solid and aqueous phases (reaction 9).[8,23,24]

$$NO_{2(g)} + HO\cdot_{(g)} + M \rightarrow HNO_{3(g)} \qquad (8)$$

$$NH_{3(g)} + HNO_{3(g)} \leftrightarrow NH_4NO_{3(s,\,aq)} \qquad (9)$$

Sulfates are predominantly a result of the daytime oxidation of sulfur dioxide (SO_2). Sulfur released into the atmosphere as gaseous sulfur dioxide originates from fossil fuel combustion via electricity generation and heating; smelting and the burning of biomass are additional sources.[8,19] Both gas (reactions 10–12) and aqueous phase (reactions 13–15) chemistry produce sulfuric acid (H_2SO_4) and sulfate aerosol.[8,19,25]

$$HO\cdot_{(g)} + SO_{2(g)} + M \rightarrow HOSO_2\cdot_{(g)} \qquad (10)$$

$$HOSO_2\cdot_{(g)} + O_{2(g)} \rightarrow HO_2\cdot_{(g)} + SO_{3(g)} \qquad (11)$$

$$SO_{3(g)} + H_2O_{(g)} + M \rightarrow H_2SO_{4(g)} + M \qquad (12)$$

Due to the low vapor pressure of sulfuric acid, once produced it rapily condenses on existing aerosol particles or forms aqueous droplets.[8,19,25] Similar to nitric acid, sulfuric

acid undergoes neutralization by ammonia which produces aqueous or solid ammonium sulfate aerosol (reaction 16).[8,19,24,26]

$$SO_{2(g)} + H_2O_{(l)} \leftrightarrows SO_2{\cdot}H_2O_{(aq)} \quad (13)$$

$$SO_2{\cdot}H_2O_{(aq)} \leftrightarrows HSO_3^- + H^+ \quad (14)$$

$$SO_2{\cdot}H_2O_{(aq)} + H_2O_{2(aq)} \leftrightarrows H_2SO_{4(aq)} + H_2O_{(l)} \quad (15)$$

$$2NH_{3(g)} + H_2SO_{4(aq)} \leftrightarrows (NH_4)_2SO_{4(s,\,aq)} \quad (16)$$

Less frequently quantified water-soluble ions such as chloride (Cl^-), phosphate (PO_4^{3-}), calcium (Ca^{2+}), magnesium (Mg^{2+}), and potassium (K^+) contribute to a smaller fraction of the bulk of aerosol material. Crustal material suspended in the atmosphere by wind erosion or human activity such as construction, mining, and road dust contributes to calcium and magnesium particulate matter.[8,14] Sea-spray and coal burning are two sources of chloride compounds with the former only being significant in oceanic coastal regions.[14] Phosphate sources are less well-known and include biomass burning and mineral dust.[27] Potassium is also a tracer for air pollution as a result of burning biomass.

In addition to hydrochloric, nitric, and sulfuric acid droplets, low molecular weight organic acids may account for a significant portion of atmospheric aerosol acidity. Oxalic (HOOCCOOH), acetic (CH_3COOH), and formic (HCOOH) acids are the most frequently detected organic acids in the atmosphere.[13,28-32] Formic and acetic acids are found primarily in the gas phase while oxalic acid is found in the particulate phase. Sources of organic acids include direct emissions from biogenic sources, motor vehicle exhaust, as well as biomass burning.[8,13,14,20,29-31] Secondary formation of organic acids, resulting from the oxidation of VOCs in the atmosphere, is another important source.[8,13,14,20,29-31] VOCs react with ozone as well as nitrate and hydroxyl radicals in the

troposphere, facilitating secondary organic aerosol (SOA) development.[17,32] Both gas and particulate phase oxidation of VOCs contribute to SOA. Isolating individual VOCs that specifically contribute to organic acids has proven difficult due to the vast number of possible precursor compounds. What has been determined is the initial oxidizing species as well as mixing ratios of nitrogen oxides, both playing a major role in oxidation and extent of formation of various secondary organic species. Controlled laboratory experiments have contributed most of the current knowledge of SOA production.[17,32] Several olefins that are potential precursors of both formic and acetic acids, as well as other larger chain organic acids, include ethylene, propene, isobutene, and 1-pentene, among others.[8,29,30] Criegee intermediates resulting from reactions between ozone and alkenes produce carboxylic acids by reacting with water vapor present in the troposphere.[8]

Chicago, Illinois: Industry and Meteorology

Population and Major Air Pollution Sources

Considered the third-largest city in the United States, Chicago's population of about 2.7 million residents and an additional 6.8 million in the surrounding metropolitan–Northwest Indiana–Wisconsin area[33,34] makes Chicago a major urban hub with a well-established industrial sector. Two large airports, O'Hare and Midway International Airports, are located within city limits. In addition, intercity passenger and freight rail traffic is high due to Chicago's location along the network of U.S. railways. Chicago is the main intermodal hub in the nation and sees roughly 37,500 freight railcars per day.[35] Local industry includes paint and solvent manufacturing and oil refineries. Vehicle

emissions from several interstate highways add to local pollution, as does industry in Northwest Indiana featuring steel plants, coke ovens, oil refineries, cement production, among other manufacturing.[36] The industry mentioned, in addition to other local sources, contributes to air pollution measured in close proximity of the city. Additive to local pollution, regional pollution transport is also a contributing factor to air pollutants measured in Midwestern cities.[12,22] The Midwest has a large agricultural and industrial presence from which pollutants can be transported to the Chicago region and beyond.

Lake Breeze

Geography and meteorology play a large role in the chemical evolution and transport of natural and anthropogenic air pollutants. Large bodies of water directly influence weather regimes and pollution transport along cities' coastlines. With a mesoscale meteorological event, such as a lake breeze, polluted and processed air is recirculated over coast and inland, also potentially cycling emitted pollutants.[37] Chicago's location on the southwest shore of Lake Michigan makes the city susceptible to lake breeze circulation year-round, especially in the spring or early summer months when temperature differences between land and lake are large. Several lake breeze studies along the western Lake Michigan shoreline have found that pollutants, specifically tropospheric ozone, are recirculated and transported both inland as well as north along the coastline.[37-43] Therefore, lake breezes affect local air quality via distribution of initial anthropogenic emissions and processed air containing secondary species brought back onshore by the breeze's circulation. A depiction of the circulation of a local lake breeze is shown in Figure 1.

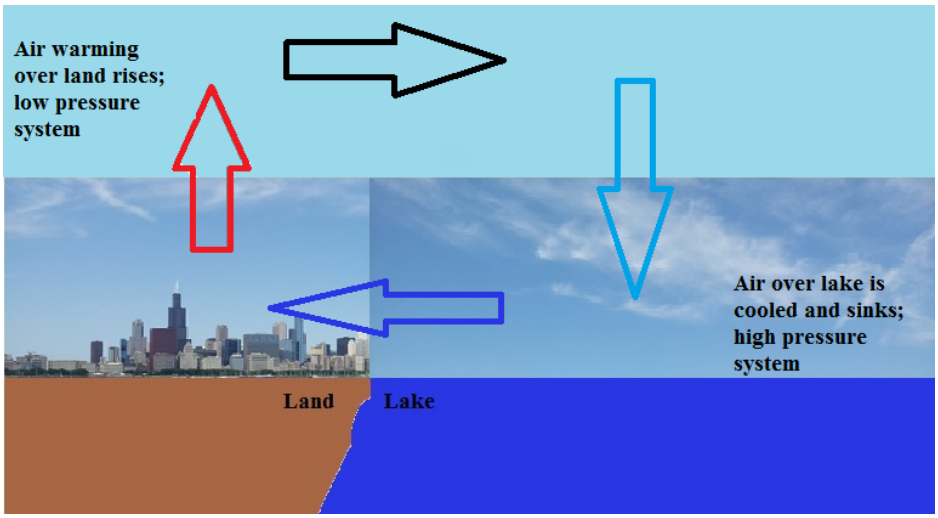

Figure 1. Depiction of the Chicago lake breeze. Lake breeze circulation; air warmed from solar and infrared radiation rises above land creating a low pressure system (red arrow), while air in contact with lake water is cooled and dense resulting in a high pressure system (light blue arrow). Outflow (black arrow) and inflow (navy blue arrow) complete the circulatory air pattern.

A local lake breeze typically forms in the morning hours, on days with little cloud cover and the presence of offshore, light winds.[41,43] If winds are too strong, the necessary temperature gradient between the air above land and air above adjacent lake waters will not develop.[41] As water warms more slowly than land due to its larger heat capacity, cool water temperatures result in cooler, more dense air above the body of water, creating a higher air pressure above the water surface. The air over adjacent land warms from the sun and absorbs additional energy emitted from the land below. The warm air rises and creates a low-pressure system over the land mass. To equalize the pressure difference, cool air flows from over the lake towards land, forming the circulation pattern known as a lake breeze. Air constituents residing relatively stationary above the lake due to calm conditions in the morning prior to the breeze, undergo chemical reactions as solar radiation increases throughout the morning hours. With the onset of a lake breeze, this air mass now containing processed constituents is transported back onshore, leading to a

short-term increase in concentration of secondary air constituents before leveling off as the circulation progresses. The initial front of the lake breeze is narrow, measuring between one and two kilometers (km) in thickness.[41] The strength and duration of a lake breeze is dependent on temperature variability between air above land and adjacent lake and the resulting pressure gradient. While the extent of the onshore air mass migrating inland varies, it has been measured as far as 40 km inland from the western shore of Lake Michigan.[41] During the onset of a local lake breeze, temperatures decline or level off and wind speeds increase as well as shift to onshore flow (i.e. easterly, northeasterly, and southeasterly). Humidity may increase or decrease during lake breeze circulation.[42] An opposite pattern, called a land breeze, can develop during the nighttime hours, when land temperatures are cooler than bordering water temperatures.[42] Offshore flow of a land breeze at night transports a stable air mass of primary pollutants over the lake, which can recirculate back onshore in the event a lake breeze develops the following day.[37]

Theory of Multivariate Statistical Methods

Overview

A large amount of data accumulates resulting from extensive studies on air pollution. Multivariate statistical techniques are used to discover underlying relationships buried in large data sets that are not observed using traditional descriptive statistics. Redundant information is eliminated using multivariate techniques, making the data more manageable for interpretation. Relationships between meteorological parameters and air pollutants are important to establish as both emission sources and weather regimes influence air quality via transport and transformation of air pollutants across regions.

Both principal component analysis (PCA) and factor analysis (FA) have been applied to air pollutant and meteorological data from all over the world in order to identify sources of pollutants monitored in a particular study.[44-50] Canonical correlation analysis (CCA) has been used to evaluate atmospheric data considerably less than PCA or FA. CCA has been utilized to determine linear relationships between air pollution variables and meteorological parameters.[44,49,50] Regardless of the technique used, uncovering variables' relationships can allow researchers to gauge pollution transport, identify potential pollutant sources, and better predict local pollution episodes.

Canonical Correlation Analysis

Canonical correlation analysis is a multivariate statistical method which determines the extent of existing linear relationships, or lack thereof, between two sets of data containing multiple variables in each set.[51] Generally, one data set corresponds to variables defined as independent, while the other data set contains variables classified as dependent.[51] For each data set, linear combinations are derived; canonical weights within linear combinations are generated in such way that maximum correlation is achieved between the linear combinations of the first data set and the linear combinations of the second data set.[51,52] The first canonical function derived reflects the maximum linear correlation possible between the two original data sets. Each successive canonical function derived maximizes residual inter-correlations between data sets not explained by previous canonical functions. Therefore, each canonical variate pair is orthogonal and uncorrelated to one another.[51] The maximum number of canonical functions that can be derived depends on how many variables are within each data set being used in the

analysis. The number of variables in the smaller of the two data sets is the limiting factor.[51] For example, if the first data set has seven variables and the second data set has four variables, no more than four canonical functions are derived in CCA.

Shown below are the general equations[adapted from 53] for linear combinations of data set no. 1 (U) and data set no. 2 (V); combined, they represent a canonical function (U, V).

$$U = a_{11}X_1 + a_{12}X_2 + a_{13}X_3 + a_{14}X_4 \ldots . a_{1n}X_n \qquad (17)$$

$$V = b_{11}Y_1 + b_{12}Y_2 + b_{13}Y_3 + b_{14}Y_4 \ldots . b_{1q}Y_q \qquad (18)$$

In equation 17, symbols X_1, X_2, X_3, $X_4 \ldots X_n$ represent each original variable within data set no. 1; a_1 denotes the canonical weights in the linear combination (U) and "n" distinguishes that each weight value is different for each variable. In equation 18, the Y_1, Y_2, Y_3, $Y_4 \ldots Y_q$ represent each original variable within data set no. 2; b_1 stands for each canonical weight in linear combination (V) and "q" distinguishes that each weight value is different for each variable. All successively derived canonical functions follow the equations displayed above.

Within each canonical function are derived canonical weights corresponding to the amount of influence each original variable has in the linear combination.[51,53] The larger the weight, the more influence a particular variable associated with the weight value has in the linear combination. In addition to canonical functions, several other pieces of information are derived in CCA. Canonical correlations corresponding to the linear correlation between each derived canonical function, the statistical significance of each canonical function, and the simple correlations between original variables and respective derived canonical variates are used as additional resources from CCA output to interpret the data.[51] Terminology of CCA results varies by reference; therefore,

interchangeable terms are listed for clarity in Table 1. Additionally, linear combinations are used to calculate canonical scores, which project original variables' observations in canonical function space. These score plots can be examined to identify extreme cases, outliers, and trends.[51]

Table 1. Summary of CCA terminology of synonymous association.[50]

Main Term	Synonymous Term(s)
Linear combination	Canonical variate
Canonical function	Canonical variate pair Canonical variable
Canonical weight	Canonical coefficient
Canonical loading	Canonical structure loading

Traditionally, canonical weights are the CCA result most interpreted through their magnitude and size.[51] However, it is also beneficial to interpret canonical loadings, simple correlations between original variables and respective canonical variates. Canonical loadings reveal additional information when original variables display collinearity or multicollinearity between themselves.[51,53] Collinearity is defined as the correlation between two variables; multicollinearity refers to multiple variables having correlation to one another.[54] If original variables exhibit collinearity prior to CCA, canonical weights can be misleading.[53] It is important to note absence or presence of collinearity of original variables to determine whether canonical weights, loadings, or both, should be interpreted. See Johnson and Wichern (1998) for in-depth derivation of mentioned CCA component results.

Principal Component Analysis

Principal component analysis functions as a statistical method for dimension reduction of a multivariate set of data. Through PCA application, original variables are transformed into new variables; this transformation is completed to retain the variance of the original data, but express this variability in a fewer number of new variables, thus eliminating redundant information.[55] The new variables are expressed as linear combinations of original variables.[55] These linear combinations are referred to as principal components (PCs) or eigenvectors and follow the same general format as equations 17 and 18. The coefficients or loading values within a linear combination can be used to interpret relationships across a set of original variables and for classification purposes.[55]

By rotation of the axes the original data occupy, loading values within principal components are generated to maximize the amount of variance explained by the new variable. The first PC captures the largest variance of the original data and is associated with the largest eigenvalue.[55] The second PC derived lies orthogonal to the first and captures variance not explained by the first PC. Each successive PC maximizes the data variance not expressed by the PCs preceding it. All PCs derived are orthogonal and uncorrelated with one another.[55] Furthermore, the eigenvalue associated with each PC becomes smaller with each successive new linear combination. Eigenvalues aid in determining how many PCs are retained for interpretation. When following Kaiser's Rule, all principal components with an associated eigenvalue of less than one are not interpreted because the information gained is insignificant.[55] An additional tool to

determine the number of PCs to retain for interpretation is called a Scree Plot, a graph of eigenvalue versus corresponding PC number.[52,55] Consideration of a large change in slope between points in a Scree Plot is used to determine which PCs to retain.[52,55] PC eigenvalues in the area of large slope are retained, whereas values located where the plot's curve levels off are not considered.

PCA is applied to either the covariance or the correlation matrix of the original data. A correlation matrix is chosen when variables within the original data set were measured on varying scales; variables are standardized before PCA is applied.[55] Similarly to CCA, PCA score plots projecting PC scores in new variable space are generated for interpretation. Additional information on PCA can be found in Johnson and Wichern (1998) as well as Wilks (2011).

CHAPTER II

EXPERIMENTAL DETAILS

Sampling Location and Period

Aerosol sample collections, as well as the monitoring of trace gas mixing ratios and meteorology, were completed at Loyola University Chicago's Lakeshore Campus, located in the Rogers Park neighborhood of Chicago, Illinois. Instrumentation utilized in all air pollution studies was located atop Mertz Hall, a 60-meter (m) tall student residence building that is 200 meters west of the Lake Michigan shoreline. The sampling location is roughly 13 kilometers (km) north of Chicago's downtown centre. Residential areas border the university campus to the north, east, and south. A map depicting the sampling location is shown in Figure 2.

Figure 2. Map depicting Chicago (black circle) and Loyola University Chicago sampling location (A) in relation to Lake Michigan and surrounding area (maps.google.com 2012).

Air pollution studies were completed on weekdays during the summer season, as Chicago is most susceptible to lake breezes during this period and secondary air pollutant concentrations were expected to be the highest. Data collection was completed only on days when precipitation was not forecasted or did not occur. Trace gas instruments can be damaged due to water vapor and aerosol material is removed from the local atmosphere via wet deposition. A total of 66 days of aerosol, trace gas, and meteorological measurements were taken over the course of three consecutive summer studies in 2010, 2011, and 2012. Table 2 lists collection periods and the total number of collection days completed during each summer. The purpose of each summer study was to investigate air pollution levels during lake breeze and non-lake breezes days, determining a baseline of pollution concentrations and whether lake breeze circulation patterns affected the development of secondary pollutants in the local atmosphere. Furthermore, the data collected during summer 2010–2012 studies could be compared to an initial study that took place at the same location almost a decade earlier, during summers 2002–2004.[38-40]

Table 2. Summary of air pollution collection periods.

Summer of Collection	2010	2011	2012
Period of sampling	July 12–August 6	July 5–August 5	July 2–August 7
Total number of days	17	24	25

Instrumentation Utilized in Data Collection

Trace Gas and Meteorology Monitoring

Mixing ratios of trace gases, ozone and nitrogen oxides, were continuously measured with one-minute resolution using Thermo 49C O_3 and 42C NO–NO_2–NO_x Analyzers, respectively (Thermo Environmental Instruments, Inc., Franklin, MA).

The principle of operation of the Thermo 49C O_3 Analyzer is ozone's absorbance of ultraviolet (UV) radiation at 254 nanometers (nm). A gaseous sample of air is drawn into a "sample inlet" tube of the instrument and is then controlled by solenoid valves. One part of the inlet flow is directed through a scrubber to remove any presence of ozone before passing through the analysis chamber. This aliquot of air is designated as "reference". The other part of inlet air is passed through the analysis chamber, bypassing the scrubber, and consists of "sample" air. Two flow sensors control the flow of reference and sample air channels. The analysis chamber consists of two separate 38-centimeter (cm) cells, one attributed as a reference cell and the other a sample cell. A UV lamp is located at one end of the cells and two detectors at the other end, which independently monitor the intensity of light in the reference (I_o) and sample (I) cells. Using the Beer-Lambert law (equation 19), where epsilon (Ɛ) is the molar absorptivity coefficient of ozone at 0 °C and one atmosphere (308 cm^{-1}), b is the length of the cells (38 cm), the instrument directly calculates c, the concentration of O_3 (ppm).[57] A flowchart of the instrument air flow and main components is shown in Figure 3a.

$$I \div I_o = e^{-\varepsilon bc} \qquad (19)$$

Chemiluminescence is the principle of operation of the Thermo 42C NO–NO_2–NO_x Analyzer. When ozone and nitric oxide react, a characteristic luminescence is produced due to the nitrogen dioxide formed being in an excited state (NO_2^*). Emission of infrared light occurs when excited nitrogen dioxide molecules decay to a lower energy state (reactions 20 and 21).

$$NO + O_3 \rightarrow NO_2^* + O_2 \qquad (20)$$

$$NO_2^* \rightarrow NO_2 + h\nu \qquad (21)$$

The intensity of emitted light has a linear relationship to the concentration of nitric oxide present. Air drawn into the instrument first passes through a filter to remove particles. Then the air is split into two separate samples, with one sample entering the analysis chamber without further treatment for direct determination of NO by chemiluminescence. The other sample of air passes through a converter, containing molybdenum (Mo), to convert NO_2 to NO before entering the analysis chamber. In the analysis chamber, NO reacts with O_3 to produce NO_2^*. The chemiluminescence emitted when NO_2^* returns to its ground state is detected by a photomultiplier tube (PMT) and translated into a concentration by electronic conversion. By switching between samples, both NO only as well as NO + NO_2 can be determined. To calculate NO_2 concentration, the difference in concentrations of both modes is computed by the instrument.[58] A diagram of airflow through the instrument is shown in Figure 3b.

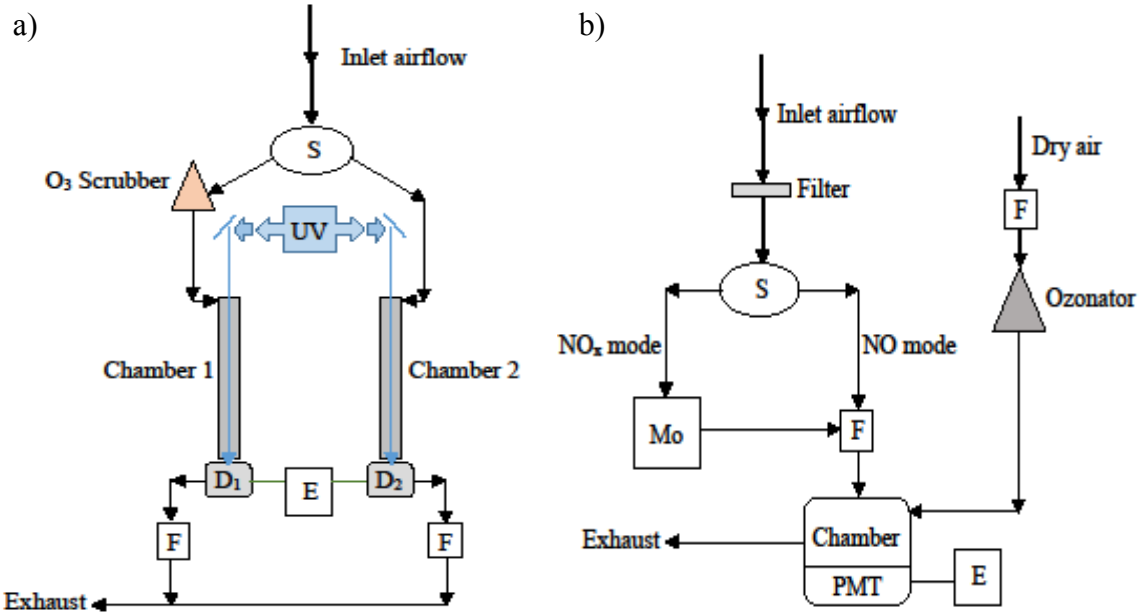

Figure 3. Flow chart of airflow through components of a) Thermo 49C O_3 Analyzer and b) Thermo 42C NO–NO_2–NO_x Analyzer. *S* solenoid, *UV* ultraviolet lamp, *D_1, D_2* detectors, *E* electronics for data processing, *F* flow sensors, *Filter* particulate filter, *Mo* molybdenum converter, *Ozonator* ozone generator, *PMT* photomultiplier tube. These are adaptations of extensive schematics in the instrument instruction manuals.[57,58]

Both trace gas instruments were calibrated with the assistance of staff at the Illinois Environmental Protection Agency Northbrook station. The Thermo 49C O_3 Analyzer is a USEPA Designated Equivalence Method for measuring ambient ozone concentrations, EQOA–0880–047.[59] The Thermo 42C NO–NO_2–NO_x Analyzer is a USEPA Reference Method for measuring ambient nitrogen dioxide concentrations, RFNA–1289–074.[59]

A Vantage Pro™ 2 Weather Station (Davis Instruments, Hayward, CA) concurrently recorded meteorological parameters with 15-minute resolution. Weather station equipment included an anemometer (for wind speed and direction), barometer, humidity and temperature sensors, and a rain collector. The equipment was mounted on a metal pole attached to the roof of Mertz Hall, roughly 15 feet above the building's roof. Trace gas and weather instrumentation recorded data 24 hours a day during each summer pollution study.

Aerosol Collection

Atmospheric aerosols were collected using two pre-washed 47-millimeter (mm) Whatman™ QM-A quartz fiber filters placed back-to-back inside a Teflon filter holder connected to a Gast® vacuum pump (IDEX Corporation). A flow meter (Dwyer Instruments Inc.) inserted between the filter holder and pump regulated the volume of air passing through the filter. All of the described components were connected using chemically inert tubing. The flow rate, 1.699 cubic meters per hour (m^3 $hour^{-1}$), was constant during each daily collection of every summer. Prior to use in aerosol collection, all of the quartz fiber filters were pre-washed following an already established procedure.[38-40] For this, the filters were placed into individual sterile petri dishes (Pall

Corporation), 10 milliliters (mL) of Nanopure™ H_2O was added, and then the petri dishes were shaken at 50 rotations per minute (rpm) by a mechanical shaker for 15 minutes. The washing procedure was repeated before the filters were dried in an oven. The dried filters were then stored in sterile petri dishes, wrapped in Parafilm®, and placed in a sealed plastic bag until aerosol collections. Pre-washing the filters was carried out to remove contaminants.[38-40]

Two aerosol samples were collected each weekday during all summer air pollution studies. The first aerosol sample period, defined as segment A, was from 0700 to 1000 local time (LT). Segment B, the second aerosol sampling period, was from 1100 to 1300 LT. Aerosol collection was designed to capture short-term pollution development, pollutants on non-lake breeze days, and pollution levels before and during a local lake breeze. This design enabled quantifying air pollutants during these scenarios. The method of collection was initially developed and tested during summer 2002–2004 studies at the same location.[38-40] During summers 2002–2004, it was observed that a local lake breeze was most frequent between the hours of 1000 and 1100 LT.[38-40] Therefore, the 1-hour gap between collection segments A and B was inserted so the segment B collection could potentially capture aerosol concentrations during or after a lake breeze had occurred.[38-40] In summer 2010, an aerosol sample sequence using segment A [0700–0900 LT], B [0900–1100 LT], and C [1100–1300 LT] collection periods was explored to try to increase the probability of capturing pre and post lake breeze pollutant concentrations. It was not continued, as it did not prove to be a viable adjustment to the method. Methodology in summers 2011–2012 and instrumentation used in summer 2010–2012 studies, described herein, was consistent with previous 2002–2004 studies in

order to increase the amount of data available to evaluate lake breeze versus non-lake breeze pollution and also compare results and assess differences from the earlier study.

New, pre-washed quartz fiber filters were used in all segmented aerosol collections on each day. After collection, the Teflon filter holder was detached from the ring stand and transported to Flanner Hall in a plastic container sealed with a lid. In the laboratory, filters were transferred from the Teflon filter holder to individual sterile petri dishes using tweezers. All petri dishes were wrapped in Parafilm®, placed into sealed plastic bags, and frozen at -6 degrees Celsius (°C) to prevent sample degradation.

Aerosol Filter Extraction and Analysis

Filter Extraction Method

The method described herein was first utilized in summer 2002–2004 studies when it was validated as a method to extract water-soluble aerosol material from quartz fiber filters.[38-40] Prior to extraction of aerosol material, petri dishes containing the samples were removed from the storage freezer and equilibrated to room temperature. All quartz fiber filters used in aerosol sampling were transferred to individual Nalgene® HDPE (high-density polyethylene) bottles using tweezers. Five milliliters of Nanopure™ H_2O was added to each of the HDPE bottles using a micro-pipet. The HDPE bottles were capped and placed in a VWR® ultrasonic bath (35 kilohertz) for 20 minutes. New, pre-washed quartz fiber filters not used in collections were extracted using the same procedure and considered blank or control filters. Once sonication of quartz filters was completed, a one milliliter aliquot of aqueous aerosol extract from each HDPE bottle was removed and filtered using a 13-millimeter (mm) syringe filter with a 0.45 μm PVDF (polyvinylidene fluoride) membrane attached to a one milliliter luer-slip plastic syringe.

This micro-filtration removed large fibrous filter material that may otherwise damage analytical instrumentation during analyses. New syringes and syringe filters were used every time to filter each aqueous aerosol sample extract. After micro-filtration, aqueous aerosol sample extracts were transferred to micro-centrifuge tubes and stored in refrigeration until analyses. All HDPE bottles containing quartz filters and remaining aqueous extract were stored in plastic bags and frozen at -6 °C in case additional analyses was required.

Analysis of Extracted Aerosol Material

All aqueous quartz fiber filter extracts of blanks and aerosol samples were analyzed for water-soluble cations and anions using a Metrohm 761 Compact Ion Chromatograph (IC) with chemical suppression (Metrohm USA, Inc., Riverview, FL) and conductivity detection. The suppression module was used only for anion analysis mode to reduce the conductivity of the eluent. Instrument operating conditions for both cation and anion analysis of aqueous aerosol sample extracts and blank filter extracts are displayed in Table 3. Ion-exchange chromatography is a common method of quantification of water-soluble cations and both inorganic and organic anions present in atmospheric aerosols.[13,14,28,30,38,39,60,61] High sensitivity and selectivity along with a relatively short duration of sample analysis has made ion chromatography an invaluable tool. Ion chromatography separates ions in an aqueous sample based on an ion's affinity to the stationary phase. A flow chart depicting components of an IC system and system flow for cation and anion mode is show in Figure 4.

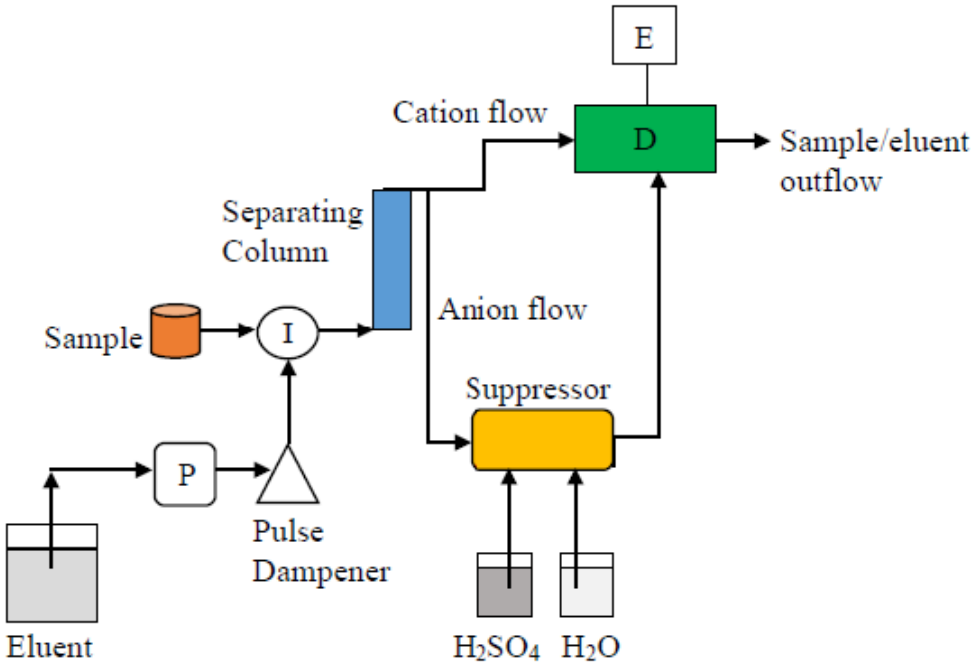

Figure 4. Flowchart of IC system components for cation and anion analysis. *Eluent* mobile phase, *P* high-pressure pump, *Pulse Dampener* pulse dampener, *I* 6-port injection valve & sample loop, *Separating Column* cation or anion guard column & column, *D* conductivity detector, *E* electronics for data processing, *Suppressor* 3-chamber suppressor unit, H_2SO_4, H_2O suppressor solutions.

The major components of an ion chromatograph (IC) system include an eluent (mobile phase), high-pressure pump, pulse dampener, sample loop, 6-port injector valve, guard column, separation column (stationary phase), suppressor, and detector. All of the IC components are connected by polyetheretherketone (PEEK) tubing.[62] An aqueous sample is manually injected into the sample loop and then enters the system via a 6-port injector valve. A high-pressure pump draws eluent through the system and the pulse dampener removes mechanical noise due to the pump's two pistons. Once injected, the sample is transported, via the mobile phase (eluent), to a separating column containing the stationary phase of opposite charge to the analyte ions. The ions are separated in the column based on their size and charge. The separated analyte ions along with the mobile phase are pumped through a conductivity detector. The detector measures changes in

conductance due to analyte ions in comparison to a baseline conductivity of the mobile phase ions only. A chromatogram displays the ions present in the sample as conductivity (y-axis) versus time (x-axis).[62] Analyte concentration is proportional to conductivity and calibration of the instrument is completed by analyzing a set of standards and graphing a calibration curve. The ion concentrations of each sample are determined by comparing the conductivities of standards and sample. For anion analysis, an extra step is added which reduces the background noise originating from the eluent. The eluent ($Na_2CO_3/NaHCO_3$) contains carbonate (CO_3^{2-}) and bicarbonate (HCO_3^-) at 3.5 and 1.0 millimolar (mM), thus the baseline conductivity is high.[62] This in turn impacts the detection limit of analysis for all other ions. As a result, both carbonate and bicarbonate anions should be removed before detection. A packed-bed suppressor inserted after the separating column but before the conductivity detector is used for this purpose.[62] The Metrohm suppressor module (MSM) is coated with a cation exchange resin ($R\text{-}SO_3\text{-}H$) and both dilute H_2SO_4 and H_2O are supplied to the suppressor for regeneration and rinsing in between sample injections. The suppressor's role is to convert both CO_3^{2-} and HCO_3^- ions into carbon dioxide (CO_2) and H_2O. Reactions 22, 23 show conversion of eluent ions while reaction 24 is an example of analyte ion conversion.

$$NaHCO_{3(aq)} + R\text{-}SO_3\text{-}H_{(aq)} \leftrightarrows H_2O_{(aq)} + CO_{2(aq)} + R\text{-}SO_3\text{-}Na_{(aq)} \quad (22)$$

$$Na_2CO_{3(aq)} + 2R\text{-}SO_3\text{-}H_{(aq)} \leftrightarrows H_2O_{(aq)} + CO_{2(aq)} + 2R\text{-}SO_3\text{-}Na_{(aq)} \quad (23)$$

$$NaNO_{3(aq)} + R\text{-}SO_3\text{-}H_{(aq)} \leftrightarrows HNO_{3(aq)} + R\text{-}SO_3\text{-}Na_{(aq)} \quad (24)$$

Table 3. Ion chromatograph method conditions for cation and anion analysis.

Instrument Conditions	Cation	Anion
Eluent (millimolar, mM)	3.0 $H_2C_2O_4$	3.5 Na_2CO_3 and 1.0 $NaHCO_3$
Guard column	Metrosep C2	Metrosep A Supp 4/5
Separation column	Metrosep C2-150	Metrosep A Supp5-250
Column particle size (micrometer, µm)	7	5
Sample loop volume (microliter, µL)	20	20
Flow rate (milliliter per minute, mL min^{-1})	1.0	0.7
System pressure (megapascal, MPa)	8	13
Chemical suppression	No	Yes
Suppressor solutions (mM)	N/A	100 H_2SO_4 and Nanopure H_2O
Duration of analysis (minutes)	13	30

IC Calibration

Standard solutions containing quantifiable ions in cation and anion mode were prepared and analyzed to first determine the retention time of each ionic species. Cation standard solution included sodium (Na^+), ammonium (NH_4^+), potassium, (K^+), magnesium (Mg^{2+}), and calcium (Ca^{2+}) while the anion standard solution contained fluoride (F^-), acetate ($C_2H_3O_2^-$), formate (CHO_2^-), chloride (Cl^-), bromide (Br^-), nitrate (NO_3^-), benzoate ($C_7H_4O_2^-$), phosphate (PO_4^{3-}), sulfate (SO_4^{2-}), oxalate ($C_2O_4^{2-}$). Example chromatograms for cation and anion analyses of multi-ion standard solutions are shown in Figure 5. A calibration curve was then produced by analyzing several multi-ion standard solutions of different concentration. After calibration, aqueous aerosol extract of each sample filter was analyzed in both cation and anion analysis mode. Triplicate analyses were carried out for each sample filter extract to obtain an average concentration and standard deviation. Both front and back sample filters were analyzed for each collection to account for breakthrough or front filter overloading. Unused, pre-cleaned quartz filter aqueous extracts were analyzed by IC in triplicate and denoted as blanks or

control filters. Each summer of collection had designated blank filters corresponding to the different packages of Whatman™ QM-A quartz fiber filters used in respective collections. The blank concentrations were subtracted from the sample filter concentrations of the respective ion to obtain net aerosol ion concentrations (in parts per million, ppm) for all quantified analyte ions.

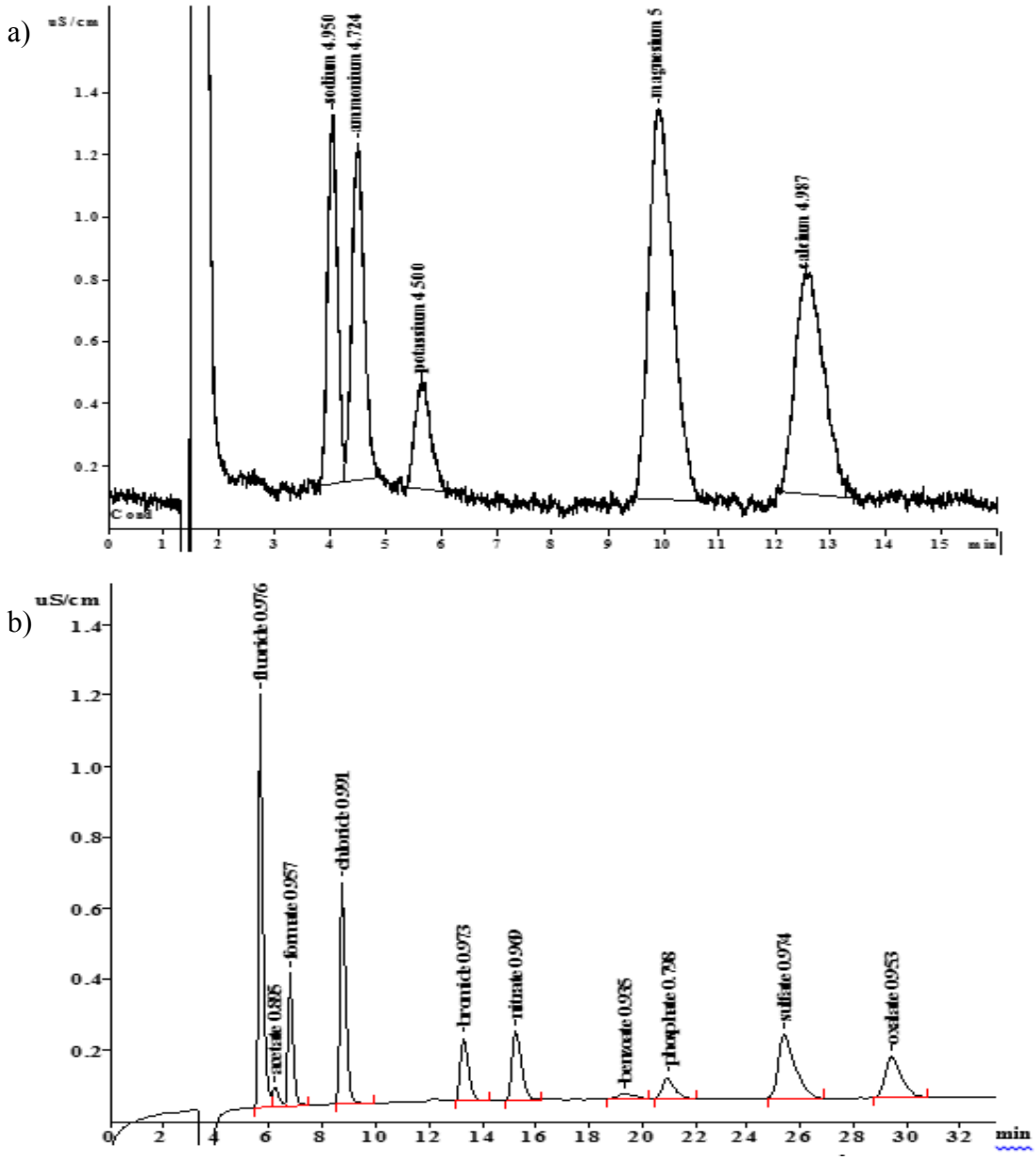

Figure 5. a) Cation and b) anion chromatograms; conductivity in microSiemens per centimeter (µS cm^{-1}) versus time in minutes (min).

Sample Data Processing

The following calculations were completed for each ion quantified to obtain final concentrations in microgram per cubic meter (μg m^{-3}).

1. First, the average blank filter ion value was subtracted from the respective quantified ion in a sample to obtain a net concentration in parts per million (ppm).
2. Next, the average value of net ion concentration was calculated from the three replicate sample analyses of the sample filter extract.
3. The average value of net ion concentration was multiplied by five milliliters, to account for dilution. The result is absolute mass of each ion in micrograms (μg).
4. Finally, absolute mass (μg) was divided by the total volume of air collected (segment A or B, 5.097 or 3.398 cubic meters (m^3), respectively) resulting in mass per volume, expressed as microgram per cubic meter (μg m^{-3}).

An example calculation for chloride concentrations determined in the segment A collection on Monday, July 2, 2012 is shown in Table 4. If any filter breakthrough occurred during collections, which meant particulate matter passed through the top filter and was deposited on the back filter, concentrations of both filters were added together.

Meteorology and Trace Gas Data Processing

All meteorological and trace gas data were downloaded at the completion of each summer study. Because the resolution of the weather station (15-minute) and Thermo trace gas (1-minute) equipment was higher than that of the segmented aerosol collections, all meteorological parameters and trace gas mixing ratio data between 0700–1000 and 1100–1300 LT were averaged to match the periods of segment A and B aerosol collections, respectively.

Table 4. Sample data processing to account for triplicate analyses, blanks, dilution factor, and the total volume of air collected. Data from Monday, July 2nd, 2012 segment A. Blank average and runs 1–3 (ppm), dilution (µg), volume of air collected (m^3), final concentration (µg m^{-3}). Dilution = net average x 5 mL; Final concentration = Dilution value ÷ volume of air.

Ion Detected	Blank Average	Run 1	Run 1-blank	Run 2	Run 2-blank	Run 3	Run 3-blank	Net Average	Dilution [x 5 mL]	Volume of air	Final Conc.
Chloride	0.033	0.452	0.419	0.445	0.412	0.454	0.421	0.417	1.670	5.097	**0.328**

CHAPTER III

SUMMER 2010–2012 AIR POLLUTION STUDY RESULTS

Overview

Descriptive statistics including data from all 66 days of study were reported to show the ionic composition and dominant species present in the local atmosphere in summers 2010–2012. All collection days were then categorized into one of three groups, namely reference, lake breeze, or variable. Through categorization, assessing differences between non-lake breeze (reference) days and lake breeze days was completed. Variability in pollution on reference and lake breeze days were discussed separately and categorized results were used to evaluate whether the circulation of a local lake breeze contributed to variance in local secondary pollutant concentrations. We hypothesized that a lake breeze would induce a strong increase in the concentration of secondary air pollutants due to transport of a chemically processed air mass initially over the lake towards the city and inland. This spike in pollutants was thought to be larger than a typical non-lake breeze, reference day pollution pattern of a gradual increase in secondary air pollution due to photochemical and chemical reaction processing. Variable days were not discussed as no pattern in the variability of recorded wind direction was found. The large variability in wind direction during variable days did not make it conducive to extract meaningful information regarding air pollution concentrations for this group of sampling days.

Pollutant Concentrations and Meteorology

Air Pollutants

With respect to all 66 collection days, chloride, nitrate, sulfate, and oxalate were the most common ions quantified in aqueous aerosol extracts and detected on all days of study during both A and B segment collections. Acetate and formate were also quantified on the majority of sampling days. Potassium, phosphate, calcium, and magnesium ions were less frequently quantified and detected on less than half of the total sampling days. Fluoride, benzoate, and bromide were either not detected in any sample filter extracts or their blank filter concentrations were higher than sample concentrations. The observed ionic pollutants quantified are consistent with summer 2002–2004 studies except for acetate and formate, which had larger blank concentrations than sample concentrations during those studies.[38-40] Sodium and ammonium peaks were not resolved in summer 2010–2012 sample analyses therefore results for these ions are not discussed. Descriptive statistics of all air pollutant data for summers 2010–2012 are shown in Tables 5–8. Overall, the trend in ionic pollutant averages, found by pooling all three summers' segment A and B data together, from highest to lowest concentration was sulfate > nitrate > calcium > phosphate > formate > acetate > oxalate > chloride > potassium > magnesium. Total ion concentrations for each summer study, referring to both segment A and B data combined, showed variability of ion concentrations during each summer but not a change in the overall dominant ionic species (Figure 6). The bulk of water-soluble aerosol species quantified was inorganic (Figures 7–9). Sulfate and nitrate ions had the

highest concentrations in all three summer studies; this is consistent with summer 2002–2004 studies completed at the same sampling site.[38-40]

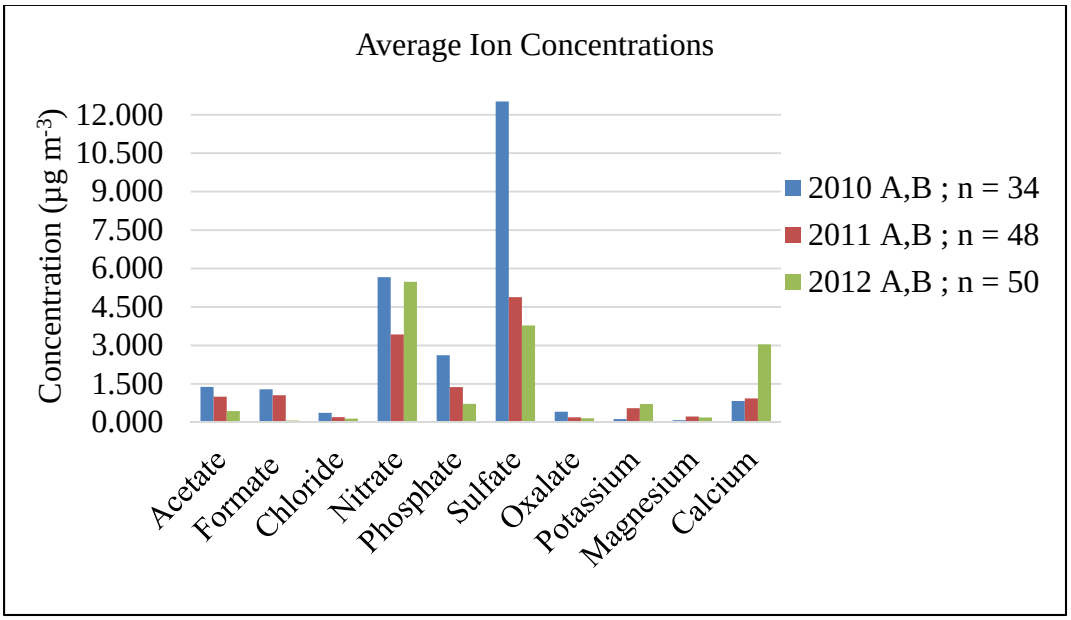

Figure 6. Total ion concentrations for all 66 days; overall averages for segments A and B.

Sulfate concentrations ranged from 0.435 to 41.014 µg m^{-3} over all three summers. There was also high variability in the concentration of nitrate, 0.315–17.541 µg m^{-3}. Average sulfate concentrations in summers 2010, 2011 were higher than nitrate concentrations (Figure 6). Conversely, in summer 2012 average nitrate concentrations were higher than sulfate concentrations. Sulfates are primarily neutralized by available ammonia in the atmosphere; any excess ammonia present then neutralizes nitric acid, to form ammonium nitrate particles. In high temperatures, ammonium nitrate converts to its gas-phase precursors, nitric acid and ammonia, as it is more volatile than ammonium sulfate.[8] Humidity and temperature varied each summer, discussed later in this chapter, and may have contributed to the difference seen in yearly averages of nitrate and sulfate ion concentrations.

Table 5. Summer 2010 pollutant concentrations. Segment A and B minimum, maximum, and average concentrations reported separately for ions [μg m^{-3}] and trace gases (ppb); SE_b is the standard error based on variability of blank filters' ion concentrations.

Pollutants	A_{min}, A_{max}	$A_{avg} \pm SE_b$	SD	B_{min}, B_{max}	$B_{avg} \pm SE_b$	SD	A, B_{avg}
Acetate	0.066, 4.108	1.529 ± 0.053	1.106	0.202, 2.315	1.146 ± 0.053	0.653	1.381
Formate	0.094, 2.487	1.490 ± 0.112	0.679	0.047, 2.399	1.070 ± 0.112	0.775	1.287
Chloride	0.068, 1.646	0.494 ± 0.014	0.448	0.017, 0.749	0.245 ± 0.014	0.218	0.370
Nitrate	1.918, 13.698	5.168 ± 0.011	3.032	2.089, 16.879	6.155 ± 0.011	3.353	5.662
Phosphate	0.071, 13.772	3.906 ± 0.847	5.123	0.090, 1.915	0.593 ± 0.847	0.365	2.617
Sulfate	2.668, 41.014	15.651 ± 0.069	10.654	1.305, 26.242	9.379 ± 0.069	6.264	12.515
Oxalate	0.256, 1.280	0.482 ± N/A	0.235	0.184, 0.495	0.337 ± N/A	0.009	0.410
Potassium	0.012, 0.120	0.054 ± N/A	0.042	0.041, 0.587	0.314 ± N/A	0.386	0.128
Magnesium	0.046, 0.051	0.049 ± 0.520	0.004	N/A	ND	N/A	0.049
Calcium	0.139, 1.506	1.040 ± 1.307	0.781	N/A	ND	N/A	1.040
Ozone	15.76, 43.27	29.21	8.23	31.15, 66.77	48.54	9.32	38.87
Nitrogen oxides	2.88, 50.48	19.72	13.78	3.12, 29.63	10.99	7.94	15.36

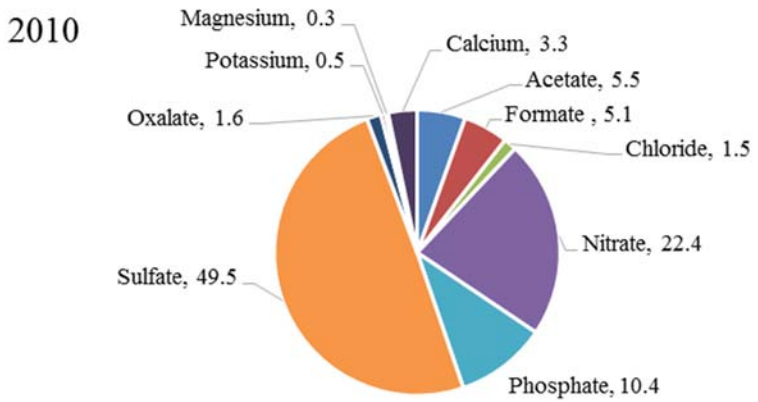

Figure 7. Summer 2010 percent (%) composition of quantified aerosol ions based on total concentration (both segment A, B data).

Table 6. Summer 2011 pollutant concentrations. Segment A and B minimum, maximum, and average concentrations reported separately for ions [μg m^{-3}] and trace gases (ppb); SE_b is the standard error based on variability of blank filters' ion concentrations.

Pollutants	A_{min}, A_{max}	$A_{avg} \pm SE_b$	SD	B_{min}, B_{max}	$B_{avg} \pm SE_b$	SD	A, B_{avg}
Acetate	0.027, 2.952	1.040 ± N/A	0.856	0.177, 1.843	0.958 ± N/A	0.532	1.002
Formate	0.062, 5.379	0.954 ± 0.003	1.172	0.035, 4.546	1.166 ± 0.003	0.950	1.058
Chloride	0.022, 2.079	0.249 ± N/A	0.408	0.025, 0.333	0.152 ± N/A	0.090	0.202
Nitrate	0.315, 5.568	2.697 ± 0.004	1.520	0.550, 10.837	4.189 ± 0.004	3.152	3.427
Phosphate	0.005, 9.754	1.572 ± 0.096	2.960	0.006, 11.250	1.169 ± 0.096	2.824	1.377
Sulfate	0.435, 15.330	5.206 ± 0.007	3.638	0.820, 13.594	4.544 ± 0.007	3.181	4.882
Oxalate	0.047, 0.391	0.174 ± N/A	0.098	0.051, 0.507	0.213 ± N/A	0.138	0.193
Potassium	0.003, 3.036	0.570 ± 0.011	0.725	0.078, 1.862	0.527 ± 0.011	0.492	0.552
Magnesium	0.019, 0.341	0.132 ± N/A	0.097	0.015, 1.934	0.382 ± N/A	0.700	0.224
Calcium	0.064, 1.754	0.772 ± 0.075	0.690	0.047, 6.593	1.102 ± 0.075	2.152	0.929
Ozone	15.76, 54.17	33.80	8.54	27.51, 78.04	47.59	15.87	40.55
Nitrogen oxides	0.02, 54.33	14.99	12.75	0.64, 42.83	8.18	8.89	11.66

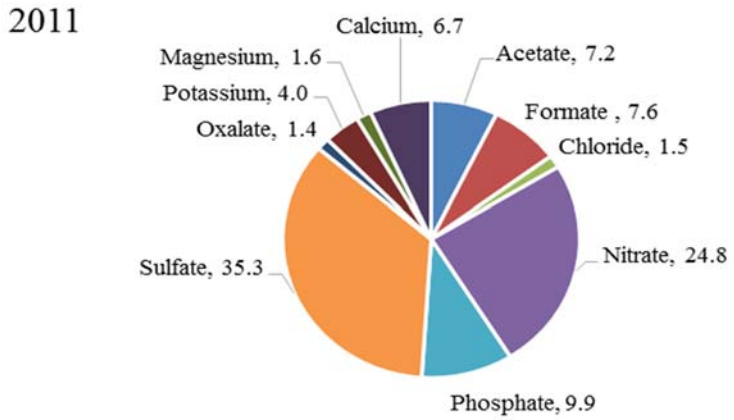

Figure 8. Summer 2011 percent (%) composition of quantified aerosol ions based on total concentration (segment A, B data).

Table 7. Summer 2012 pollutant concentrations. Segment A and B minimum, maximum, and average concentrations reported separately for ions [μg m^{-3}] and trace gases (ppb); SE_b is the standard error based on variability of blank filters' ion concentrations.

Pollutants	A_{min}, A_{max}	$A_{avg} \pm SE_b$	SD	B_{min}, B_{max}	$B_{avg} \pm SE_b$	SD	A, B_{avg}
Acetate	0.100, 0.908	0.393 ± 0.010	0.191	0.078, 0.938	0.480 ± 0.010	0.264	0.436
Formate	0.003, 0.175	0.080 ± 0.004	0.058	0.012, 0.208	0.058 ± 0.004	0.056	0.070
Chloride	0.014, 0.734	0.180 ± 0.006	0.152	0.034, 0.255	0.106 ± 0.006	0.059	0.143
Nitrate	0.944, 11.648	4.112 ± N/A	2.329	1.409, 17.541	6.854 ± N/A	3.687	5.483
Phosphate	0.205, 5.225	0.886 ± 0.258	1.268	0.157, 1.181	0.560 ± 0.258	0.298	0.718
Sulfate	1.045, 7.956	3.574 ± 0.007	1.676	1.327, 10.084	3.978 ± 0.007	2.133	3.776
Oxalate	0.033, 0.316	0.153 ± 0.002	0.079	0.035, 0.291	0.163 ± 0.002	0.080	0.158
Potassium	0.142, 2.856	0.654 ± N/A	0.673	0.048, 4.101	0.786 ± N/A	1.084	0.713
Magnesium	0.009, 0.483	0.172 ± N/A	0.111	0.011, 0.416	0.208 ± N/A	0.096	0.190
Calcium	0.179, 6.061	2.677 ± 0.177	1.441	0.467, 5.991	3.423 ± 0.177	1.659	3.042
Ozone	14.92, 56.16	38.48	10.67	44.45, 94.43	67.03	15.31	52.46
Nitrogen oxides	1.80, 50.61	22.39	13.38	1.44, 20.38	8.10	4.88	15.25

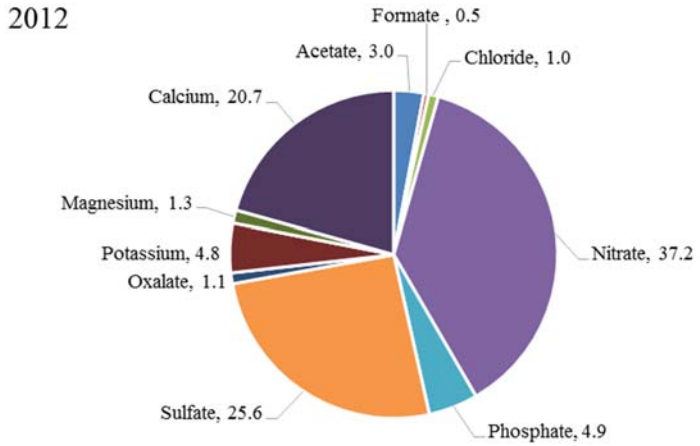

Figure 9. Summer 2012 percent (%) composition of quantified aerosol ions based on total concentration (segment A, B data).

Several studies used nitrate to sulfate ion ratios as an indicator for whether pollution concentrations were influenced more by stationary or mobile source emissions. High nitrate to sulfate ratios indicated vehicular emissions were an important source of air pollution. Low ratios suggested stationary emission sources were more influential on air pollution composition.[11,14,63] Local stationary sources influenced air pollution during summer 2010 and 2011 studies, based on calculated average nitrate to sulfate ratios of 0.673 and 0.807, respectively. Conversely, in summer 2012 mobile sources had more influence on local pollution, with an average nitrate to sulfate ratio of 1.559. Other studies found sulfate transported to the Midwest region significantly affected local concentrations of sulfate.[12,22,64,65] Wind direction variability in our study, discussed later in this chapter, contributed to variability in sulfate concentrations. In all summers, nitrate to sulfate ratios increased from A to B segments, likely due to atmospheric processing of pre-cursor pollutants and variability of meteorology. High nitrate to sulfate ratios of two and five were measured at two urban areas in California while low ionic ratios were found in China.[14,66] The difference in ratio values was attributed to China burning coal for energy and Southern California using other means for electricity generation.[14,66] Both urban areas had the commonality of a large automobile presence.[14] In comparison, nuclear energy and coal burning were the top two electricity generation methods in Illinois during 2010–2012.[67-69] Chicago also has a large motor vehicle presence. Our nitrate to sulfate ion ratios were less than both of the other urban studies,[14,66] possibly due to the combination of energy generation sources as well as variability in pollution sources and meteorology between all cities mentioned.

Chloride, calcium, magnesium, phosphate, and potassium ion concentrations were low, compared to those of sulfate and nitrate. Average chloride concentrations ranged from 0.106 to 0.494 μg m^{-3}. Common sources of chloride aerosols are sea-spray and road salt. In areas like Chicago, far away from marine sources, coal burning and road dust comprise the largest chloride sources. Variability in the concentration of calcium may be due to insolubility of species, such as for calcium silicates or calcium carbonate. As a crustal material, limestone quarrying and cement kilns were found to be possible sources of calcium released into the Chicago atmosphere.[12] Construction on the Loyola University Chicago campus, including ground excavation and brick and cement work, increased the amount of observed dust near the sampling location during summer 2012. This likely contributed to an elevated calcium ion concentration average (3.042 μg m^{-3}) in 2012, compared to summer 2010 (0.829 μg m^{-3}) and 2011 (0.929 μg m^{-3}) averages. Potassium, magnesium, and calcium ion sources include direct emission into the atmosphere and an earlier Chicago study found local contributing sources to be coal burning, soil, refinery, and other industrial activity.[65] Soluble phosphate varied from 0.718 to 2.617 μg m^{-3} in summers 2010, 2011, and 2012. Phosphate had the highest blank filter concentration variability in comparison to the rest of the ions, which likely influenced its overall ion concentrations in samples. Biomass burning, erosion, and using phosphate based fertilizer all contribute to airborne phosphate aerosol.

Daily formate concentrations ranged from 0.013 to 5.379 μg m^{-3}, while acetate and oxalate varied from 0.027 to 4.108 μg m^{-3} and 0.033 to 1.280 μg m^{-3}, respectively. Studies have shown that up to 60% of aerosol material could include low molecular

weight organic acids.[70] In our study, organic acid anions made up between 5 and 15% of the overall total aerosol composition. Several studies used the ratio of formate to acetate to determine whether atmospheric presence was from a direct source (ratio less than one) or in situ photochemical formation (ratio greater than one).[13,61,71-72] Formate to acetate average ratios in summers 2010–2012 are shown in Table 5. During summers 2010 and 2011, overall (segment A and B data combined) average formate to acetate ratios were 1.385 and 1.381, respectively. Most 2010 and 2011 segment A and B ratio values were less than one, indicating direct emissions played a larger role than secondary formation. However, on several days, ratios were much larger than one (max. 4.367) thus affecting the overall average. A Grubb's Test determined none of the ion ratios were removable as outliers. Thus, overall summer 2010, 2011 ionic ratio averages were greater than one so photochemical production played a larger role in formate and acetate concentrations than direct emissions. Conversely, in summer 2012 the average formate to acetate ion ratio (0.198) suggested direct emissions played a larger role in the atmospheric presence of the organic acid anions than oxidative pathways due to photochemistry. During all summers, the ratio value increased from segment A to B on most collection days, indicating either higher formate or lower acetate concentrations were present later in the day. Khwaja (1995) stated that motor exhaust increased the fraction of acetic acid in the atmosphere while vegetation emissions increased formic acid.

In addition, other studies used Pearson correlations between organic acid anions and temperature or ozone to provide evidence that photochemical activity was the source of the organic acid ions.[13,71] In our study, neither a correlation between formate and

temperature nor acetate and temperature were found. Low, negative correlations between acetate and ozone as well as formate and ozone suggested photochemical activity was not a main source in the local Chicago atmosphere. While lack of Pearson correlations supports ionic ratio results indicating direct emissions played a larger role in local formate and acetate concentrations during summer 2012 pollution, the Pearson correlations, or lack thereof, contradict the summer 2010, 2011 ratio values. More emphasis should be placed on the ionic ratio values as lack of Pearson correlation only signifies that no linear relationships were present. Based on the raw data, both photochemical and direct emissions played a role in the presence of formate and acetate during our studies. Other factors must also be considered including the presence of precursor chemical species to organic acids.

With respect to trace gas mixing ratios, yearly ozone and nitrogen oxides did not fluctuate as greatly in comparison to aerosols. Mixing ratios of nitrogen oxides typically peaked during segment A collections due to heavy traffic emissions between 0700 and 0900 LT. This was also observed in summer 2002–2004 studies.[38-40] Average segment A mixing ratios of nitrogen oxides in summers 2010–2012 were 19.7, 15.0, and 22.4 parts per billion (ppb), respectively, while B segment averages ranged from 8.1 to 11.0 ppb. On a typical summer day with light winds and little cloud cover, ozone mixing ratios showed a diurnal pattern with morning lows and highs in the early afternoon hours.[38-40] Average ozone mixing ratios in segment A collection ranged from 29.2 to 38.5 ppb and from 47.6 to 67.0 ppb in segment B collections. Figure 10a depicts a typical diurnal pattern of trace gas mixing ratios commonly observed in local measurements, while

Figure 10b depicts average mixing ratios over all three summers. Ozone mixing ratios increased from summers 2010–2012; this trend was also observed in Illinois' statewide monitoring of ozone.[73,74] Local nitrogen oxides decreased from summer 2010 to 2011, then increased in summer 2012 (Figure 10b). Statewide Illinois monitoring site data showed that nitrogen dioxide mixing ratios decreased between summers 2010–2012.[73,74] It is unclear why our data showed an increase in nitrogen oxides from summers 2011 and 2012, but local sources such as construction vehicles might have played a role. The location of the sampling site near a main roadway potentially influenced this as well.

a)

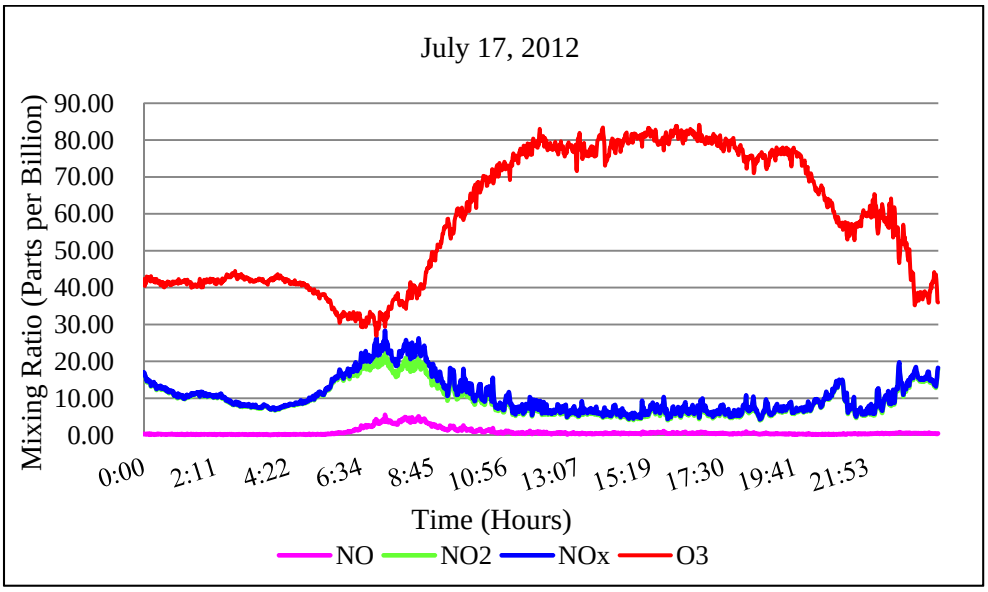

b)

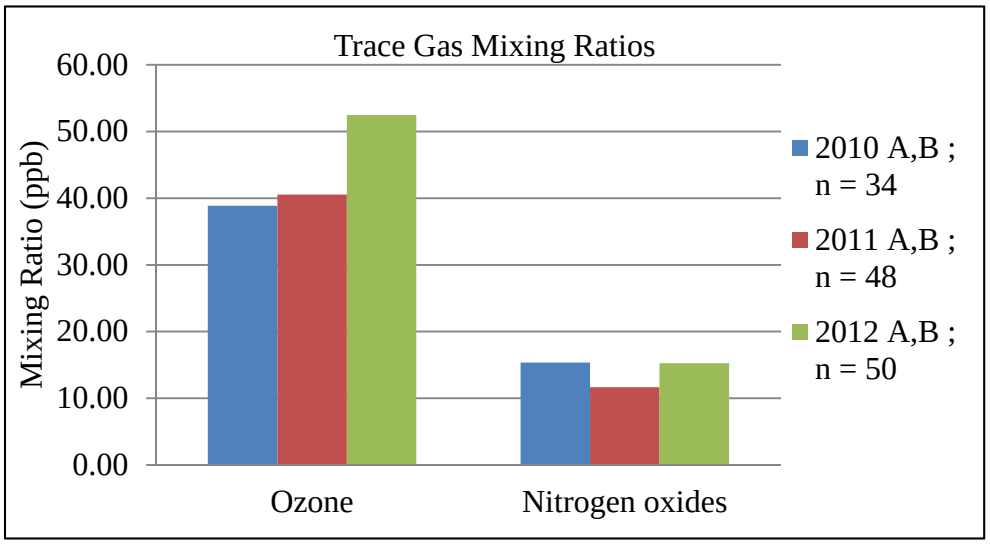

Figure 10. a) Time series of ozone and nitrogen oxide mixing ratios recorded on July 17, 2012 and b) average trace gas mixing ratios during each summer study.

Meteorology

Variability of recorded wind direction during both A and B aerosol sampling segments for all 66-collection days is displayed in Figure 11. A general wind rose to reference cardinal and inter-cardinal direction has been provided (Figure 11a). Each summer had a slightly different dominant wind direction profile, which is presented in

Figure 11b. Westerly winds were the most dominant originating wind direction in summer 2010, followed by northeasterly through southeasterly degrees. In summer 2011, northerly winds were the most frequently recorded, while northeasterly/easterly winds followed in frequency. Southwesterly and southeasterly winds were the most commonly observed direction of wind in summer 2012. Variability of wind speed and corresponding wind direction is shown in Figure 11c. The strongest winds were recorded when originating from a westerly direction, shown in the green shaded area (8.8–11.0 m s^{-1}). Wind speeds were higher in the westerly direction (green and blue) overall compared to the northerly and southeasterly direction with had more red shaded area (3.6–5.7 m s^{-1}).

a)

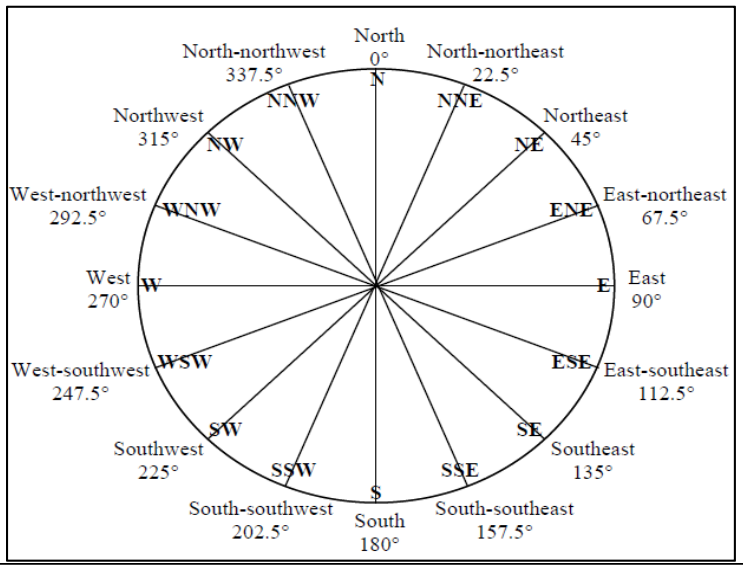

b)

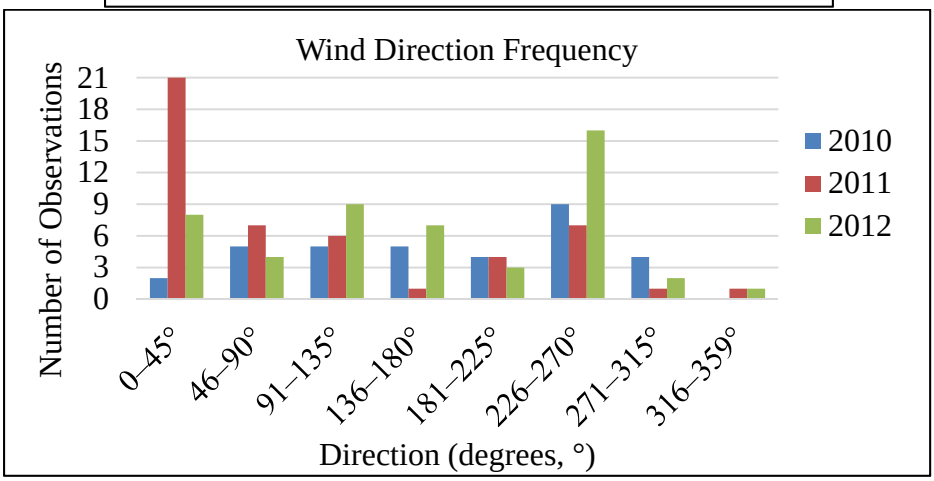

c)

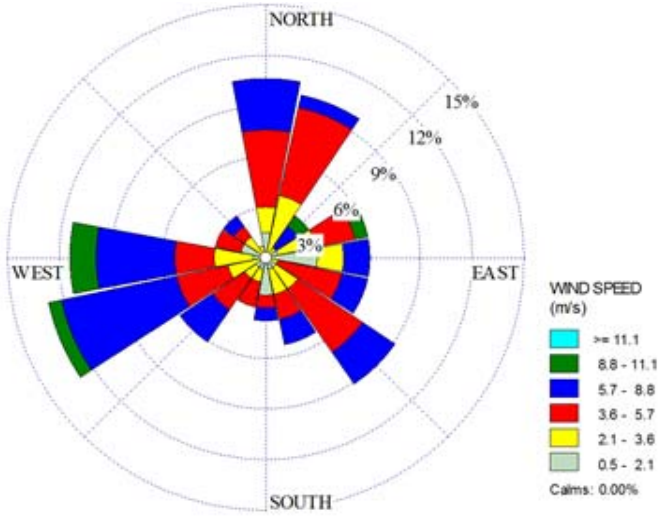

Figure 11. a) Wind rose of cardinal and inter-cardinal directions, b) frequency of wind direction, and c) wind speed variability for segments A and B on all 66-collection days.

Temperature, wind speed, and humidity averages were not highly variable (Table 8) between summer studies. There were no identifiable extremes, although summer 2011 was cooler temperature wise in comparison to 2010 and 2012 and had higher observed humidity. Summer 2012 had the most days when recorded temperatures reached or exceeded 30 °C during segment A and B sampling in comparison to summers 2010 and 2011.

Table 8. Descriptive statistics for recorded meteorology during all summer studies.

	2010		2011		2012	
	Min, Max	A, B_{avg}	Min, Max	A, B_{avg}	Min, Max	A, B_{avg}
Temperature (°C)	21.6, 31.4	25.7	18.9, 33.8	24.6	21.3, 35.4	26.5
Wind speed (m s^{-1})	0.5, 10.0	3.8	0.7, 11.0	4.8	1.1, 9.8	4.8
Humidity (%)	30, 86	68	52, 95	77	39, 90	66

Correlation Matrix of Air Pollutant and Meteorological Variables

Correlation matrices are useful to uncover univariate relationships. A correlation matrix (Table 9) was generated using Minitab® 16 Statistical Software (Minitab, Inc., State College, PA, USA 2010) to determine univariate relationships between air pollutants and meteorology during all 3-summer studies' combined data. Multivariate relationships between pollutants and meteorology are discussed in Chapters IV and V.

Potassium and nitrate had a moderate, positive correlation (0.326), which may be attributed to biomass burning.[76,77] Potassium may also result from coal burning. Other univariate pollutant-pollutant relationships included calcium and magnesium (0.539), indicating the same local primary source which could include road dust, soil, cement kilns, and quarrying.[12] Calcium is also correlated to nitrate (0.353) and ozone (0.452), however, these relationships are likely due to similar meteorological transport and not atmospheric chemistry as ozone and nitrate are secondary pollutants while calcium is a

primary pollutant. Acetate is correlated with formate (0.623), phosphate (0.620), and oxalate (0.388), indicating these ions may have originated from similar local sources. Formate is correlated with phosphate (0.409) and to oxalate (0.388). Phosphate and oxalate are also correlated (0.301). Particulate phosphorus is released into the atmosphere in soil derived dust and due to industrial and agricultural activity. Therefore, the correlation of phosphate to all of the organic acid anions may not be chemical but rather meteorological based. The correlation between chloride and sulfate (0.510) as well as chloride and oxalate (0.375) is indicative of a vehicular source of the ions.[77] Nitrate is correlated with sulfate (0.403), ozone (0.508), and temperature (0.412). Sulfate is correlated with oxalate (0.399) but not to any meteorology unlike in an earlier study of sulfate in Chicago.[78] Ozone is anti-correlated with nitrogen oxides (-0.432) and humidity (-0.342) but is positively correlated with temperature (0.587). This is expected as tropospheric ozone production is dependent on solar intensity and low humidity. Nitrogen oxides are destroyed in ozone production (see reactions 1–3).[8] Temperature is used as a proxy in place of solar intensity when solar intensity data is not available. Nitrogen oxides and wind direction are correlated (0.441), indicating NO_x emission sources to the south and west while to the north and east of the sampling site no major sources appear to be present. A more in depth discussion of relationships between air pollutants and meteorology is carried out in Chapters IV and V through multivariate statistical analyses as univariate relationships, while important, do not realistically portray multi-interaction of chemical species with subsequent meteorological changes.

Table 9. Correlation matrix of air pollution and meteorological variables. *K* potassium, *Mg* magnesium, *Ca* calcium, *Ac* acetate, *Fo* formate, *Cl* chloride, *P* phosphate, *N* nitrate, *S* sulfate, *Ox* oxalate, O_3 ozone, NO_x nitrogen oxides, *Sp* wind speed, *T* temperature, *D* wind direction, *H* humidity. Values greater than or equal to $\pm$ 0.300 are highlighted in bold.

	K	Mg	Ca	Ac	Fo	Cl	P	N	S	Ox	O_3	NO_x	Sp	T	D
Mg	-0.070														
Ca	0.222	**0.539**													
Ac	0.019	0.139	-0.285												
Fo	-0.158	0.123	**-0.355**	**0.623**											
Cl	-0.102	0.016	-0.208	0.185	0.201										
P	-0.126	0.129	-0.079	**0.620**	**0.409**	0.216									
N	**0.326**	0.139	**0.353**	-0.110	-0.236	0.222	-0.136								
S	-0.065	0.029	-0.095	0.153	0.128	**0.510**	0.112	**0.403**							
Ox	-0.035	-0.081	-0.017	**0.388**	**0.417**	**0.375**	**0.301**	0.180	**0.399**						
O_3	0.091	0.071	**0.452**	-0.225	**-0.300**	-0.230	-0.239	**0.508**	-0.109	-0.034					
NO_x	0.059	0.299	0.052	0.015	0.007	0.245	0.035	0.197	0.262	0.012	**-0.432**				
Sp	-0.012	-0.235	-0.040	-0.184	-0.043	-0.233	-0.063	-0.030	-0.095	-0.157	0.198	-0.172			
T	0.001	0.133	**0.453**	-0.022	-0.019	-0.076	-0.160	**0.412**	0.048	0.200	**0.587**	0.029	0.206		
D	0.036	0.158	0.282	0.083	0.026	-0.028	-0.016	0.224	0.128	0.251	0.009	**0.441**	0.106	**0.530**	
H	-0.029	-0.092	**-0.322**	0.076	0.161	0.155	0.283	-0.257	0.045	-0.182	**-0.342**	-0.071	-0.051	**-0.587**	**-0.446**

Pollution Plots

Pollution plots, graphically representing air pollutant concentrations based on wind direction recorded during sampling, were separately generated for all ions and trace gases (Figure 12) to determine if a trend in air pollutant concentration based on wind direction was present. Pearson correlations indicated there was a linear relationship between nitrogen oxides and wind direction but the other pollutants were not correlated with wind direction. The pollution plots allowed for visual analysis of a frequency of higher air pollution concentrations in a specific range of wind direction or lack thereof. While several observations in the acetate and formate pollution plots (Figure 12a,b) in the westerly direction showed higher concentrations compared to the other observations, overall there is no apparent directional dependence. Chloride ions did not show elevated concentrations (Figure 12c) in a specific wind direction and the same was found for phosphate ion concentrations (Figure 12d). Nitrate and sulfate ions both exhibited some dependence on wind direction, as the pollution plots (Figure 12e,f) showed several elevated concentrations of both ions occurred when the wind direction was southeasterly. Oxalate, potassium, and magnesium ions' pollution plots also revealed there was little to no dependence of their concentrations on wind direction (Figure 12g-i). For calcium, several observations showed higher concentrations clustered in the westerly and southerly direction, but no clear trend was noticeable (Figure 12j). Nitrogen oxide mixing ratio were clearly dependent on wind currents as most of the observations in the westerly and southerly direction had higher concentrations than other wind directions (Figure 12k). There was no clear dependence of ozone mixing ratios on wind direction (Figure 12l).

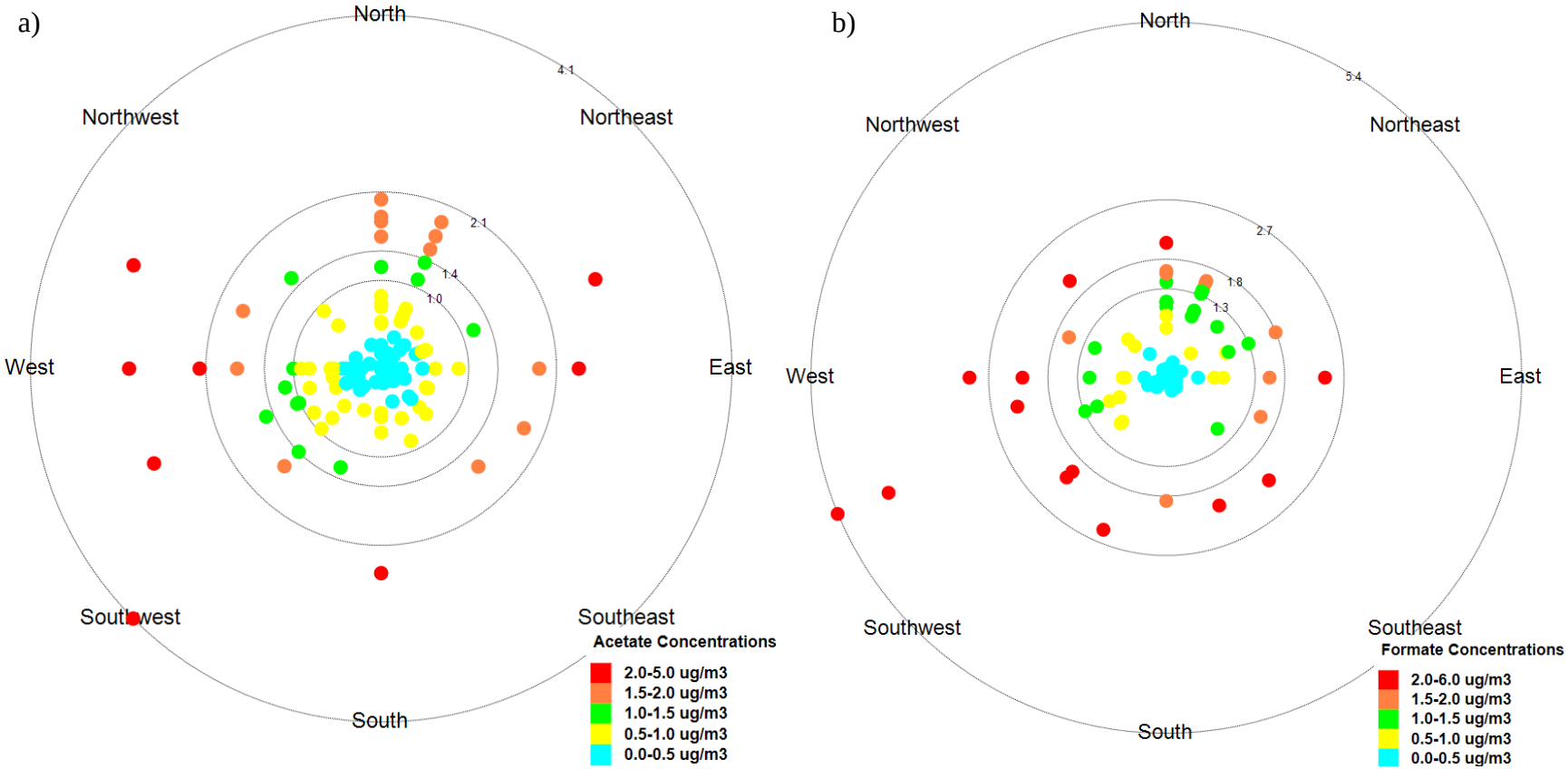
a)
North
Northwest
Northeast
West
East
Southwest
Southeast
South
4·1
2·1
1·4
1·0
Acetate Concentrations
2.0-5.0 ug/m3
1.5-2.0 ug/m3
1.0-1.5 ug/m3
0.5-1.0 ug/m3
0.0-0.5 ug/m3
b)
North
Northwest
Northeast
West
East
Southwest
Southeast
South
5·4
2·7
1·8
1·3
Formate Concentrations
2.0-6.0 ug/m3
1.5-2.0 ug/m3
1.0-1.5 ug/m3
0.5-1.0 ug/m3
0.0-0.5 ug/m3

c)

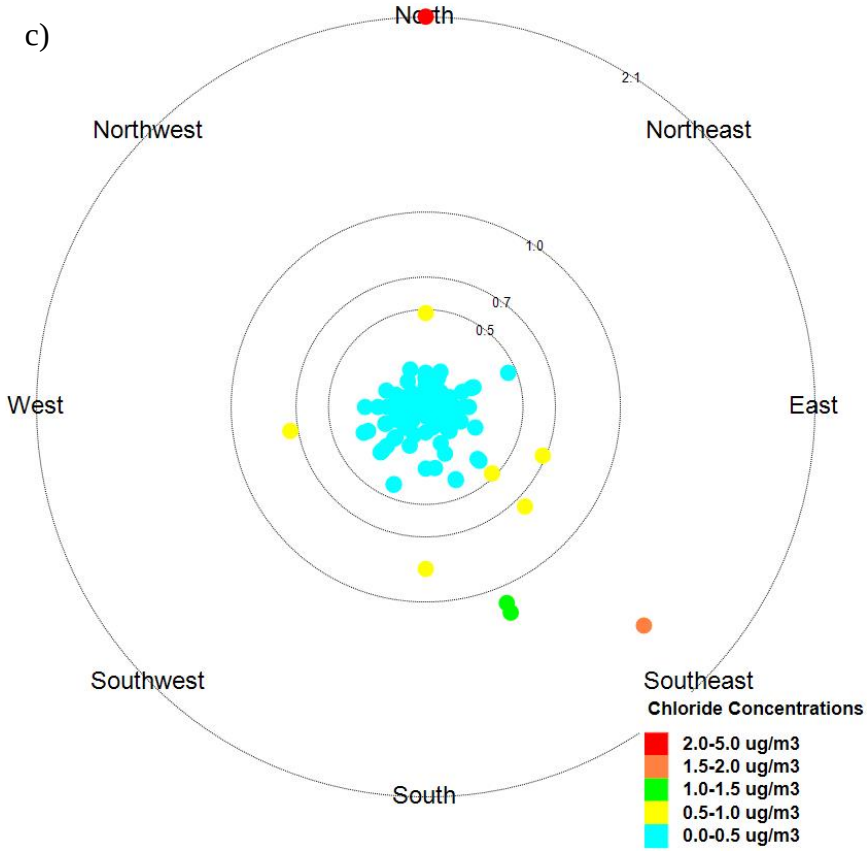
North
Northeast
East
Southeast
South
Southwest
West
Northwest
2.1
1.0
0.7
0.5
Chloride Concentrations
2.0-5.0 ug/m3
1.5-2.0 ug/m3
1.0-1.5 ug/m3
0.5-1.0 ug/m3
0.0-0.5 ug/m3

d)

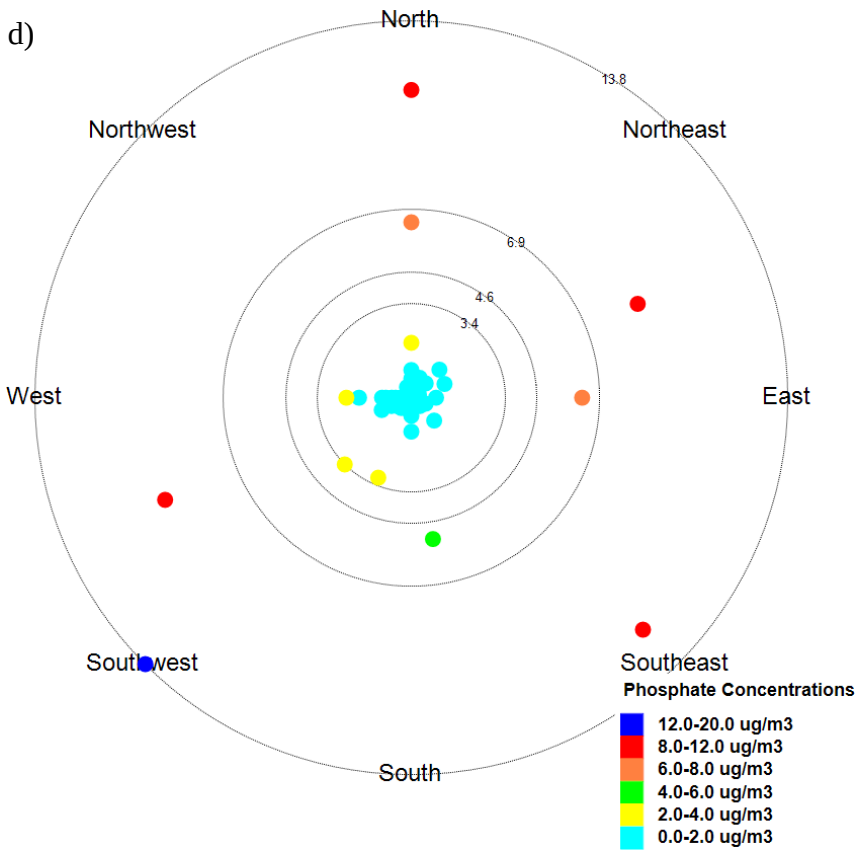
North
Northeast
East
Southeast
South
Southwest
West
Northwest
13.8
6.9
4.6
3.4
Phosphate Concentrations
12.0-20.0 ug/m3
8.0-12.0 ug/m3
6.0-8.0 ug/m3
4.0-6.0 ug/m3
2.0-4.0 ug/m3
0.0-2.0 ug/m3

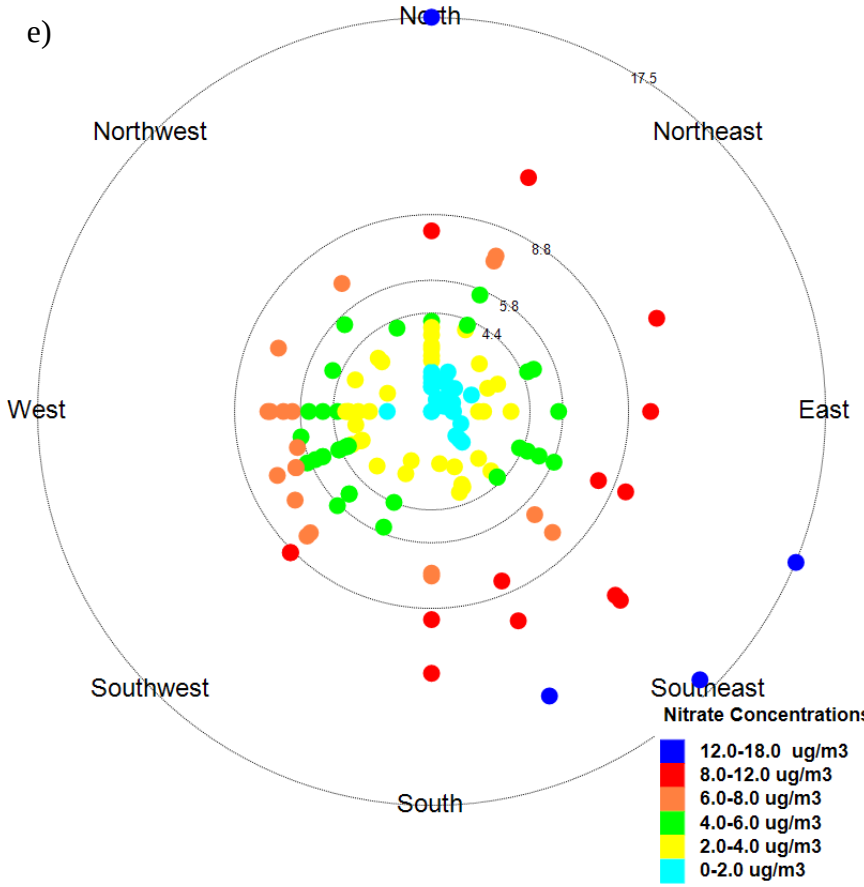
e)
North
Northwest
Northeast
West
East
Southwest
Southeast
South
17.5
8.8
5.8
4.4
Nitrate Concentrations
12.0-18.0 ug/m3
8.0-12.0 ug/m3
6.0-8.0 ug/m3
4.0-6.0 ug/m3
2.0-4.0 ug/m3
0-2.0 ug/m3

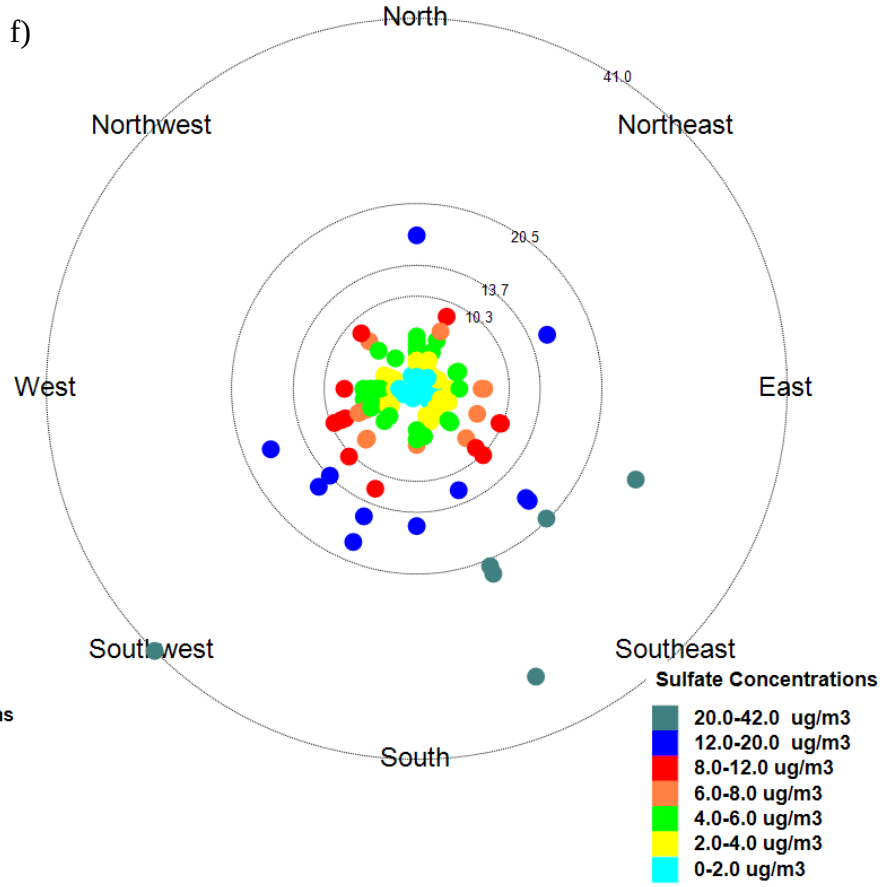
f)
North
Northwest
Northeast
West
East
Southwest
Southeast
South
41.0
20.5
13.7
10.3
Sulfate Concentrations
20.0-42.0 ug/m3
12.0-20.0 ug/m3
8.0-12.0 ug/m3
6.0-8.0 ug/m3
4.0-6.0 ug/m3
2.0-4.0 ug/m3
0-2.0 ug/m3

g)

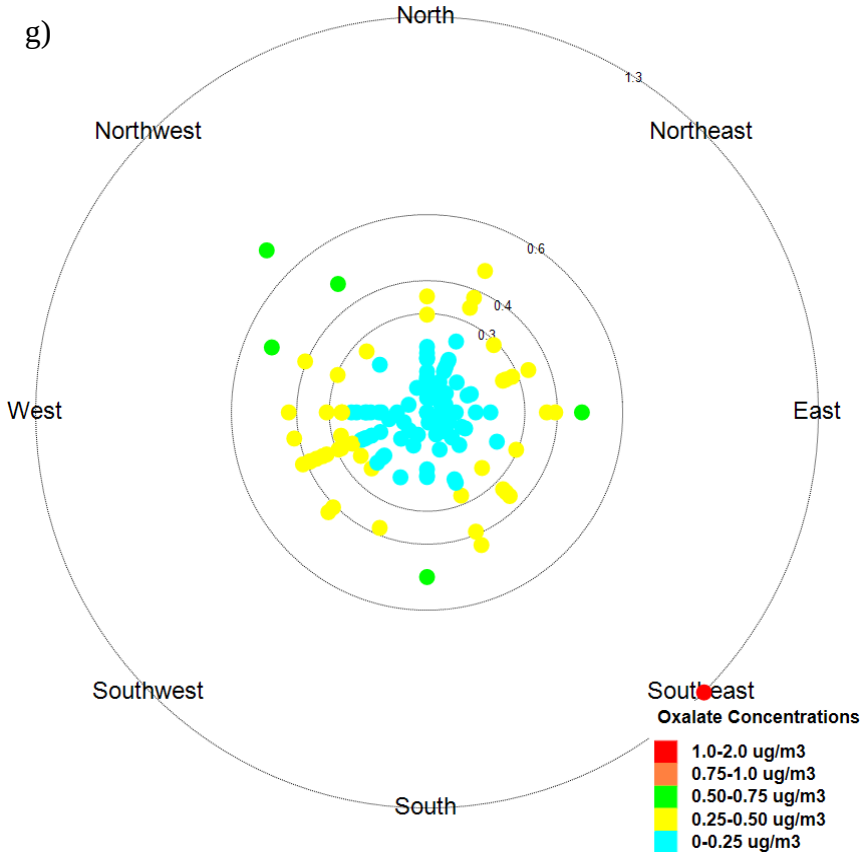
North
Northeast
East
Southeast
South
Southwest
West
Northwest
1·3
0·6
0·4
0·3
Oxalate Concentrations
1.0-2.0 ug/m3
0.75-1.0 ug/m3
0.50-0.75 ug/m3
0.25-0.50 ug/m3
0-0.25 ug/m3

h)

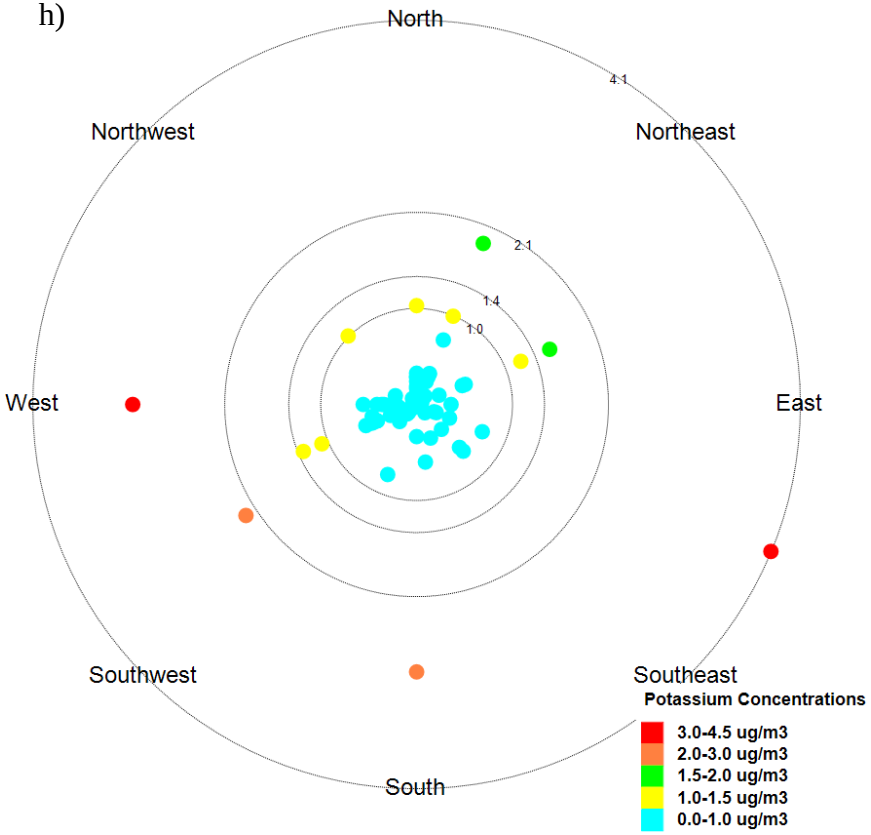
North
Northeast
East
Southeast
South
Southwest
West
Northwest
4·1
2·1
1·4
1·0
Potassium Concentrations
3.0-4.5 ug/m3
2.0-3.0 ug/m3
1.5-2.0 ug/m3
1.0-1.5 ug/m3
0.0-1.0 ug/m3

i)

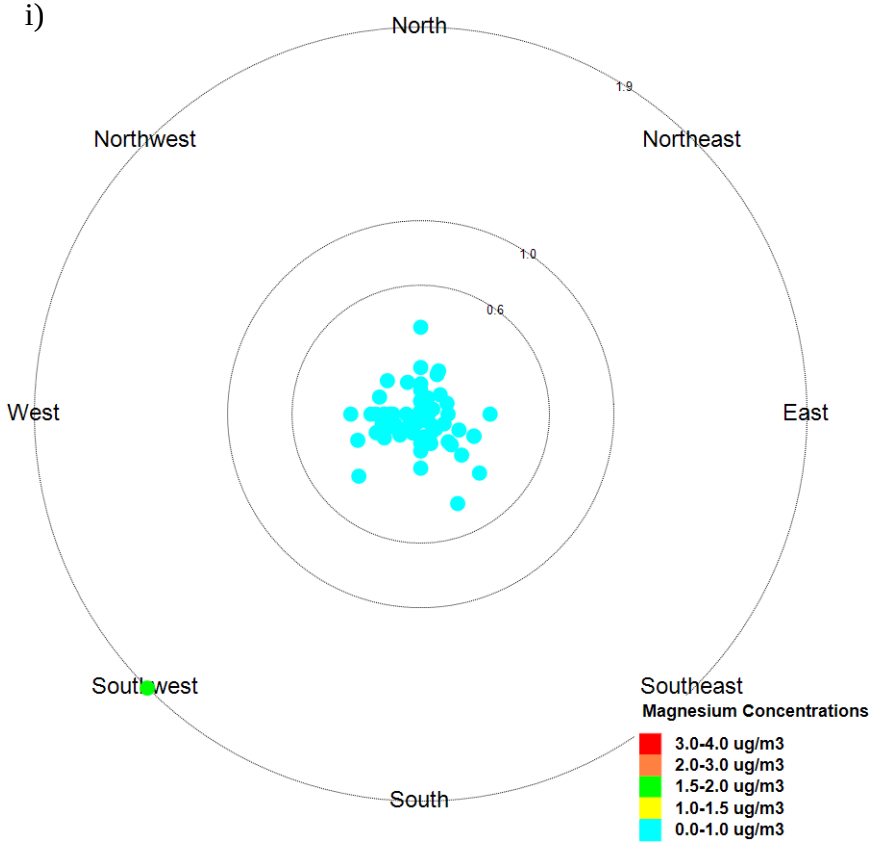
North
Northwest
Northeast
West
East
Southwest
Southeast
South
1.9
1.0
0.6
Magnesium Concentrations
3.0-4.0 ug/m3
2.0-3.0 ug/m3
1.5-2.0 ug/m3
1.0-1.5 ug/m3
0.0-1.0 ug/m3

j)

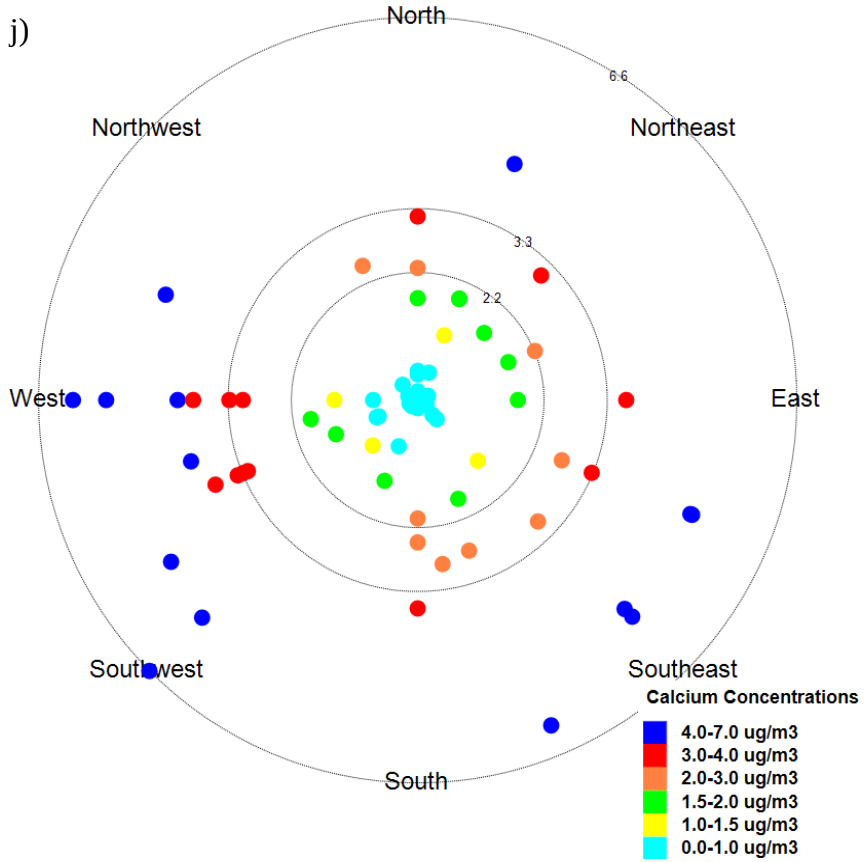
North
Northwest
Northeast
West
East
Southwest
Southeast
South
6.6
3.3
2.2
Calcium Concentrations
4.0-7.0 ug/m3
3.0-4.0 ug/m3
2.0-3.0 ug/m3
1.5-2.0 ug/m3
1.0-1.5 ug/m3
0.0-1.0 ug/m3

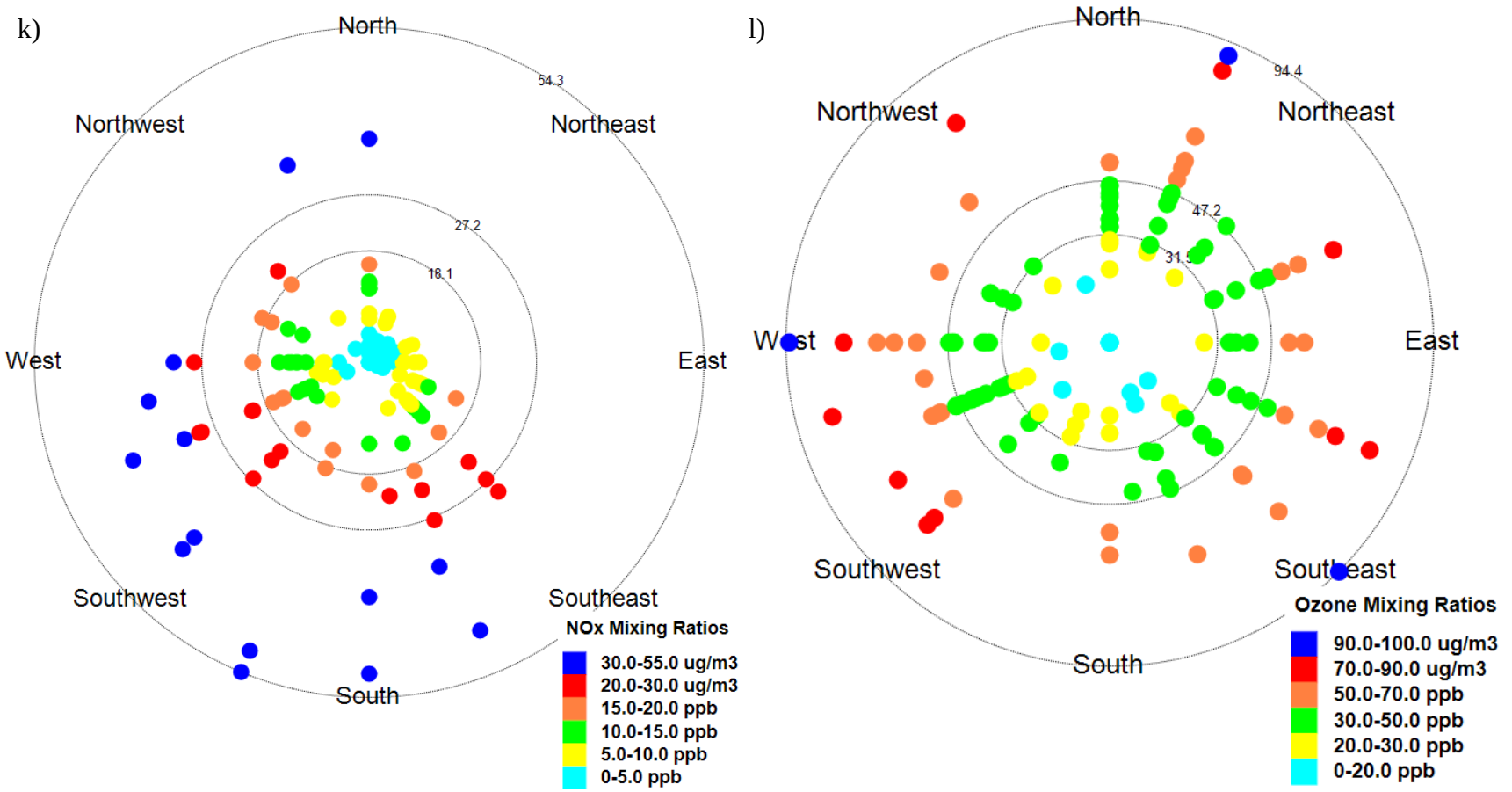

Figure 12. Pollution plots of ionic and trace gas pollutants quantified in summers 2010–2012; both segment A and B data included for a) acetate, b) formate, c) chloride, d) phosphate, e) nitrate, f) sulfate, g) oxalate, h) potassium, i) magnesium, j) calcium, k) nitrogen oxides, and l) ozone.

Summer 2002–2004 versus Summer 2010–2012 Data

A 57-day study was completed at the sampling site at Loyola University during summers 2002–2004.[38-40] Percent change between both three-summer sampling periods was calculated for all pollutant and meteorological variables to gauge pollution changes from period 2002–2004 to period 2010–2012. In the following equation, [X] refers to the three-year cumulative average of a variable.

$$\% \text{ change} = \frac{[X] \text{ in } 2010–2012 \; – \; [X] \text{ in } 2002–2004}{[X] \text{ in } 2002–2004} \times 100$$

Average mixing ratios of nitrogen oxides (-49.0%) decreased and an increase in ozone mixing ratios (18.2%) was found. The observed decline in nitrogen oxides and increase in ozone is also supported by the 2012 Illinois Environmental Protection Agency Annual Air Quality Report. Reported was a decrease in nitrogen oxides measured at statewide monitoring sites and an overall decline in industrial NO_x emissions.[73,74] Statewide ozone mixing ratios have varied from 2002 to 2011 for 1-hour maxima and 8-hour ozone values, showing an initial decline for 2002 to 2004, variability in 2005–2009, and then an increase from 2009 to 2011.[73,74] Local three-year average temperatures rose from 22.7 °C in summers 2002–2004 to 25.6 °C in 2010–2012, an increase of 12.6%. Relative humidity also increased by 16.4%, from an average of 61% in summers 2002–2004 to 71% in summers 2010–2012. Average wind speed decreased by roughly 14% in summers 2010–2012 compared to the earlier study. Observed warmer temperatures (a proxy for solar intensity) in summers 2010–2012 likely contributed to elevated ozone levels. A lack of air mass mixing and transport of air pollution due to lower wind speeds possibly allowed ozone and other secondary pollutants to accumulate in the area instead

of being transported elsewhere. In summers 2002 and 2003, southwesterly winds were the most dominant direction while in summer 2004 westerly winds were most frequently reported. These are different wind profiles compared to the summer 2010–2012 study.

Calcium (171.1%), magnesium (34.7%), potassium (11.0%), nitrate (7.7%), phosphate (14.1%), and oxalate (53.3%) ion concentrations increased from summers 2002–2004 to 2010–2012. In contrast, sulfate concentrations decreased by 5.2%. With respect to gaseous sulfur dioxide emissions in Illinois an overall decrease was reported.[73,74] The decrease in statewide emissions may explain lower sulfate in aerosols in the most recent study. Less transport of regional sulfate to the area may also be a factor, as wind speeds were lower and wind direction regimes were different in the recent air studies. Similar to sulfate, lower average concentrations of chloride were measured in summers 2010–2012 (0.223 μg m^{-3}) than in 2002–2004 (0.304 μg m^{-3}), a 26.8% decrease.

Illinois was one of 27 states grouped into the 2005 USEPA Clean Air Interstate Rule (CAIR), addressing pollution migration over state lines. It required drastic cuts of power plant sulfur dioxide and nitrogen oxides emissions using either a cap and trade system or other methods devised by states individually. CAIR was replaced by CSAPR (Cross-State Air Pollution Rule) by the USEPA in 2011, which set a pollution limit for each state and established new allowances on emissions (USEPA Office of Air and Radiation, 2013). The observed decrease in nitrogen oxides in the multi-summer studies completed at Loyola University Chicago may be a result of the implementation of CAIR and CSAPR. Similarly, less sulfate, of which sulfur dioxide is a precursor, also may be a result of these regulations.

Day Classifications

All 66 air pollution sampling days during the summers of 2010, 2011, and 2012 were classified as either a reference, lake breeze, or variable day, depending on the dominant wind direction recorded during segment A and B aerosol sample collections. Defined criteria for each type of classification day is displayed in Table 10. Based on the classification guidelines, there were a total of 37 reference, 13 lake breeze, and 16 variable days. The frequency of classification days per summer is shown in Table 11. The classification of collection days streamlined data processing and analyses to facilitate comparison of pollutants on non-lake breeze [reference] and lake breeze days. Variable days are not discussed as the large variability of wind direction on these days did not reveal any pattern in pollutants, which made it unsuccessful to assess pollution data.

Table 10. Classification criteria for reference, lake breeze, and variable days.

Reference Day	Lake Breeze Day	Variable Day
Steady wind direction throughout A and B segment collections	Wind direction changes from an initial degree to northeasterly to southeasterly (minimum of 70° shift from initial direction)	More than one wind direction during A and B collections, sporadic and inconsistent

Table 11. Frequency of reference, lake breeze, and variable days each summer.

Collection Year	2010	2011	2012	Total
Reference day	12	14	11	37
Lake breeze day	2	5	6	13
Variable day	3	5	8	16
Number of collection days	17	24	25	66

Reference Day Wind Direction

The reference day category included days where a steady degree of wind was recorded during both A, B segmented collections. Most of the collection days throughout each summer were identified as reference days. While wind direction on a particular day

remained steady, reference days varied between each other with respect to wind direction (Figure 13). Southwesterly winds dominated reference days in summer 2010; southeasterly & northerly winds were also frequently recorded. In summer 2011, northerly winds were the most frequently recorded on reference days, followed by southeasterly winds. Westerly winds predominated during reference days in summer 2012, while northerly and southerly winds were also recorded.

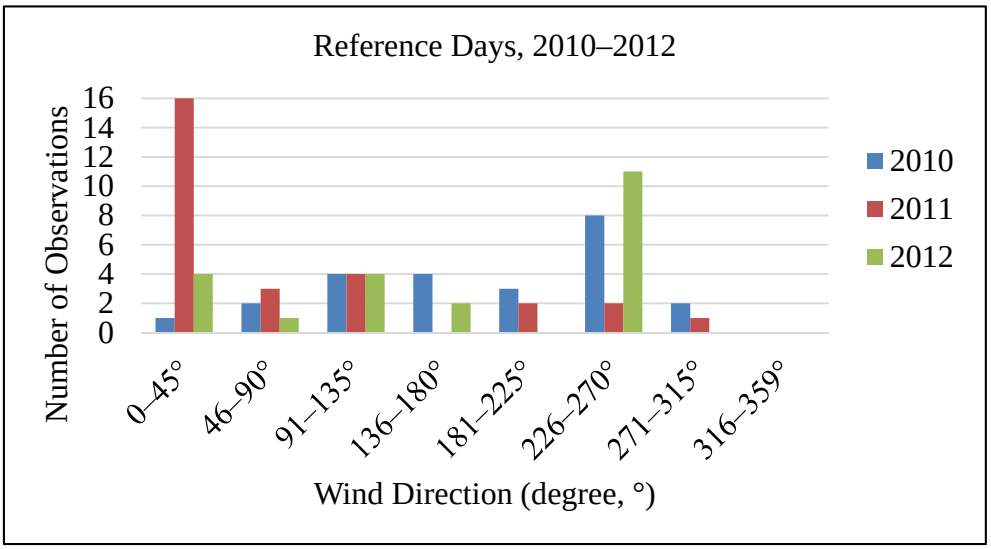

Figure 13. Graph of wind direction frequency each year for only reference days; both A and B segment data for 37 reference days.

Lake Breeze Onset Variability

A local lake breeze was observed on 13 of the 66 collection days. A lake breeze was characterized by an initial observance of consistent offshore winds, followed by a minimum of 70° shift in winds towards an onshore, easterly direction. The onshore wind then remained steady in an easterly direction. Approximately 20% of all summer 2010–2012 collection days had an observed lake breeze. This value is consistent with what was observed in summer 2002–2004 studies at the same location, as well as in other Chicago

lake breeze research.[22,38-40] Not all lake breezes were equal with respect to the onset time of its circulation, its strength, and the effect on measured aerosol concentrations. Lake breeze onset was defined as the initial time when recorded winds had shifted to an onshore, easterly direction. The occurrence of lake breeze onsets based on recorded time that the wind direction changed to easterly is displayed in Figure 14.

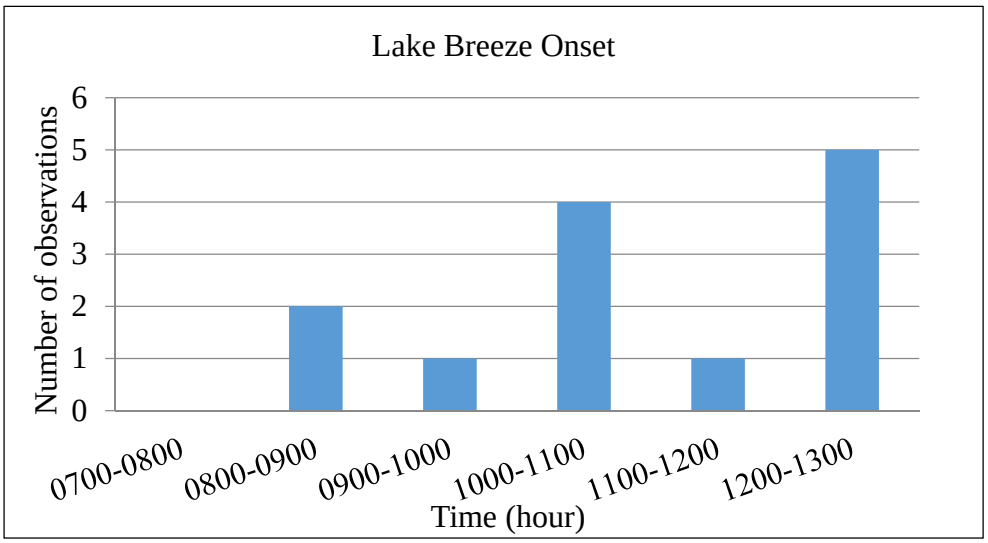

Figure 14. Variability of local lake breeze onset during summers 2010–2012, grouped into hourly periods.

The most common periods when a lake breeze onset was observed were between the hours of 1000 and 1100 LT and also between 1200 and 1300 LT. Roughly one-third of the lake breezes had an observed onset between 1000 and 1100 LT. Five lake breezes began in the early afternoon between 1200 and 1300 LT, during segment B aerosol collections. Upon reviewing meteorological conditions (Table 12) on all 13 lake breeze days it was found that the shift to easterly winds occurred early to mid-morning when segment A temperatures were between 24 and 26 °C. In comparison, on days when a lake breeze developed around noontime or later, recorded early to mid-morning temperatures

in segment A were around 30 °C. Furthermore, higher wind speeds were recorded on days when a lake breeze onset occurred later in the day. Prior to a lake breeze onset, on days when the breeze happened in the early afternoon, segment A wind speed varied from 4.7 to 7.9 m s^{-1}. This is considerably higher than wind speeds recorded during segment A collections on days with earlier lake breeze onsets (1.7–2.8 m s^{-1}). Higher winds may have delayed the development of the temperature gradient needed for lake breeze circulation, thus causing a later observed onset of the local lake breeze. Additionally, warmer air temperatures in segment A contributed to a delay in the temperature differential between land and lake. Air mass mixing due to higher winds may have delayed air above the lake to cool and air above land to warm.

Table 12. Lake breeze day meteorology averages during segment A collections.

Date of Lake Breeze	Onset Time (LT)	Temperature (°C)	Direction (°)	Speed (m s^{-1})	Humidity (%)
July 13, 2010	1050–1150	24.1	135	2.1	75
July 21, 2010	1030–1100	26.9	292.5	1.4	68
July 5, 2011	1000–1100	25.3	270	2.7	52
July 6, 2011	0800–0900	24.5	0	1.7	68
July 11, 2011	0915–0930	24.3	270	1.8	85
July 21, 2011	1245–1300	30.3	247.5	7.9	68
August 1, 2011	1230–1300	27.0	247.5	4.7	80
July 3, 2012	1215–1245	27.4	247.5	7.8	57
July 5, 2012	1245–1300	30.7	247.5	3.3	56
July 9, 2012	0845–0900	23.8	337.5	2.1	65
July 13, 2012	1015–1030	27.2	225	2.5	57
August 2, 2012	1230–1245	24.8	247.5	6.2	61
August 3, 2012	1015–1030	26.8	180	1.3	74

Data in Table 12 was analyzed using an unpaired, two independent sample Student *t* test to determine if the onset time of a local lake breeze could be statistically attributed to segment A meteorology. All reported *p* values are one-tail unless otherwise specified as the focus was on differentiating whether the higher segment A temperature

and wind speeds observed when a lake breeze occurred later on a collection day were significant in terms of affecting circulation onset. Separate Student *t* tests were calculated for each meteorological parameter based on the following two scenarios:

Scenario 1) sample 1 = lake breeze data when onset occurred during 0700–1100 LT;
sample 2 = lake breeze data when onset occurred during 1100–1300 LT.

Scenario 2) sample 1 = lake breeze data when onset occurred during 0700–1200 LT;
sample 2 = lake breeze data when onset occurred during 1200–1300 LT.

In scenario 1, average segment A wind speed had a significant effect on lake breeze onset time, $t(5) = 3.43$, $p = 0.009$. Similarly, in scenario 2, there was a significant effect with respect to wind speed, $t(4) = 4.44$, $p = 0.006$. There was also a significant effect with respect to temperature, $t(6) = 2.22$, $p = 0.034$, in scenario 2. Wind direction and humidity segment A values were not statistically different at 95% confidence level in scenarios 1 and 2. To increase the sample size of the data pool, lake breeze data from summers 2002–2004 were added to the data set in Table 12 for a total of 34 days of lake breeze data. Student *t* tests were calculated with the larger set of data for the same two scenarios. There was a significant effect with respect to temperature for both scenario 1 [$t(13) = 2.76$, $p = 0.008$] and scenario 2 [$t(7) = 2.92$, $p = 0.011$]. There was also a significant effect with respect to wind speed for scenario 1 [$t(16) = 1.74$, $p = 0.050$] and scenario 2 [$t(8) = 2.65$, $p = 0.015$]. Neither humidity nor pre-lake breeze wind direction affected the onset time of a lake breeze significantly.

Reference versus Lake Breeze Day Pollution

One of the goals of this project was to evaluate whether the concentrations of secondary air pollutant species were elevated as a result of a lake breeze when compared to non-lake breeze, reference day pollution levels. Data for 37 reference days and 10 lake breeze days observed during summer 2010–2012 studies was evaluated using an unpaired, two independent sample Student *t* test. Reference days were the first independent sample group and lake breeze days collectively were the second set of sample data. Segment A data averages of air pollutant concentrations on the included days were used as pre-lake breeze or baseline levels of pollution. Three of the 13 lake breeze days were not included because the observed onset of breeze circulation occurred in segment A, so baseline comparison data pre-lake breeze was not available.

Table 13. Descriptive statistics of summer 2010–2012 ion concentrations (μg m^{-3}) and trace gases (ppb) separately for reference and lake breeze days.

Pollutant	Reference Days		Lake Breeze Days	
	A_{avg}	B_{avg}	A_{avg}	B_{avg}
Acetate	0.971	0.843	1.080	0.589
Formate	1.041	1.025	0.503	0.537
Chloride	0.327	0.165	0.162	0.156
Nitrate	3.786	5.252	4.818	8.173
Phosphate	2.714	0.935	0.366	0.452
Sulfate	8.524	5.680	6.222	6.685
Oxalate	0.263	0.230	0.265	0.281
Potassium	0.427	0.386	0.722	0.624
Magnesium	0.151	0.190	0.221	0.223
Calcium	1.897	2.639	2.544	2.683
Ozone	33.18	52.36	39.72	71.40
Nitrogen oxides	16.63	8.35	22.86	9.41

The null hypothesis, H_0, of the test was no difference in the average of reference and lake breeze pollution in segment B and any variability was due to chance. Thus, local pollution levels on reference and lake breeze days were the same and a lake breeze that

occurred in the sampling gap or in segment B did not induce changes in pollution concentrations. All reported *p* values are two-tail unless otherwise noted. A Student *t* test was calculated for the following two cases of data:

Case 1) Comparing average segment B concentrations of each pollutant on both lake breeze and reference days

Case 2) Comparing the average difference (B minus A) in the concentration between segment A and B collections of each pollutant on lake breeze and reference days.

The null hypothesis was rejected ($p < 0.05$) for nitrate and ozone in case 1. A significant effect in the average of segment B nitrate concentrations, $t(20) = 3.06$, $p = 0.006$, was found suggesting lake breeze circulation contributed to elevated nitrate concentrations. Similarly, average segment B ozone mixing ratios on lake breeze days compared to reference days were significantly different, $t(13) = 3.47$, $p = 0.004$. In case 2, the null hypothesis was rejected for chloride, nitrate, sulfate, and ozone. The large, positive average difference between segment A and B concentrations of both nitrate and ozone on lake breeze days was significant, $t(17) = 2.52$, $p = 0.022$ and $t(11) = 2.77$, $p = 0.018$, respectively. On reference days the average difference of sulfate concentrations was negative (mean, M = -2.84, standard deviation, SD = 7.36) but was positive on lake breeze days (M = 0.463, SD = 2.236), indicating average sulfate concentrations increased from segments A to B on lake breeze days and decreased on reference days. The lake breeze effect on sulfate was found to be statistically significant, $t(44) = 2.36$, $p = 0.023$. Furthermore, average chloride concentration on lake breeze days (M = -0.006, SD = 0.065) was statistically different than the reference day average (M = -0.162, SD =

0.403), t(42) = 2.25, $p = 0.030$. The null hypothesis could not be rejected for calcium, magnesium, potassium, acetate, formate, phosphate, or oxalate for either case 1 or 2.

Thus, the hypothesis that all secondary aerosol species would have elevated concentrations on lake breeze days due to recirculation of processed air masses is not fully supported by Student *t* test results. Sulfate, nitrate, and ozone concentrations were affected by a local lake breeze, based on summer 2010–2012 data. The remaining air pollutants were not significantly affected. The same Student *t* test scenarios were applied to data of the same pollutant species from 32 reference and 10 lake breeze days in summers 2002–2004. During those particular summers none of the pollutants for case 1 or 2 had significantly different concentrations.

Conclusion

As a result of completed air pollution studies during summers 2010–2012 several concluding remarks can be made. Overall, the trend in ionic pollutant averages from highest to lowest concentration was sulfate > nitrate > calcium > phosphate > formate > acetate > oxalate > chloride > potassium > magnesium. The bulk of aerosol material was inorganic. A majority of air sampling days were classified reference days, with consistent observed wind direction throughout segment A and B sampling periods. A lake breeze circulation was observed on 20% of the total number of sampling days. Utilizing a Student *t* test revealed that most air pollutants were not affected by lake breeze circulation in our summer studies. However, high-resolution segment A and B aerosol sampling effectively illustrated variability in local pollution concentrations during each day of collection.

While sulfate and nitrogen oxides' concentrations have declined since the summer 2002–2004 studies were completed, ozone, nitrate, chloride, calcium, magnesium, potassium, phosphate, and oxalate ions have increased. Reported statewide total PM_{10} emissions have declined in the past decade indicating local sources and regional transport of air pollutants may have played a larger role in pollution variability during summer 2010–2012 studies. The combined 6-summer study results showed similar trends with statewide reported data in the Illinois Environmental Protection Agency's Air Quality Reports for 2011 and 2012 with respect to nitrogen oxides and ozone. Pollution plots of summer 2010–2012 pollutants showed some air pollutants had higher concentrations when recorded wind direction was westerly or southerly during sampling. This is likely due to the concentrated industrial activity to the south and west of the sampling site, including the Northwest Indiana region.

CHAPTER IV

MULTIVARIATE STATISTICAL ANALYSIS CASE STUDY: APPLICATION TO SUMMER 2002–2004 AIR POLLUTION DATA

Overview

A case study was completed that explored the viability and robustness of applying two multivariate statistical methods, canonical correlation analysis (CCA) and principal component analysis (PCA), to the pollutant and meteorological data collected at Loyola University Chicago. The theory and description of each statistical method was explained in Chapter I. Aerosol, trace gas, and meteorological data from an initial pollution study completed in the summer months of 2002, 2003, and 2004 at the same sampling location was utilized in this case study. The purpose of statistical analysis was to determine the extent of existing underlying linear relationship(s), or lack thereof, between meteorological parameters and pollutant concentrations in addition to reducing original data dimensionality to assist in interpreting results for patterns or outliers. The advantage of both techniques is that associated relationships between multiple variables' interactions are uncovered. Results of the multivariate case study have been published.[50]

Description of Data Matrix

Fifty-five weekdays of aerosol, trace gas, and meteorological data were accumulated during summer 2002–2004 studies. The data included concentrations of ammonium, calcium, nitrate, sulfate, and oxalate ions, nitrogen oxides and ozone trace

gas mixing ratios, and four meteorological parameters: temperature, wind speed, wind direction, and humidity. All were included in the data matrix. Other ionic species were below detection limit or poorly resolved and therefore not included in statistical analyses. The final data set consisted of 110 observations and 11 variables. Since all of the variables' values in the original data had varying levels of resolution due to differing instrument sampling frequency, meteorological data and trace gas mixing ratios were averaged to match the timeframe of aerosol sampling segments A and B.

All variables were standardized by subtracting each variable's observed value by its respective average and then dividing by its standard deviation. Observations of included species with concentrations below detection limits were left blank in contrast to other studies published using multivariate statistical techniques which substituted detection limits or averages for missing data values prior to statistical application.[49,80,81]

The statistical program used for CCA was SAS® 9.2 Software (SAS Institute Inc, Cary, NC, USA 2008). The results of CCA presented in SAS® included testing significance of canonical functions as well as derived canonical weights, canonical loadings, and canonical scores for each canonical function. PCA was applied to data using Minitab® 16 Statistical Software (Minitab, Inc., State College, PA, USA 2010) and results included eigenvalues, eigenvectors, and principal component scores. Score plots for both CCA and PCA results were also generated using Minitab® 16 Statistical Software.

The original data, 110 observations of 11 variables (four meteorological parameters and seven air pollutants), was arranged in one data matrix (for PCA) and split into two data matrices (for CCA): the first containing concentrations (μg m^{-3}) of

measured air pollutants (ammonium – A, calcium – C, nitrate – N, sulfate – S, and oxalate – Ox, along with mixing ratios of ozone – O_3, and nitrogen oxides – NO_x) and the second containing observed meteorological parameters during air sampling (wind speed – Sp, temperature – T, wind direction – D, and humidity – H). Throughout the results section, the original variables may be denoted by the symbol associated with them as presented above. The meteorological parameters were considered predictor/independent variables and air pollutants were considered response/dependent variables.

Canonical Correlation Analysis

Canonical Variate Pairs

Four canonical functions were derived in CCA. The first three functions were statistically significant at the 0.05 level; therefore, the fourth canonical function was not reported since its interpretation would not add significant value. Linear combinations derived corresponding to meteorological parameters are denoted Met1, Met2, and Met3 whereas linear combinations corresponding to air pollutants are denoted A.Poll1, A.Poll2, and A.Poll3. The canonical correlation of each canonical function (Met no., A.Poll no.) as well as the canonical weights corresponding to respective air pollution and meteorology linear combinations are displayed in Table 14. Canonical weight values $\pm$ 0.300 were interpreted but other variables' weights below this threshold may also be mentioned to put a canonical function interpretation into context.

Table 14. Standardized canonical weights for air pollutant (A.Poll) and meteorological parameter (Met) canonical variables along with canonical correlations for each canonical variate pair (Met no., A.Poll no.).

Can. Function	Met1, A.Poll1	Met2, A.Poll2	Met3, A.Poll3
Can. Correlation	0.821	0.562	0.461
Wind speed	0.203	**0.552**	**-0.779**
Temperature	**0.901**	**0.369**	**0.582**
Wind direction	-0.297	-0.058	**0.618**
Humidity	-0.109	**0.900**	**0.486**
Ammonium	-0.112	**0.819**	**0.714**
Calcium	0.100	0.119	-0.273
Nitrate	-0.005	-0.127	**0.526**
Sulfate	0.035	-0.119	**-0.543**
Oxalate	0.226	0.201	**0.498**
O_3	**0.900**	**-0.835**	**-0.561**
NO_x	0.148	**-1.261**	0.100

The first canonical variate pair had a canonical correlation of 0.821, indicating that A.Poll1 and Met1 are highly correlated. Furthermore, 72.0% of the variance in A.Poll1 is explained by Met1. A.Poll1, the first air pollutant linear combination, is mostly influenced by ozone (0.900) and to a much lesser extent by oxalate (0.226) and nitrogen oxides (0.148). The canonical weights of the other variables in A.Poll1 are near zero. Temperature (0.901) is the dominant independent variable in the first linear combination, Met1, corresponding to weather parameters. Therefore, according to the first canonical variate pair the mixing ratio of ozone is positively correlated to temperature whereas nitrogen oxides mixing ratio has low correlation. Thus with rising temperature, ozone mixing ratios are increasing at a much larger rate as opposed to nitrogen oxide mixing ratios. It is well documented that ozone formation increases with temperature, mostly due to the photolytic destruction of nitrogen oxides, as high temperatures are associated with abundant sunlight. Hence, an anti-correlation between the two species is reflected in the

first canonical variate pair by the contrast in their respective canonical weight values. Also interpreted through the canonical weights of the first function is the positive relationship between oxalate and temperature. The concentration of oxalate, however, is presumed to be of low correlation due to the small value of its weight. This is the extent of interpretable information contained in the first canonical variate pair. Figure 15a depicts a plot of the canonical scores generated by A.Poll1 and Met1. Overall, no yearly trends are observed, nor are there obvious outliers; the positive linearity of canonical scores can be seen, numerically stated earlier by the canonical correlation value (0.821). There are six score points that extend further from the linearity than the rest (no. 15, 17, 23, and 44–46) of the scores along A.Poll1. All six of these scores are from segment B collections. Three of the scores are from 2002 measurements completed on July 30 (no. 15), August 1 (no. 17), and August 12 (no. 23) while the remaining scores are from measurements completed on June 24–26 in 2003 (no. 44–46, respectively). After reviewing original data on these dates of collection, it was found all of these scores had above average ozone mixing ratios ranging from 78.29 to 97.86 ppb. Score no. 46 had the highest recorded ozone mixing ratio of all six mentioned observations (97.86 ppb). Score no. 46 is also the highest in terms of location on A.Poll1. This supports the interpretation that A.Poll1 is highly influenced by ozone mixing ratios. The observed elevated mixing ratios of ozone offer explanation to the scores' location.

The canonical correlation of the second canonical variate pair (Met2, A.Poll2) was 0.562, indicating there is moderate linear correlation between canonical variates. The amount of variance in A.Poll2 that is explained by Met2 is 16%. Ammonium (0.819), nitrogen oxides (-1.261), and ozone (-0.835) residuals not explained by the first canonical

variate have the largest canonical weights and influence on A.Poll2. The weight of ammonium is positive, while the weights of both ozone and nitrogen oxides are negative, implying the presence of an inverse relationship. The weights of wind speed and humidity, 0.552 and 0.900, respectively, indicate these meteorological variables have the most influence on Met2. This canonical variate pair suggests that moderate to high winds and very humid conditions are predictors of large ammonium concentrations. The second function can therefore distinguish humid/non-humid days as well as differences in observed wind speed and its effect on ammonium concentrations and nitrogen oxide mixing ratios. The large negative canonical weight value associated with nitrogen oxides indicates that on days of high humidity and moderate winds, mixing ratios of nitrogen oxides are low. This could be a result of increased mixing of air masses, which also explains the large negative weight associated with ozone. While the small canonical weight associated with wind direction implies little to no influence of wind direction on Met2, it is important to note that to the west and northwest of the sampling site areas with considerable agricultural signature are present. This may influence measureable ammonium in the area, increasing concentrations when the origin of the wind direction is from the west and northwest.

The second canonical function is shown in Figure 15b. There is a clear outlier point present in the A.Poll2 vs. Met2 score plot. An observation (no. 30) during summer 2003 is highly negative on A.Poll2 in comparison to the other canonical scores. This indicated that one or more of the original variables with corresponding large negative canonical weight had substantial influence on the observation’s calculated score. Upon further inspection of observed values in the original data set, the location of no. 30 is due

to unusually high mixing ratios, greater than 100 ppb, of nitrogen oxides (negatively weighted in A.Poll2) measured during and after the normal traffic rush hour period on July 1, 2003 during segment A collection. The large negative canonical weight of nitrogen oxides on A.Poll2 directly contributed to the large negative score for the observation. Furthermore, winds originated from the southwest (202.5°) and turned south-southeast (157.5°). Both are directions in which heavily industrialized areas are located. While wind direction is not weighted significantly in Met2, it may have played a role in the large mixing ratio of nitrogen oxides observed, resulting in the outlier score.

The third statistically significant canonical function derived in CCA had a canonical correlation of 0.461. This canonical function represents residuals of variable correlations which were not expressed by the first two canonical functions. Roughly 9.0% of the variance in A.Poll3 is explained by Met3. Therefore, even though it is statistically significant it does not reveal much new information. Wind direction is the only information provided in Met3 that was not significantly weighted in the previous two canonical functions. All residuals of the secondary pollutants have significant weights of varying sign but interpretation is not clear since these are residual values of low canonical correlation. The score plot (Figure 15c) for this canonical function shows no clear correlation of scores but there are several outlier points, specifically no. 3, 25, 38, 42, 64, 77, and 86. All of these observations are from segment A collections. Along Met3, no. 25 and 38 are on the negative end while no. 42 is near the origin and no. 3, 64, 77, and 86 are on the positive end. The scores' locations along this axis are directly related to a combination of wind speed, wind direction, temperature, and humidity residuals. No. 25 and 38 had recorded wind speed in upwards of three times the wind speeds of

observations 3, 64, 77, and 86, which contributed to the distinct difference in location as the Met3 canonical weight for wind speed is negative (-0.779). Wind direction and temperature have the next largest influence on scores' location, with positive canonical weights of 0.618 and 0.582, respectively. Observed wind direction for no. 38 was from the north, 0°, therefore this score's location was the only outlier score not affected by wind direction. The remaining scores' observed wind direction varied from southwesterly to northwesterly while temperatures ranged from 21.9 to 26.1 °C. Variability in observed humidity values for outlier points aids in final score location as well. Along the A.Poll3 axis original data for scores no. 38 and 64 were references as these scores are at the opposite ends of this axis. Canonical weights for five of the seven pollutant variables are $\pm$ 0.300. Sulfate and ozone canonical weights are negative (-0.543 and -0.561, respectively) while ammonium (0.714), nitrate (0.526), and oxalate (0.498) have positive weights. Original data showed score no. 38 observations for sulfate and ozone were three times higher than values for score no. 64. Furthermore, score no. 64 had observed ammonium and nitrate concentrations three and four times higher, respectively, than those found for score no. 38. The described variability explains the two extremes in terms of location along the A.Poll3 axis for scores no. 38 and 64.

a)

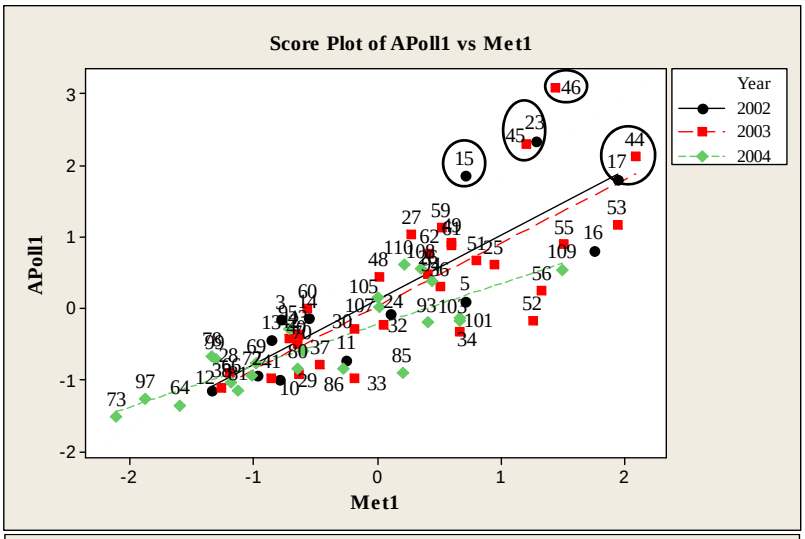

b)

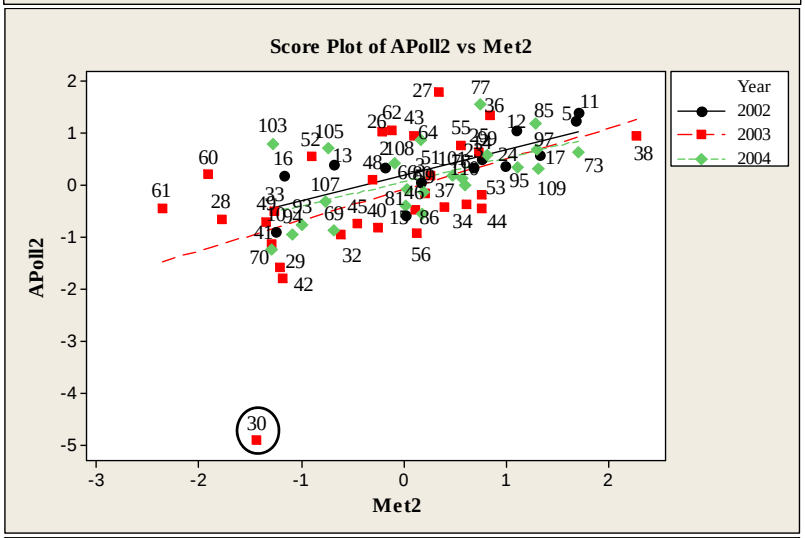

c)

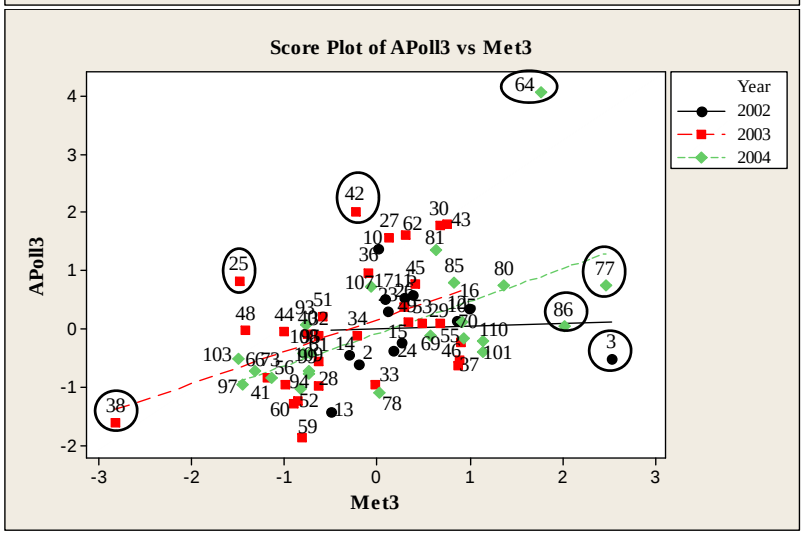

Figure 15. CCA score plots. a) A.Poll1 vs. Met1, b) A.Poll2 vs. Met2, and c) A.Poll3 vs. Met3). Scores are distinguished by collection year (different symbols). The number next to each point corresponds to an observation number, used to identify collection dates.

Canonical Loadings

Canonical loadings were interpreted in addition to canonical weights to uncover additional information regarding relationships between air pollutants and meteorology. Canonical loadings represent the simple correlation between original variables and their respective canonical variate whereas canonical weights are values derived for each variable that maximize linear correlation between data sets.[51,52] Distinction of these two CCA outputs are noted in Table 15.

Table 15. Distinguishing the difference between canonical weights and loadings.

CCA Output	Information Extracted
Canonical weight	Weight is derived and dependent on variance and the maximum inter-correlation between two data sets' variables
Canonical loading	Coefficients reflect how important original variable was in deriving its canonical weight in a canonical function

A correlation matrix (Table 16) of the original data unveiled collinearity of several air pollutants and low to moderate correlations between meteorological parameters. Ammonium and calcium are positively correlated with nitrate, 0.699 and 0.664, respectively. Nitrate is also correlated with sulfate (0.548) and oxalate (0.611). Oxalate is correlated with both ozone (0.622) and sulfate (0.752). This can explain why ozone was the only large canonical weight in A.Poll1, the first canonical variate for air pollutants. Numerical values of the simple correlations between original variables and their respective canonical variate are presented in Table 17.

Table 16. Correlation matrix of air pollutant and meteorological variables in summers 2002–2004. *A* ammonium, *C* calcium, *N* nitrate, *S* sulfate, *Ox* oxalate, O_3 ozone, NO_x nitrogen oxides, *Sp* wind speed, *T* temperature, *D* wind direction, *H* humidity.

	A	C	N	S	Ox	O_3	NO_x	Sp	T	D
C	**0.392**									
N	**0.699**	**0.664**								
S	**0.377**	**0.484**	**0.548**							
Ox	**0.520**	**0.458**	**0.611**	**0.752**						
O_3	0.241	0.157	**0.433**	**0.416**	**0.622**					
NO_x	**0.302**	**0.365**	**0.357**	0.026	0.073	**-0.424**				
Sp	-0.127	-0.058	-0.228	0.010	0.043	0.165	**-0.379**			
T	**0.360**	**0.383**	**0.572**	**0.506**	**0.682**	**0.686**	0.068	0.014		
D	0.065	0.086	0.031	-0.042	-0.047	-0.100	0.196	0.213	0.143	
H	0.078	-0.163	-0.176	-0.212	-0.292	**-0.376**	-0.117	0.074	**-0.448**	-0.127

Table 17. Canonical loadings (structure correlations), correlations between original variables and their canonical variates, summers 2002–2004.

	A.Poll1	A.Poll2	A.Poll3
Ammonium	0.337	0.347	**0.787**
Calcium	0.284	-0.001	0.290
Nitrate	**0.567**	-0.118	**0.538**
Sulfate	**0.535**	0.155	-0.012
Oxalate	**0.812**	0.066	0.242
Ozone	**0.960**	0.126	-0.088
Nitrogen Oxides	-0.368	**-0.643**	**0.583**
	Met1	Met2	Met3
Wind Speed	0.262	**0.623**	**-0.505**
Temp	**0.944**	0.013	0.311
Wind Direction	-0.121	0.195	**0.519**
Humidity	**-0.555**	**0.736**	0.216

Manly (2005) suggested interpreting loading values greater than $\pm$ 0.500 and that threshold was implemented in this work. The correlations expressed by the loadings resulted in supplementary information to what was found in interpreting the canonical weights. Nitrate, sulfate, oxalate, and ozone are all positively correlated with A.Poll1 (Table 17). In the simple correlations of meteorological parameters, temperature is highly correlated with Met1 while humidity is negatively correlated with Met1. Therefore, A.Poll1 is a good measure of conditions of high ozone mixing ratios and oxalate concentration as well as moderate nitrate and sulfate concentrations; Met1 is a measure of high temperature and low humidity. Overall, this interpretation suggests higher temperature and lower humidity result in larger observed values of ozone and oxalate. This result agrees with the classification of these two pollutants as secondary, produced in the atmosphere due to various chemical reactions.[8] The correlation of nitrate and sulfate with temperature requires additional exploration.

As ammonium nitrate's (NH_4NO_3) volatility increases with increasing temperatures and low humidity, reforming gaseous nitric acid (HNO_3) and ammonia (NH_3) in the troposphere[8,23] other species of particulate nitrate must contribute to the moderate, positive correlation between nitrate and temperature. Organonitrates have been measured in various aerosol studies in urban locations and were found to contribute significantly to organic mass of aerosols.[83-85] These molecules are present mainly due to the reaction between nitric oxide (NO) and peroxy ($RO_2\cdot$) radicals during the day as well as the product of alkene and nitrate radical reactions at night.[8,85] Based on this information, organonitrates most likely play an important role in the atmospheric signature in Chicago with respect to nitrate formation.

Sulfate aerosols are produced in the atmosphere either via gaseous or aqueous phase oxidation of SO_2, sulfur dioxide. Both pathway reaction rates are dependent on a variety of factors and oxidation of SO_2 in the aqueous phase is considered to be the major source of atmospheric sulfate aerosols.[8] This contradicts the canonical loading result of a moderate sulfate correlation with high temperature/low humidity. As both Scheff (1984), Lee and Hopke (2006) found, the Midwest experiences significant amount of regional transport of sulfate, thus locally measured sulfate may not have been produced in the immediate area. This would explain the contradiction in the CCA sulfate loading correlation result for A.Poll1 and Met1.

The only pollutant variable in A.Poll2 with a correlation value of $\pm$ 0.500 is nitrogen oxides (-0.643). Wind speed (0.623) and humidity (0.736) both have large positive correlations with Met2. These correlations confirm the results in the second linear combination for meteorology (Met2), which weighted humidity and wind speed

significantly. However, in the linear combination of A.Poll2, ammonium was weighted highly positive and nitrogen oxides highly negative. Ammonium is not significantly correlated to A.Poll2 according to the canonical loading. Overall, this interpretation indicated that high winds are good predictors of low mixing ratios of nitrogen oxides.

Original variables correlated with A.Poll3 included ammonium, nitrate, and nitrogen oxides. Wind speed and the direction from which winds originated are moderately correlated with Met3. Therefore, when wind speed was lower and originating from a large degree [180°, S; 270°, W; 0°/360°, N], higher ammonium and nitrate concentrations were measured along with high nitrogen oxide mixing ratios. This contradicts what was expressed earlier by the second pair of canonical weights regarding wind speed. Because the third canonical function is based on correlations not already expressed in the first two canonical variates and the canonical correlation was low (0.461), it is difficult to estimate the value of this canonical loading information. Thus, more consideration should be put on the wind speed result uncovered in the second canonical variate pair since its correlation was larger.

Principal Component Analysis

Principal component analysis was applied using the correlation matrix as original data were measured on varying scale. Out of eleven principal components (PCs) derived in PCA, the first four (PC1–PC4) were retained for further interpretation. These four principal components accounted for 77.0% of the variability in the original data. The number of principal components retained was determined using Kaiser Criterion and a Scree plot. PC1 through PC4 each had eigenvalues greater than one and were retained. The Scree plot (Figure 16) confirmed retention of PCs 1–3 for interpretation; however, it

is arguable whether the slope between PC3 and PC4 is large enough to retain PC4. Table 18 displays each of the retained principal components, specifically the loading values corresponding to each of the original variables within the PCs. Only loading (absolute) values greater than or equal to ± 0.300 were included in PC interpretations. The eigenvalue and variance explained by each PC is also displayed (Table 18) along with the cumulative percentage of variance of all of the PCs.

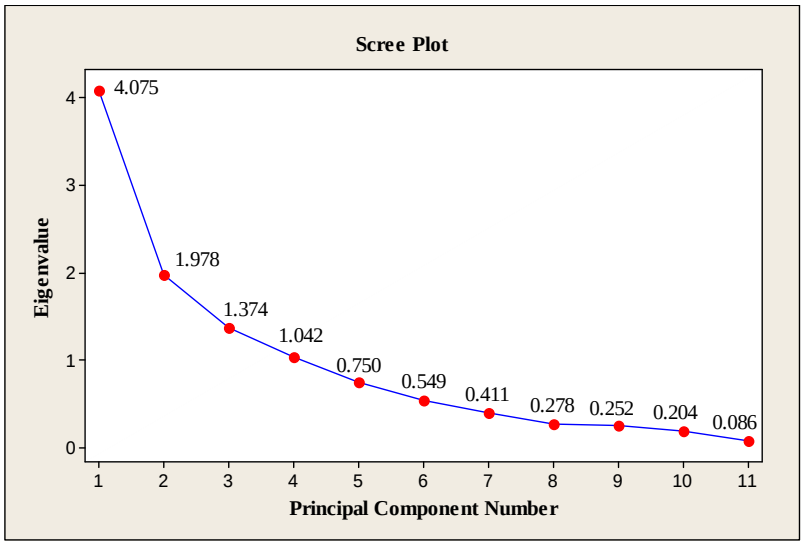

Figure 16. PCA scree plot used in determining the number of principal components (PCs) to retain for interpretation.

Table 18. Principal components' loading values, eigenvalues, and percent variance explained by each PC. Cumulative variance of all principal components is also displayed.

	PC1	PC2	PC3	PC4
Ammonium	**0.305**	**-0.307**	0.251	-0.146
Calcium	0.280	**-0.381**	0.073	-0.140
Nitrate	**0.383**	-0.281	-0.117	-0.150
Sulfate	**0.365**	-0.009	0.049	-0.279
Oxalate	**0.431**	0.057	-0.019	-0.030
Ozone	**0.376**	**0.366**	-0.112	-0.013
Nitrogen Oxides	-0.066	**-0.614**	-0.094	0.286
Wind Speed	0.102	**0.341**	**0.570**	0.023
Temperature	**0.402**	0.146	-0.049	**0.311**
Wind Direction	0.036	-0.144	**0.631**	**0.525**
Humidity	-0.211	-0.097	**0.411**	**-0.635**
Eigenvalue	4.075	1.978	1.374	1.042
Variance (%)	37.0	18.0	12.5	9.5
Cum. Var. (%)	37.0	55.0	67.5	77.0

Principal Component Interpretation

PC1 has the largest eigenvalue (4.075) and explains 37.0% of the original data variance. Ammonium (0.305), nitrate (0.383), sulfate (0.365), oxalate (0.431), and ozone (0.376) loading values in PC1 indicate a similar pattern with relation to temperature (0.402). The loading values are all positive, suggesting a moderately positive association between variables. All of these pollutants listed are secondary in nature, produced in the atmosphere due to chemical reactions.[8] Therefore, this PC is indicative of an overall measure of secondary aerosol production in the Chicago region. Because NH_4^+ is also weighted, PC1 could also convey neutralization of aerosol acidity as NH_4^+ neutralizes nitrate and sulfate.

PC2 explains 18.0% of the total variance of the data and its associated eigenvalue was 1.978. PC2 identifies the consumption of nitrogen oxides in the photochemical production pathway of tropospheric ozone as their loadings are of opposite sign, -0.614

and 0.366, respectively. Additionally, wind speed (0.341) has a positive loading in PC2, while ammonium (-0.307) and calcium (-0.307) both have negative loadings. Note that the ammonium loading in this PC represents residuals that were not explained in PC1. This result shows that with large wind speeds low concentrations of these aerosol species are measured at the sampling site. Mixing of air masses due to wind may cause dilution of the species resulting in low collection yields.

The only variables with significant loading values in PC3 were meteorological variables: wind direction (0.631), humidity (0.411), and wind speed (0.570). Wind speed residuals not explained by PC1 or PC2 were weighted in PC3. PC3 explains 12.5% of the total variance in the original data. Due to variable weights, it can be inferred that PC3 is an overall measure of the state of meteorology during the sampling period. It is only possible to interpret how meteorology affects ammonium as the other pollutants' loading values are near zero. A correlation between humidity and NH_4^+ is present. Furthermore, the loading of wind direction (0.631) indicates that the direction from which the wind originates affects observed NH_4^+. Larger concentrations of NH_4^+ are present when wind direction is large i.e. westerly direction. Up to this point, 67.5% of the variance in the total data has been explained. PC4 explains an additional 9.5% of the variance of the original data and is the last principal component retained for interpretation. Residuals of temperature (0.311), wind direction (0.525), and humidity (-0.635) not expressed by PCs 1–3 are expressed in PC4. The loading values for air pollutants were below the defined threshold for interpretation, thus PC4 does not yield any further information. The absence of new information in PC4 supports the findings from the Scree Plot, which suggested retaining only PC1 through PC3 as the slope between PC3 and PC4 was small.

Score Plot Interpretation

Score plots of PC2 vs. PC1 and PC3 vs. PC1, projecting original data in the dimensionality of principal components, are displayed in Figure 17. The scores are differentiated by year of collection indicated by data points' shape and color (2002 round, 2003 square, and 2004 diamond). The scores on the positive end of PC1 in Figure 17a, circled and labeled no. 1, have a significant contribution from high temperature and large secondary air pollutants' recorded values, coinciding with the larger factor loadings on PC1 for these variables. For example, observations no. 23 and 46 were very warm (28.4 and 29.5 °C, respectively) with high ozone (78.3 and 97.9 ppb) and sulfate (18.8 and 22.7 μg m^{-3}) concentrations. The majority of the points in the positive section of PC1 are from late morning, early afternoon collections which explain high temperatures and an increase in the oxidative nature of the atmosphere, resulting in large secondary air pollutant concentrations. On the contrary, observations in a small cluster labeled no. 2 at the far left, negative end of PC1, including no. 38, 73, 78, 97, and 99, were among the coolest days on record. For example, temperatures of 16.8 °C and 17.0 °C were recorded on observations 38 and 73, respectively. Many of the points are from morning aerosol collections, when temperatures are lower. The combination of low concentrations of nitrate, sulfate, oxalate and ozone and high humidity may explain the negative scores on PC1 (circled no. 2 & no. 3), as the loading value for humidity is moderately negative.

The difference between the positive and negative scores of no. 30, 64, 56, 108 and 109 vertical axis in the PC2 vs. PC1 plot may be explained by nitrogen oxide mixing ratios as well as ammonium, ozone, and wind speed data. Observations no. 30 and 64 had very large negative scores on PC2. Nitrogen oxides and nitrate concentrations observed

were large while wind speed values and ozone mixing ratios were low for both points. Scores no. 56, 108, and 109 had very low nitrogen oxides, ammonium, and calcium concentrations and conversely had large ozone mixing ratios and wind speed values. This explains the location of observations no. 56, 108, and 109 on the positive section of PC2. In summary, several groups of observations exhibiting similar pattern of meteorology and pollutant concentrations were identified in the score plot of PC2 vs. PC1.

In the PC3 vs. PC1 score plot (Figure 17b) the focus of interpretation was on PC3 (vertical axis), as PC1 was explained earlier in the assessment of the first score plot. The position of the scores having positive or negative values on PC3 is highly dependent on the wind direction and wind speed during sampling. Scores on the positive side of PC3, such as no. 5, 10, 11, 25, and 36 circled no. 4 in the plot, are associated with high winds recorded from the northwest and southwest, moderate pollutant concentrations and, moderate to high humidity. Conversely, scores no. 30, 41, 49, 56, 60, 103, and 107 in the area labeled no. 5 have low recorded wind speeds originating from the north to the east and low pollutant concentrations. Humidity was moderate in both positive and negative score cases. The small cluster of points (no. 66, 73, 78, and 97) circled and labeled no. 6 has several common recorded observations: high west, northwest winds and low pollutant concentrations. As meteorological parameters are weighted positive on PC3, this cluster is largely positively on PC3 axis. Scores near zero or about the origin are not particularly influenced by the large loading values on either PC. Overall, several groups of observations exhibiting similar pattern of meteorology and pollutants' concentrations were identified between the two score plots.

a)

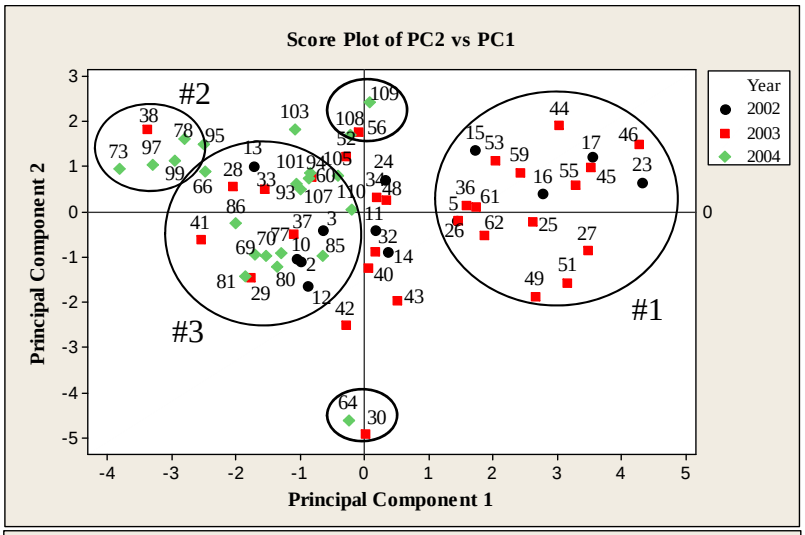

b)

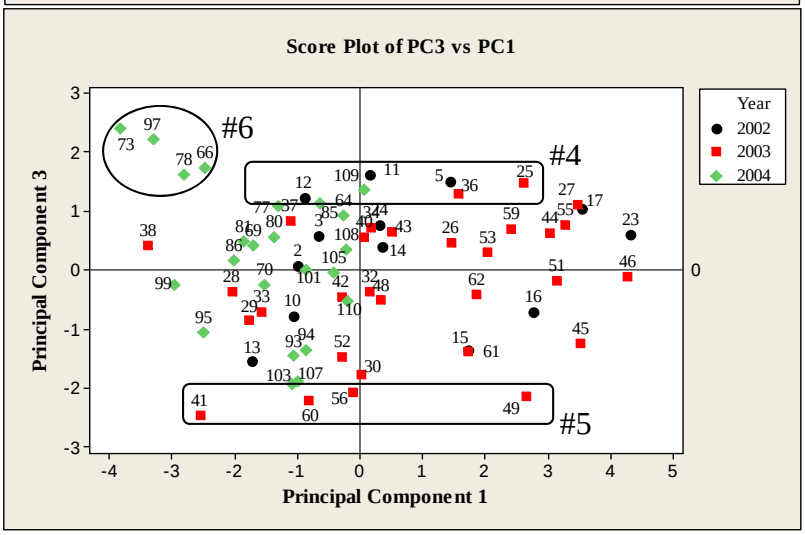

Figure 17. PCA score plots. a) PC2 versus PC1 and b) PC3 versus PC1. The label next to each point indicates an observation number, used to identify date of collection.

Conclusion

By applying canonical correlation analysis to air pollution and meteorology data, linear relationships were uncovered corresponding to the dependence of local pollutant concentration on meteorology. Three canonical functions derived in CCA were significant at the 0.05 level. Through interpretation of canonical weights it was found that temperature influenced mixing ratios of ozone positively. Canonical structure correlations also supported this, and additionally revealed oxalate was also positively correlated with

temperature. Based on air studies in other urban cities, organonitrates may contribute to Chicago's atmospheric signature as a positive correlation was found between nitrate and temperature in the first canonical loading. A moderate correlation between sulfate and high temperature/low humidity in A.Poll1 and Met1 canonical structure correlations contradicts literature as aqueous oxidation of SO_2 to form sulfate is a dominant pathway in the atmosphere. As previous studies in Midwestern cities found, regional transport might be a major component to sulfate aerosols in the Chicago area. Canonical weights of the second canonical function linked high concentrations of ammonium and nitrogen oxides mixing ratios to low wind speeds and high humidity. The corresponding canonical loading values confirmed occurrence of high ammonium concentrations on humid days with large wind speed.

Principal component analysis was used to reduce original data dimensions from 11 to 4. The four derived principal components captured 77.0% of the variance in the original data. PC1 was an overall measure of local secondary air pollutants, whereas photochemistry and wind speed were expressed in PC2. PC3 was a measure of residual meteorological conditions not already expressed and suggested the influence of wind direction on NH_4^+ concentrations. PC4 did not present new information. Using both multivariate statistical techniques resulted in independent and overlapping information about relationships between air pollutant and meteorological variables in Chicago and also between air pollutant species themselves.

CHAPTER V

MULTIVARIATE STATISTICAL ANALYSIS: APPLICATION TO SUMMER 2010–2012 AIR POLLUTION DATA

Overview

The case study discussed in Chapter IV showed that both CCA and PCA are useful methods to extract underlying information from air pollution data collected at Loyola University Chicago in summers 2002–2004. As a result, both CCA and PCA were applied to aerosol, trace gas, and meteorological data accumulated through air pollution campaigns completed during the summer months of 2010–2012 at the same sampling location. The premise of statistical analysis was the same: to reduce data dimensions and identify the presence of relationships between both pollutant-pollutant and pollutant-meteorological variables.

Description of Data Matrix

Sixty-six weekdays of aerosol, trace gas, and meteorological measurements completed during summer 2010–2012 air pollution studies were used in statistical analyses. Water-soluble anions quantified in aerosol samples and included in statistics were acetate, formate, chloride, nitrate, sulfate, and oxalate. Ammonium and calcium ion concentrations were not included in this dataset, unlike in 2002–2004, as peaks were either not resolved or below detection limit. Mixing ratios of ozone and nitrogen oxides were also included, in addition to temperature, wind speed, wind direction, and humidity.

This resulted in 132 observations of eight air pollution variables and four meteorological variables in the final matrix of data. Similar to 2002–2004 data, all of the variables' values in the original dataset had varying levels of resolution due to differing instrument sampling frequency. Meteorological data and trace gas mixing ratios were averaged to match the timeframe of aerosol sampling segments A and B. Standardization of data that was described for the previous case study was similarly applied to the 2010–2012 data matrix. One hundred thirty-two observations of 12 variables was arranged in one data matrix (for PCA) and split into two data matrices (for CCA): the first containing concentrations ($\mu g\ m^{-3}$) of measured air pollutants (acetate – Ac, formate – F, chloride – C, nitrate – N, sulfate – S, and oxalate – Ox, along with mixing ratios of ozone – O_3, and nitrogen oxides – NO_x) and the second containing observed meteorological parameters during air sampling (wind speed – Sp, temperature – T, wind direction – D, and humidity – H). Throughout this chapter, the original variables may be denoted by the symbol associated with them as presented. The statistical, data visualization programs as well as defined predictor and response variables described for the 2002–2004 case study remained consistent in the analyses herein of summer 2010–2012 data.

Canonical Correlation Analysis

Canonical Variate Pairs

The first three canonical functions derived in CCA are explained herein. The fourth canonical function was not statistically significant at the 0.05 level. Symbols AP1, AP2, and AP3 refer to the canonical variates derived for air pollution variables. Symbols M1, M2, and M3 represent meteorological parameter canonical variates. Canonical

functions (M no., AP no.), canonical correlation of each function, and canonical weights corresponding to respective pollution and meteorology linear combinations are discussed.

Table 19. Canonical functions (M no., AP no.), canonical correlations, and standardized canonical weights for air pollutant (AP) and meteorological (M) variables.

Canonical Function	M1, AP1	M2, AP2	M3, AP3
Canonical correlation	0.769	0.623	0.395
Wind speed	-0.241	**-0.389**	0.292
Temperature	**0.925**	**-0.784**	0.279
Wind direction	0.039	**1.016**	**0.641**
Humidity	-0.141	-0.229	**1.002**
Acetate	0.214	**0.347**	**-0.336**
Formate	0.011	**-0.502**	**0.978**
Chloride	-0.109	**-0.300**	-0.060
Nitrate	-0.207	0.154	0.028
Sulfate	-0.042	-0.097	**0.387**
Oxalate	**0.349**	**0.622**	**-0.727**
Ozone	**1.142**	**-0.643**	0.128
Nitrogen oxides	**0.723**	**0.457**	**0.501**

The canonical correlation between M1 and AP1, the first canonical variate pair, is high (0.769). Additionally, M1 explains roughly 60.3% of the variance in AP1. Only canonical weights greater than or equal to $\pm$ 0.300 were interpreted. The most influential variable in M1 is temperature, with a derived canonical weight of 0.925. Wind speed is not very influential with a small canonical weight. Wind direction and humidity canonical weights are near zero, indicating they have negligible impact on the first meteorological canonical variate. Overall, M1 is a measure of high temperatures. Ozone (1.142), nitrogen oxides (0.723), and oxalate (0.349) are highly weighted on AP1. Combined, the canonical function shows temperature affects the concentrations of oxalate and ozone, as well as, nitrogen oxides. The negative sign represents that low wind speeds contribute to the overall function, useful information even though the weight is

not in the range of interpretation. High temperatures influence photochemical reactions such as in the production of ozone. In contrast, nitrogen oxides are not formed in the atmosphere, but are emitted by fossil fuel combustion. It is unclear why nitrogen oxides' positive correlation with ozone and oxalate was derived, as it is known that the trace gases nitrogen oxides and ozone are anti-correlated.[8] Furthermore, nitrogen oxides are photolytically destroyed, leading to the production of tropospheric ozone.[8] Lack of air mass mixing and transport due to low winds indicated by the canonical weight of wind speed is an explanation.

A score plot generated by this canonical function is shown in Figure 18a. The large, positive correlation between M1 and AP1 canonical variates is clearly seen. No trends or clusters are present and there are only a few points that deviate from the majority, namely no. 117 and 123. Both points scored highly on AP1. Observation no. 117 corresponds to July 13, 2012 segment B measurement of which the highest average ozone mixing ratio over all three summers was recorded, 94.43 ppb. Nitrogen oxides (11.46 ppb) and oxalate (0.254 μg m^{-3}) concentrations for the same period were average in comparison to cumulative three-summer data. Score no. 123 corresponds to July 23, 2012 segment B measurement. On this day the second-highest ozone mixing ratio over all three summers was recorded, 93.37 ppb. Both nitrogen oxides and oxalate concentrations were similar to those observed for no. 117 and were 11.59 ppb for nitrogen oxides and 0.277 μg m^{-3} for oxalate. As ozone has the strong influence on score location along AP1, the well above average ozone mixing ratios for no. 117 and 123 directly contributed to their outlying positions on the score plot.

The second derived canonical variate pair (M2, AP2) had a moderate canonical correlation (0.623). The amount of AP2 variance explained by M2 is 26.5%. Both acetate (0.347) and formate (-0.502) ions are significantly weighted in AP2. The negative sign indicates an inverse relationship between species. Residual influence of ozone (-0.643), nitrogen oxides (0.457), and oxalate (0.622) not explained by AP1 is present in this function. Overall, AP2 is a measure of high acetate, oxalate, and nitrogen oxides along with low formate and ozone concentrations. This may be indicative of morning hours, when local NO_x is high due to rush hour, while O_3 is low. Interestingly, both acetic and oxalic acids have been measured directly from tailpipe emissions.[29,31,71] The commonality of magnitude and weight of both organic acid anions and nitrogen oxides suggests direct emission is an important source of the species in the local atmosphere. This supports the findings in Chapter III when referencing discussing raw data of formate to acetate ionic ratios, suggesting direct emission played a role in their presence in the atmosphere. With respect to M2, wind direction has a canonical weight of 1.016. Residuals of temperature and wind speed not explained in M1 are weighted in M2, -0.784 and -0.389, respectively. This canonical function distinguishes different wind directions and air pollutants. In cases of a large wind direction, the concentrations of acetate, oxalate, and nitrogen oxides are high while ozone and formate concentrations are low. In the area to the west and south of the sampling site, there are major roadways, an airport, and suburban, agricultural activity while to the north is residential which may explain wind direction, pollution variability. The pollution plot of nitrogen oxides in Chapter III confirms the dependence of mixing

ratios of NO_x with respect to wind direction. Lower wind speeds also contribute to accumulation of local pollutants in the atmosphere.

Figure 18b shows the score plot of AP2 versus M2. Several scores in this function deviate from the majority (no. 11, 17, 18, 39, 49, and 88). Scores no. 17 and 88 are highly positive on M2 and AP2 and correspond to segment A measurements on August 6, 2010 and July 9, 2012, respectively. Northwesterly winds combined with low temperature and wind speed resulted in the high score along M2, due to wind direction's large positive canonical weight. Low wind speed and temperature minimally influenced the score. Two scores (no. 18 and 39) along the positive end of M2 are weighted negative on AP2. Similar to no. 17 and 88, large wind direction, high temperature, and low wind speed contributed to the scores' location on M2. Formate and ozone concentrations influenced no. 18 and 39 the most along AP2. Score no. 11 corresponds to July 27, 2010 segment A measurements. Along M2, no. 11 is near zero while its location along AP2 is highly positive. A combination of above average nitrogen oxides, acetate, and oxalate concentrations contributed to the high positive score of no. 11 along AP2. Observation no. 49, an outlier, is negative along M2 due to major influence of observed low temperature and high wind speed. With respect to AP2, July 25, 2011 segment A (no. 49) had low ozone and high nitrogen oxides mixing ratios with average oxalate and acetate concentrations.

The third canonical function had a low canonical correlation of 0.395. Roughly 7.7% of the variance in AP3 is explained by M3. The only new information in AP3 is sulfate's canonical weight (0.387). Acetate, formate, oxalate, and nitrogen oxide residual

correlations not expressed earlier are weighted in AP3. In M3, humidity has a large positive canonical weight (1.002) along with wind direction residuals (0.641). This function measures the direct relationship between formate, sulfate, nitrogen oxides, wind direction, and humidity, in addition to an inverse relationship between mentioned meteorology with acetate and oxalate. In this canonical function the magnitude of acetate, formate, and oxalate canonical weights changed, with acetate and oxalate having negative (residual) weights while formate had a positive weight. The positive weight of sulfate and formate may suggest transport from southerly and easterly directions affect concentrations. The pairing of sulfate and formate canonical weights is also indicative that secondary formation of formate is important. The third canonical function score plot (Figure 18c) has several outliers (no. 10, 14, 34, 44, and 68) along M3, which are dependent on relative humidity. Scores no. 34 and 14 had low humidity (30 and 58%, respectively) compared to no. 44 and 68 (77 and 70% humidity, respectively). Scores no. 44 and 68 had the two highest formate concentrations in the study, affecting their AP3 location.

a)

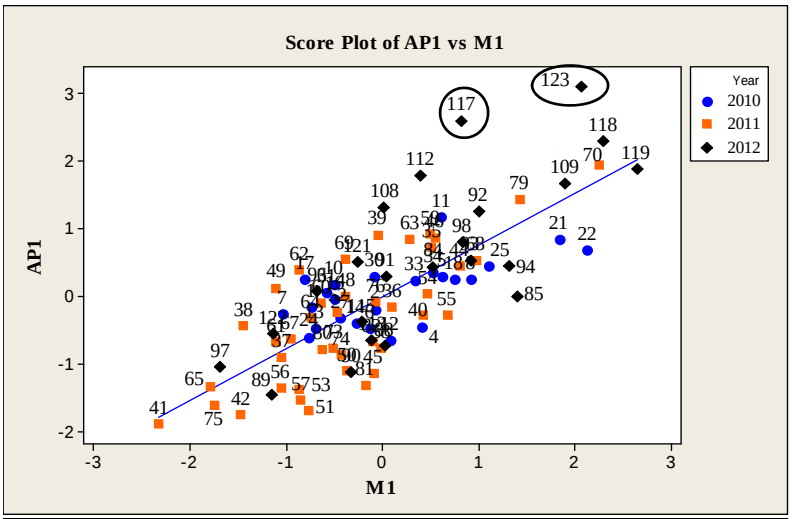

b)

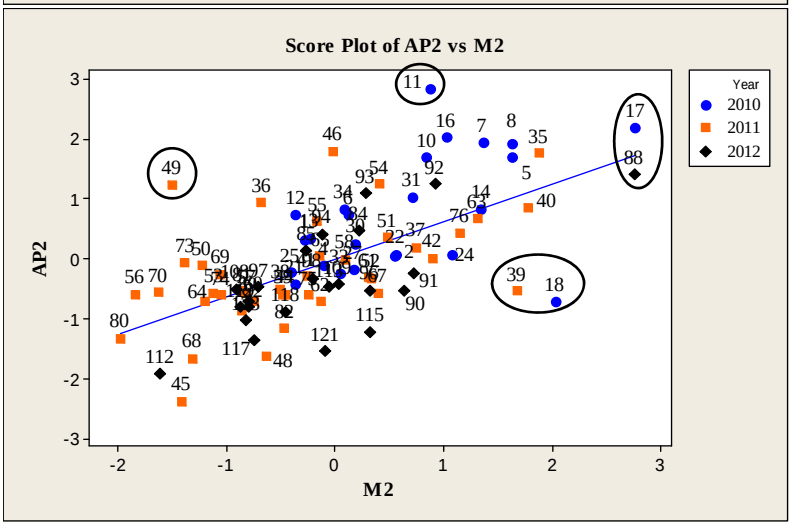

c)

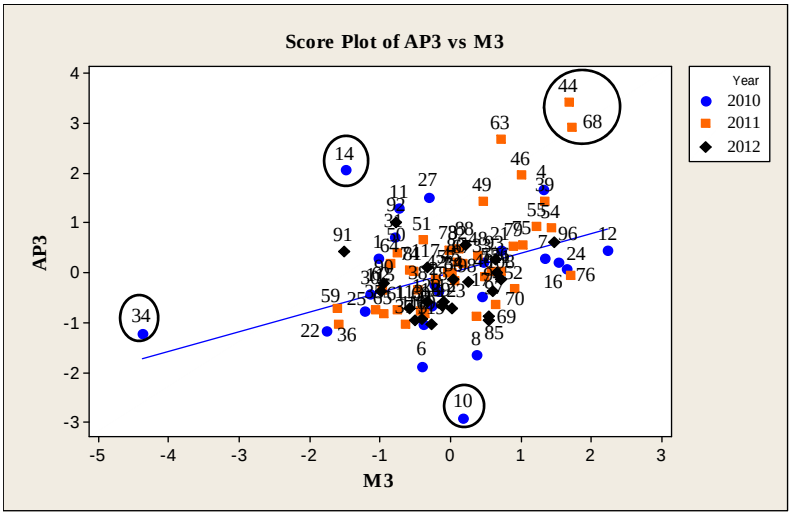

Figure 18. Score plots of a) AP1 vs. M1, b) AP2 vs. M2, and c) AP3 vs. M3. Scores are differentiated by collection year (different plotting symbols). Observation row numbers were used to identify collection sample dates.

Canonical Loadings

Canonical loadings reveal information masked in canonical weights due to multicollinearity between original variables prior to CCA application.[51] A correlation matrix of original variables (Table 20) revealed several univariate correlations between variables. Oxalate is correlated with three variables: acetate (0.388), formate (0.417), and chloride (0.375). Acetate and formate have a strong correlation, 0.623). Nitrate is correlated with both sulfate (0.403) and ozone (0.508). This may explain why nitrate and chloride standardized canonical weights were small, partialled out to original variable multicollinearity. With respect to meteorology, temperature has a positive correlation with wind direction (0.530) and a negative correlation with humidity (-0.587). The relationships of wind direction and humidity were partialled out in the canonical weights.

Canonical loading values $\pm$ 0.500 or greater were interpreted and are displayed in Table 21. AP1 is a measure of high ozone and nitrate concentrations. M1 is a measure of high temperatures and low humidity as well as wind directions with moderate degree corresponding to southerly direction (135°, SE; 180°, S; 225°, SW), shown through the canonical loading values (T: 0.960, H: -0.656, and D: 0.600). The canonical loadings of AP2 indicate that nitrogen oxides (0.674) have a strong, positive correlation with AP2 while ozone has a strong, negative correlation (-0.608). Wind direction (0.618) is strongly correlated with M2. The pollutant canonical loadings confirm the known anti-correlation between nitrogen oxides and ozone.[8] Although oxalate (0.430) does not meet the interpretation criteria, the inverse relationship expressed between ozone and oxalate suggests photochemistry is not the main pathway for this organic acid anion. This was

Table 20. Correlation matrix of air pollutants and meteorological parameters for summers 2010–2012. *Ac* acetate, *F* formate, *Cl* chloride, *N* nitrate, *S* sulfate, *Ox* oxalate, O_3 ozone, NO_x nitrogen oxides, *Sp* wind speed, *T* temperature, *D* wind direction, *H* humidity.

	Ac	F	Cl	N	S	Ox	O_3	NO_x	Sp	T	D
F	**0.623**										
Cl	0.185	0.201									
N	-0.110	-0.236	0.222								
S	0.153	0.128	**0.510**	**0.403**							
Ox	**0.388**	**0.417**	**0.375**	0.180	**0.399**						
O_3	-0.225	**-0.300**	-0.230	**0.508**	-0.109	-0.034					
NO_x	0.015	0.007	0.245	0.196	0.262	0.012	**-0.432**				
Sp	-0.184	-0.043	-0.233	-0.030	-0.095	-0.157	0.198	-0.172			
T	-0.022	-0.019	-0.076	**0.412**	0.048	0.200	**0.587**	0.029	0.206		
D	0.083	0.026	-0.028	0.224	0.128	0.251	0.009	**0.441**	0.106	**0.530**	
H	0.076	0.161	0.155	-0.257	0.045	-0.182	**-0.342**	-0.071	-0.051	**-0.587**	**-0.446**

also expressed in Chapter III Pearson correlations. In other studies, oxalate was measured in the exhaust of automobiles[31] and its positive relationship with nitrogen oxides and AP2 in this study is suggestive of automobile exhaust origin as well. Furthermore, the canonical loading correlations within AP2 and M2 suggest morning conditions of low wind speed originating from the west affect loaded pollutant species.

The canonical loading of nitrogen oxides indicate correlation to AP3. This is similar to information found in the canonical weight in AP3. Humidity has a moderate correlation with M3. Wind direction and wind speed are similarly influential in M3 to a lesser degree. These canonical loadings confirm a few of the relationships found in the third canonical function. Using information from both canonical functions and loadings offer a complete analysis of relationships present between pollutants-pollutants and pollutants-meteorology.

Table 21. Canonical loadings (structure correlations), correlations between original variables and their canonical variates, summers 2010–2012.

	AP1	AP2	AP3
Acetate	0.125	0.342	0.084
Formate	-0.031	0.074	0.470
Chloride	-0.061	0.071	0.060
Nitrate	**0.596**	-0.011	-0.002
Sulfate	0.147	0.258	0.363
Oxalate	0.303	0.430	-0.264
Ozone	**0.710**	**-0.608**	-0.269
Nitrogen oxides	0.249	**0.674**	**-0.549**
	M1	M2	M3
Wind speed	0.017	-0.472	0.400
Temperature	**0.960**	-0.180	0.173
Wind direction	**0.600**	**0.618**	0.415
Humidity	**-0.656**	-0.208	**0.568**

Principal Component Analysis

Principal component analysis was applied using the correlation matrix of data. The first four derived principal components (PCs 1–4) were retained for interpretation, based on Kaiser Criterion indicates that a principal component should be interpreted if its corresponding eigenvalue is equal to or greater than one. A scree plot (Figure 19) validates interpreting PCs 1–3. However, the slope between PC3 and PC4 points in the score plot suggests PC4 is not important and is part of the scree of the graph. Because a scree plot is subjective, PC4 was included in results.

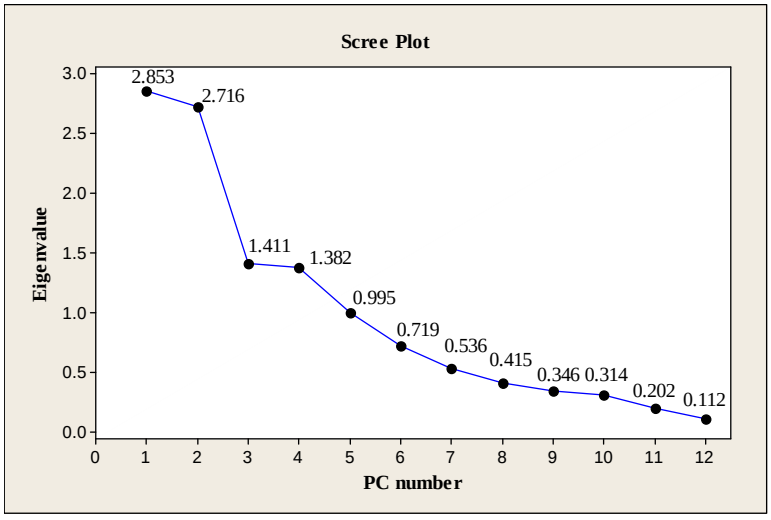

Figure 19. Scree plot of eigenvalue versus principal component (PC) number.

The first four PCs combined accounted for roughly 70% of the variance in the original data. Principal component loading values are shown in Table 22. Eigenvalue and cumulative percent variance explained by each PC are also presented. Only loading values ± 0.300 or greater were interpreted for information in each principal component.

Table 22. Principal component (PC) loading values, corresponding eigenvalues, and cumulative percentage of original data variance.

	PC1	PC2	PC3	PC4
Acetate	0.006	**0.402**	**0.408**	-0.003
Formate	-0.063	**0.411**	**0.476**	-0.016
Chloride	-0.006	**0.379**	-0.275	**0.310**
Nitrate	**0.418**	-0.020	-0.276	**0.317**
Sulfate	0.184	**0.360**	**-0.351**	0.133
Oxalate	0.197	**0.391**	0.186	0.260
Ozone	**0.351**	**-0.318**	0.113	**0.426**
Nitrogen oxides	0.157	0.248	**-0.430**	**-0.517**
Wind speed	0.092	-0.234	0.188	-0.235
Wind direction	**0.407**	0.125	0.041	**-0.448**
Temperature	**0.507**	-0.070	0.184	-0.076
Humidity	**-0.411**	0.076	-0.168	0.082
Eigenvalue	2.853	2.716	1.411	1.382
Variance (%)	23.8	22.6	11.8	11.5
Cum. Variance (%)	23.8	46.4	58.2	69.7

Principal Component Interpretation

The first principal component (PC1) explains 23.8% of original data variability. This PC is a measure of nitrate (0.418), ozone (0.351), temperature (0.507), wind direction (0.407), and humidity (-0.411), as these variables have the largest loading values. The signs of loading values indicate similarity in behavior of all positively loaded variables and an inverse relationship between humidity and the other mentioned variables. A similar weighted relationship between nitrate, ozone, temperature, and humidity was also found in CCA canonical loading values of the first pair of linear combinations. Both nitrate and ozone are secondary in nature, produced in the atmosphere by chemical reactions. The main pathway for tropospheric ozone production is nitrogen dioxide (NO_2) photolysis; nitrate ions are mainly a result of the daytime reaction of hydroxyl radicals and NO_2, forming gaseous nitric acid which can then

undergo dry deposition or uptake into clouds, fog and wet deposition. Neutralization by ammonia, $NH_{3\,(g)}$, and deposition in the form of ammonium nitrate, $NH_4NO_{3\,(s,\,aq)}$, is another pathway for nitrate aerosol.[8] PC1 is a measure of processed air, late morning or early afternoon, after rush hour emissions have decreased. In this time period of the day local temperatures are rising (large positive weight), aiding in secondary aerosol production. Winds originating from a moderate degree (135°, SE; 180°, S; 225°, SW or southerly directions) contribute to the measured pollutants via transport. The weight of nitrate and ozone suggests dependence of these species' concentrations with respect to the direction from which winds are originating.

Contrary to what is known and reported in literature, PC1 suggests that nitrate aerosol increases with high temperatures and low humidity, whereas according to Finlayson-Pitts and Pitts (2000), volatility of ammonium nitrate increases when humidity lessens and temperatures rise. Equilibrium is shifted from ammonium nitrate to gaseous nitric acid and ammonia in this case.[8] A similar correlation to PC1 was found when applying multivariate statistics to summer 2002–2004 data taken at the same location.[50] Binaku et al. (2013) suggested that organonitrate compounds play a role in the atmospheric signature of nitrate in Chicago. Many urban studies have measured organonitrate compounds in the organic aerosol fraction. The formation of organonitrates occurs during both day and night, the product of peroxy radical ($RO_2\cdot$) and nitric oxide (NO) or nitrate radical and alkene reactions, respectively.[8] The results in our recent study suggest that the nitrate signature of possible organonitrate compounds has not changed in Chicago since the previous air pollution study completed in 2002–2004.

Principal component 2 (PC2) has an eigenvalue of 2.716 and explains 22.6% of original data variance. PC2 is a measure of acetate (0.402), formate (0.411), chloride (0.379), sulfate (0.360), and oxalate (0.391). Ozone residuals (-0.318) not expressed in PC1 are negatively weighted in principal component 2. All measured organic acid anions and two inorganic ions have similar behavior in PC2. There is evidence that formate and acetate both originate in the atmosphere due to direct emissions as well as secondary formation, sources of which are location dependent.[8] If Pearson correlations between formate, acetate, and ozone exist, it is indicative that photochemistry is favored over direct emissions.[8,13,71] PC2 suggests photochemical formation is not the main source of formate and acetate in the Chicago region, as the negative sign of ozone's loading value indicates low ozone mixing ratios are present in observed cases of moderate to high formate and acetate concentrations. This confirms Chapter III results of overall ionic ratios of organic acid anions. Sulfate, which is primarily formed via aqueous oxidation of sulfur dioxide, has a loading magnitude and value proposing local oxalate might originate from in-cloud aqueous reactions. Conversely, humidity's lack of significant weight contradicts that aqueous phase chemistry has importance in the formation of sulfate and oxalate in this study. The commonality of organic acid anions and sulfate loading values may indicate that transport of species from other regions is an important source.[12,64,78]

The only new information derived in PC3 is the loading of nitrogen oxides (-0.430). Residual loadings of acetate, formate, and sulfate not expressed in PC1 or PC2 are weighted in PC3. The associated eigenvalue is 1.411 and PC3 explains 11.8% of variance in the original data. PC3 is a measure of moderate acetate, formate

concentrations and low sulfate, nitrogen oxide concentrations. With meteorology not loaded in PC3, there is no distinction of weather conditions.

PC4 consists of residual information of variables already loaded in PCs 1–3. PC4 expresses 11.5% of original data variance and has an eigenvalue of 1.382. Residuals of chloride (0.310), nitrate (0.317), ozone (0.426), nitrogen oxides (-0.517), and wind direction (-0.448) play a large role in PC4. Loading values suggest PC4 is a measure of moderate concentrations of secondary pollutants transported by winds originating from a small degree (0°/360°, N; 45°, NE; 90°, E) or northerly direction.

Score Plot Interpretation

Graphs projecting original observations in derived principal component space are shown in Figure 20. Observations (scores) are distinguished by sample year. Collections in 2010, 2011, and 2012 are represented by a circle (blue), square (orange), and diamond (black), respectively. In Figure 20a, PC2 versus PC1, there are two main clusters of points. Scores highly positive on PC1 (cluster no. 1) were influenced by a combination of high temperature and low humidity, in addition to high ozone and nitrate concentrations and large degree with respect to wind direction. These scores are from segment B collections in 2011 and 2012. For example, no. 119 and 123 were very warm days (34.1 and 32.7 °C, respectively) with high ozone mixing ratios (77.51 and 93.37 ppb, respectively) and low relative humidity (45%), combined with westerly (270°) winds. Conversely, cluster no. 2 at the negative end of PC1 encompasses scores from 2011 and 2012 segment A collections and several from 2011 segment B samples. Scores 41, 56, 65, and 89 correspond to observations of low nitrate (0.315–1.108 μg m^{-3}) and temperature

(18.9–23.5 °C), low average ozone (26.72–36.02 ppb), high humidity (70–90%), and winds originating from a small degree (northerly to easterly, 0–135°). This combination resulted in humidity dominantly affecting the location of scores. Along PC2, the vertical axis, 2012 observations are all weighted negatively while year 2010 and 2011 scores are scattered about the axis. There are two outliers with large positive scores along PC2, no. 10 and 11, corresponding to summer 2010 measurements. Low ozone mixing ratios combined with high sulfate and above average chloride, acetate, and formate concentrations resulted in a high overall score on PC2, as all of the variables listed have positive loading values with the exception of ozone.

In the score plot of PC3 versus PC1 (Figure 20b), interpreting PC3 is the focus as PC1 was already discussed. Along PC3, acetate, formate, sulfate, and nitrogen oxides influence score location. Scores with high sulfate and nitrogen oxides but low acetate and formate concentrations are on the negative end of PC3. Generally, the opposite is true for scores located on the positive end of PC3. To illustrate, no. 44 and 46 are at the opposite ends of PC3. Both are observations from 2011 segment A collections. The main influence on no. 44 is low mixing ratios of nitrogen oxides (16.85 ppb) combined with high formate (5.379 μg m^{-3}) and acetate (2.879 μg m^{-3}) concentrations. On the contrary, the negative location of no. 46 is a result of a combination of high nitrogen oxides (54.33 ppb), above average sulfate (11.974 μg m^{-3}) and low formate (0.079 μg m^{-3}) and acetate (0.521 μg m^{-3}) concentrations.

PC4 is the vertical axis in the bottom graph (Figure 20c). Points are scattered along the axis but there are two sets of score extremes. Scores no. 46, 49, and 88 are

weighted highly negative on PC4, while scores no. 10, 45, 59, 108, and 117 are highly positive on PC4 and far removed from the majority of the points. A combination of wind direction, trace gas mixing ratios, and the concentrations of both nitrate and chloride recorded on sampling days affect score location along PC4. Large positive scores have lower nitrogen oxides and higher ozone mixing ratios than the highly negative scores along PC4. Wind direction recorded for no. 10, 59, 108 and 117 were easterly and southeasterly in contrast to westerly winds for no. 46 and 88 and northerly winds for no. 45 and 49. There was no pattern for chloride and nitrate; their smaller loading values in comparison to ozone and nitrogen oxides show their influence is not as significant in comparison to the other variables. Overall, clusters and outliers identified in score plots contributed to a better understanding of similarity in the behavior of local pollution and meteorology.

a)

b)

c)

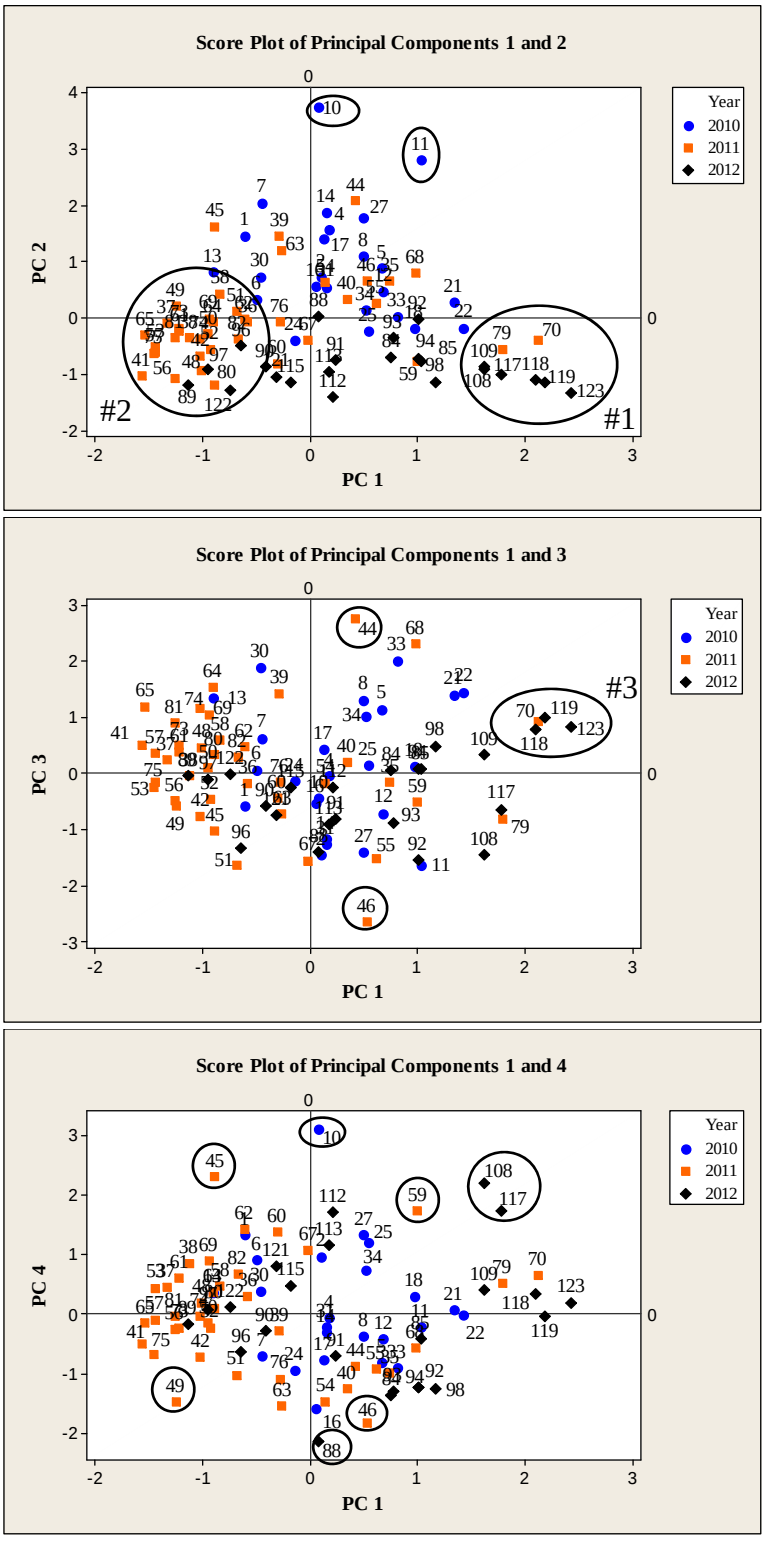

Figure 20. PCA score plots. a) PC2 versus PC1, b) PC3 versus PC1, and c) PC4 versus PC1. The label next to each point indicates an observation number, used to identify date of collection.

Conclusion

Underlying information between air pollutants and meteorology in Chicago, Illinois was found using both PCA and CCA, which proved to be effective in reducing data dimensions and uncovering relationships between variables. In CCA, three statistically significant canonical functions were derived. Through interpreting canonical weights it was found that temperature, oxalate, nitrogen oxides, and ozone have moderately strong, positive linear correlations. The second canonical function describes the linear influence of wind direction and low wind speed on both acetate and formate, as well as residuals of ozone, nitrogen oxides, and oxalate. AP3 and M3 were a measure of residual pollutant information and humidity and wind direction residuals, respectively.

In PCA, the first four principal components were significant, accounting for roughly 70% of original data variance. PC1 is a measure of local processed air masses from late morning, early afternoon hours with winds originating from the southerly direction. PC2 is a measure of both inorganic, organic ions and their inverse relationship with ozone residuals. PC3 and PC4 contain an abundance of residual information. Loadings in PC3 are indicative of morning or afternoons with lower pollutant concentrations, whereas PC4 suggests several secondary pollutants are transported via northerly winds. Overall, several underlying relationships between meteorology and air pollution concentrations were found which are useful when establishing local trends of pollution over time. These underlying relationships are important as they can aid in predicting local pollution episodes, patterns as well as potentially trace specific pollution sources based on meteorology.

CHAPTER VI

DISCUSSION

CCA and PCA in Summers 2002–2004 versus 2010–2012

Both CCA and PCA application to summer 2010–2012 air pollution and meteorological measurements (Chapter V) represented an extension to multivariate statistical analyses of air pollutants and meteorology data collected in summers 2002–2004[50], discussed in Chapter IV. Several differences in the data matrices of both 3–summer studies were the inclusion of acetate, formate, and chloride along with the absence of ammonium and calcium data for summers 2010–2012. There were also 10 additional days of field measurements in the more recent study. Even so, there were consistent relationships between variables derived as a result of applying multivariate statistical methods. Several relationships between variables derived in both 3-summer studies' data indicated consistency with respect to local air pollutant concentrations and weather.

With respect to PCA, PC1 identified relationships between nitrate, ozone, and temperature in both 3-summer studies. However, principal components 2–4 represented different relationships in either 3-summer study. For summers 2002–2004, insight on meteorological relationships was revealed in PC2 and PC3, while in summer 2010–2012 only air pollutants' relationships were derived.[50] In CCA, strong linear relationships between temperature, ozone, and oxalate identified in canonical weights, along with the

influence of nitrate on the first air pollutant linear combination were common relationships derived in both 3-summer multivariate analysis results. Temperature and humidity canonical loadings for the first meteorological linear combination were also consistent in both studies'. However, summer 2002–2004 relationships showing moderate wind speed, humidity, and temperature residuals' inverse relationship with ozone and nitrogen oxides in the second canonical function (Met2, A.Poll2) differed from relationships found in the second canonical function for summers 2010–2012. In summer 2002–2004 data, moderate temperature, wind direction, and humidity along with low wind speed were linearly correlated with high ammonium, nitrate, and oxalate as well as with low sulfate and ozone concentrations. However, the same relationships were not derived in the recent air pollution study. Similarities in the third derived canonical functions of both studies included residuals of humidity, wind speed, and wind direction influence on oxalate and sulfate concentrations. Other residual air pollutant information present was exclusive to the former or latter study, not both. Variability between both 3-summer studies can be attributed to different weather conditions and pollution concentrations, as pollutant-pollutant and meteorology-pollutant relationships affect derived components. The differences in the species included in both data matrices may have also contributed to variability in relationships between study data.

It should also be noted that in CCA and PCA score plots there were no clear trends or clusters of observations with respect to day classifications (reference, lake breeze, variable). This supports Student *t* test results that found no significant differences in the concentrations of most air pollutants on reference and lake breeze days were

present. Overall, interpreting results from applying multivariate statistics to both 3-summer studies showed that local air pollution and meteorology have some degree of consistency. However, changes over time were present as well. This highlights the importance of completing long-term air pollution studies as emission sources and regulations evolve over time in addition to changing weather patterns.

Ambient Air Quality Standards

As described in Chapter I, the USEPA regulates six criteria pollutants. Ozone, nitrogen oxides, specifically nitrogen dioxide, and particulate matter were three of the criteria pollutants measured in both 3-summer studies. National and Illinois standards for ambient air include primary and secondary values with the former value protecting public health and the latter value protecting public welfare. The ambient air primary and secondary standards dictate that one-hour O_3 averages cannot exceed 120 ppb.[73,74] None of the combined 121 sampling days in all six summer studies had an observed ozone mixing ratio that exceeded this standard during segment A and B sampling. One-hour NO_2 mixing ratios cannot exceed 100 ppb according to national and state primary standards.[73,74] Similar to ozone mixing ratios, none of the 121 sampling days had observed nitrogen dioxide mixing ratio one-hour averages above 100 ppb. Particulate matter primary and secondary standards for both PM_{10} and $PM_{2.5}$ are based on 24-hour averages, and cannot exceed 150 and 35 $\mu g\ m^{-3}$, respectively.[73,74] An inference was not made with respect to PM data in our study, as sampling duration was different and not all of the reported species in PM speciation by the USEPA were included in this study.

Local Pollution Emission Sources

Wind direction was found to play a large role in gauging air pollution concentrations not only from the pollutant plot (Chapter III) results, but also from the derived linear combinations in CCA and PCA for both summers 2002–2004 and 2010–2012. Both state and county level emission summaries are available through the USEPA Air Emission Sources website.[86] In addition, the website can be used to generate custom files by state and pollution source type.[86] Once generated, the files containing information on location of point source emission facilities can be visualized using Google Earth™. For example, Figure 21a is Google Earth™ image with a custom file for Illinois plotting eight point-sources of air pollution including chemical plants, concrete batch plants, electricity generation via combustion, foundries (iron and steel), non-ferrous foundries, industrial machinery/equipment plants, mineral processing plants, and petroleum refineries.[86,87] When an additional category, other industrial activity, is included (Figure 21b) there is a clear abundance of point-sources throughout Cook County and Illinois, contributing to NO_x, PM_{10} and $PM_{2.5}$, SO_2 emissions.[86,87] A similar file was generated for the state of Indiana to illustrate industrial activity in the northern portion of the state (Figure 22) as it was discussed earlier to be a contributor to Chicago area pollution when wind originated from the southeasterly direction. These results do not include any non-point pollution sources such as vehicular emissions, which should also be taken into consideration as a significant amount of NO_x and PM pollution results from automobile and other vehicle usage. However, just from the above point-source information alone, there is a large contribution to air pollution in the local area.

a)

b)

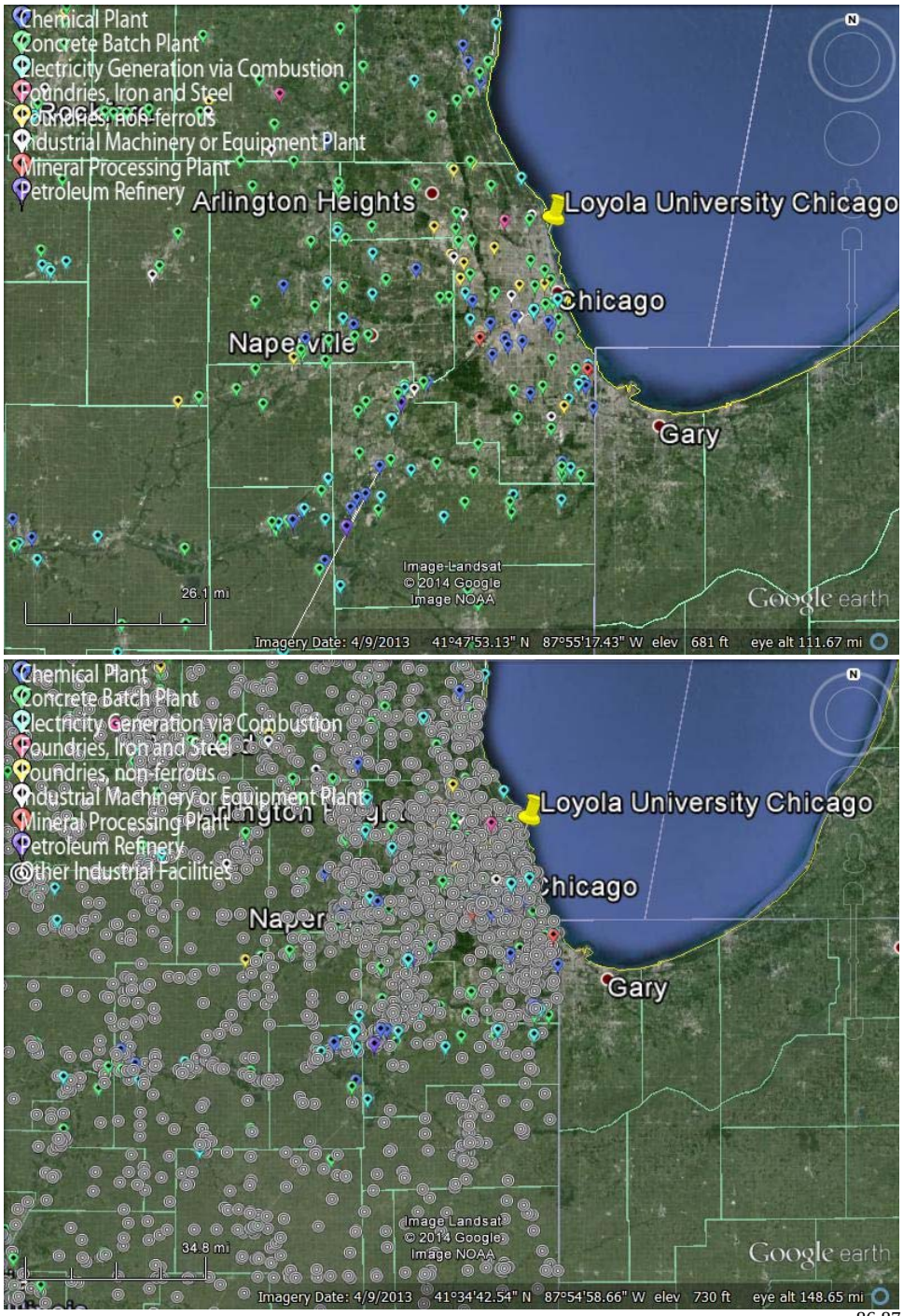

Figure 21. Google Earth™ images projecting point-source pollution in Illinois.[86,87]
a) Eight pollution point-sources and b) eight pollution point-sources with an additional category, other industrial activity.

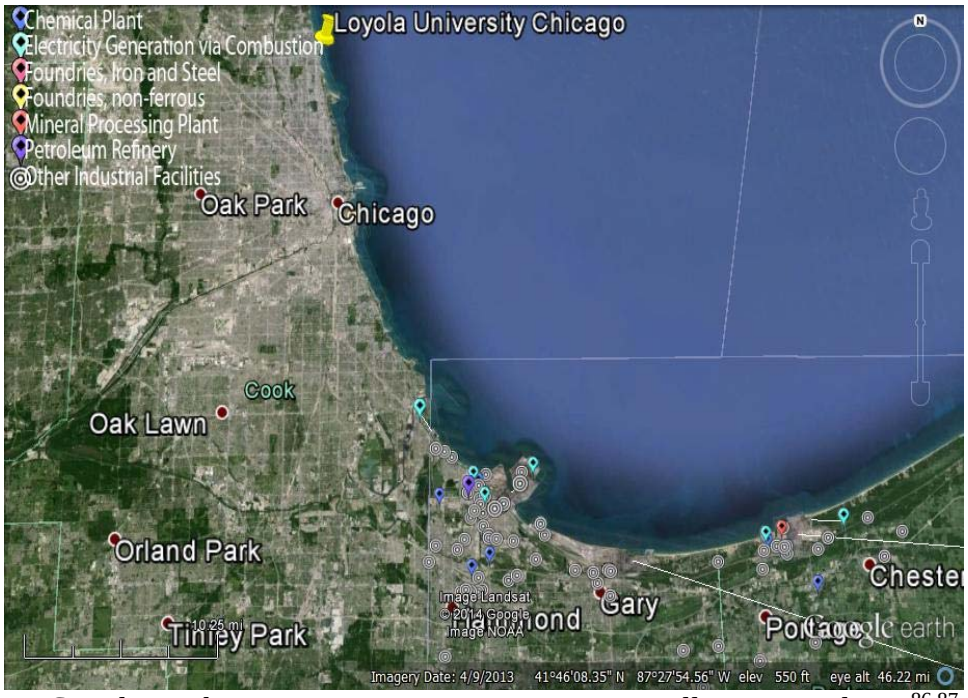

Figure 22. Google Earth™ image projecting point-source pollution in Indiana.[86,87]

Air Mass Transport

HYSPLIT Model

Models that calculate air parcel trajectories prove useful when determining the path of an air parcel prior to reaching, for example, the air sampling station at Loyola University Chicago. The HYbrid Single-Particle Lagrangian Integrated Trajectory (HYSPLIT) model[88,89] generates archived or forecasted air parcel trajectories to or from defined latitude and longitude coordinates. Trajectory calculations are based on a Lagrangian framework. Isentropic, isobaric, and model vertical velocity 72-hour backward air parcel trajectories were generated for all 66-collection days during summer 2010–2012 studies. The term backward trajectory indicated that the migration of the air parcel is calculated as how it traveled to final coordinates in Chicago, 42.0 °N and 87.7 °W. Air parcel trajectories were calculated at three different heights above ground level

(AGL): 70, 100, and 500 m. The meteorology data used in the model was the EDAS40 km archive data. Whereas backward air parcel trajectories were calculated using the HYSPLIT model for all 66-collection days, only a select few days are discussed below highlighting the capability of incorporating air parcel travel information into interpreting air pollution data.

High Pollution Days

Air parcel trajectories for two reference days in summer 2010–2012 studies when high air pollutant concentrations were observed are shown in Figure 23. The first day was July 2, 2012, which had predominantly south and southeasterly winds recorded during segment A and B sampling. Nitrate concentrations in segments A and B were 11.648 and 17.541 μg m^{-3}, respectively. These concentrations were substantially higher than the overall summer 2010–2012 average of 4.792 μg m^{-3}. Sulfate concentrations in segments A and B were 6.214 and 10.084 μg m^{-3}, respectively, which were above the 3-summer average (6.441 μg m^{-3}). The remaining ionic species had concentrations close to their respective overall 3-summer averages. Ozone mixing ratios averaged 81.96 ppb, well above the 3-summer average of 44.60 ppb. The 72-hour backward air parcel trajectory showed that prior to arriving in Chicago on July 2, 2012 the air parcel traveled from central Illinois and migrated north towards the Chicago area. Referencing the HYSPLIT results and the Google Image™ of point-source pollution, the air parcel likely accumulated PM and NO_x during migration and carried it north. This information helped to explain the elevated secondary species and trace gas concentrations observed during sampling.

The next sampling day illustrated high ozone concentrations observed when winds originated from the north. Typically, observations in both the recent and previous 3-summer studies[38-40] recorded low concentrations of pollutants when winds originated from the north or northeast direction. Lake Michigan is to the northeast of the sampling site. There is also less industrial activity to the north of the sampling site, compared to south of the sampling site. During July 6, 2012 collections, elevated ozone mixing ratios during segments A and B were recorded (53.64 and 85.70 ppb, respectively) along with higher than average (2.303 μg m^{-3}) calcium concentrations (4.738 and 4.398 μg m^{-3}). The concentration of potassium in segment B, 0.746 μg m^{-3}, was above the 3-summer average (0.581 μg m^{-3}) as well. Other ions' concentrations were near or below respective averages. Recorded wind direction during segment A and B sampling was from north-northwest to northeast in segment A and northeast in segment B. The 72-hour backward air parcel trajectory results showed the air mass traveled through Iowa, Missouri, and southern Wisconsin in the days prior to reaching the sampling site in Chicago on July 6th. This explained why elevated ozone mixing ratios were observed, as the air parcel passed over a variety of NO_x point-sources in Wisconsin including electricity generation plants, foundries, a mineral processing plant, and agriculture. By the time the air parcel reached the sampling site, the photochemically processed air mass also contained crustal elements (Ca and K). The final path of the air parcel passed over point-sources including mineral processing and cement batch plants potentially injecting crustal material into the atmosphere, leading to the observed elevated calcium and potassium ion concentrations.

a)

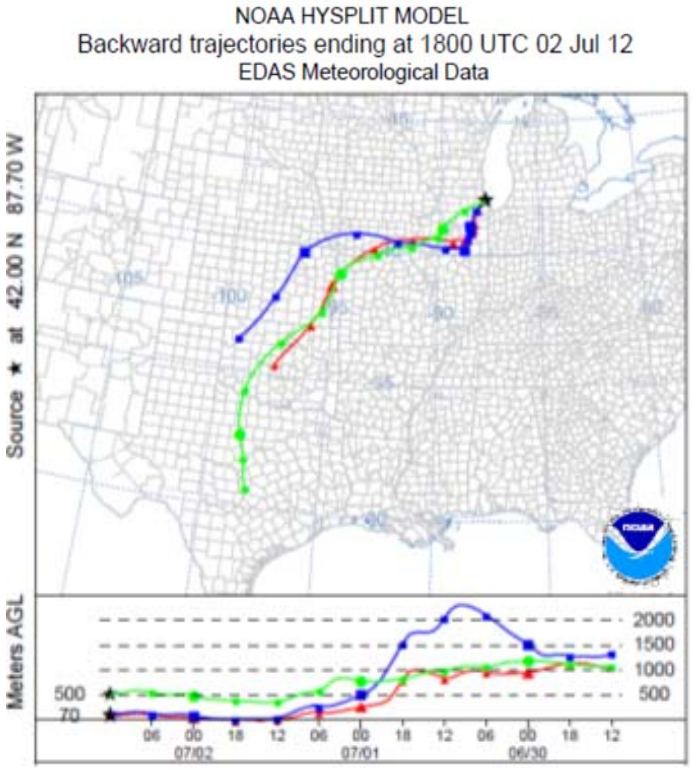

b)

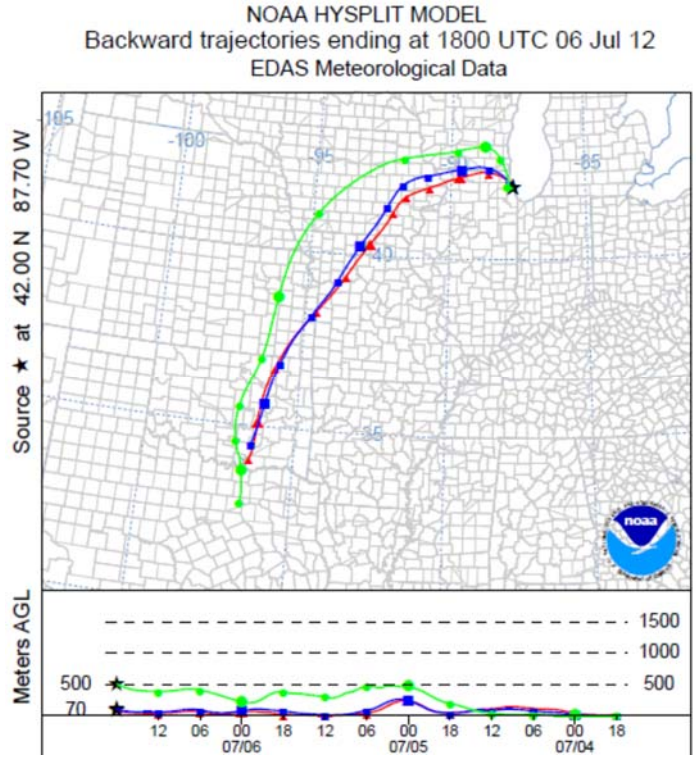

Figure 23. HYSPLIT 72-hour backward air parcel trajectories for a) July 2, 2012 and b) July 6, 2012.[88,89] Trajectories at three different heights (meters AGL), 70 (red), 100 (blue), and 500 (green) are shown.

Low Pollution Days

Air parcel trajectories for two reference days in summer 2010–2012 studies when low air pollutant concentrations were observed are shown in Figure 24. On July 7, 2011, recorded winds originated from the east and both trace gases and ionic species concentrations were low. Low concentrations were defined as being well below 3-summer study average values. The air parcel that arrived in Chicago on July 7th traveled mainly over two great lakes, Lake Superior and Lake Michigan, prior to reaching the air sampling station at Loyola University Chicago. Migration of the air parcel preceding this day of sampling is shown in Figure 24a. Calculating the backward trajectory for this sampling day offered an explanation as to why air pollutant concentrations were low, as none of the ion concentrations were higher than 1.600 μg m^{-3} and average ozone mixing ratios did not exceed 40 ppb. While migrating over each lake, the air parcel could not accumulate point-source emissions of NO_x or other pollutants and therefore, ozone development did not result. In Chapter I, low nitrogen oxide mixing ratios resulted in either a net photo-equilibrium or loss of tropospheric ozone. Furthermore, radical species needed to convert NO to NO_2, leading to ozone production, would also be low due to lack of a pollution source in the final stages of migration of the air mass south and then east to the Chicago area.

Similarly, low pollution concentrations were recorded on July 19, 2012. During segment A and B collections, winds were recorded originating from the south and southeast with respect to the sampling site. The HYSPLIT results (Figure 24b) showed the air parcel traveled through Arkansas, Missouri, central Illinois, and the northwest

portion of Indiana, of which the latter two states were found to have abundant air pollution point-sources. At first it was not understood why pollution levels were low on July 19th when the air parcel reached Chicago, as HYSPLIT backward trajectories showed the air mass traveled through areas where pollution point-sources were. One possible explanation is removal of particle pollutants due to wet deposition as it was recorded by the rain gauge at the Loyola University Chicago sampling site weather station that precipitation passed through the area in the overnight hours of July 18th and into early morning hours of July 19, 2012.

Overall, there are many factors to consider when interpreting air pollution data. Identifying both local and regional air pollution sources as well as tracing the path of air parcel migration to an air sampling site enhance the understanding of pollution variability beyond the chemical reactivity of pollutants.

a)

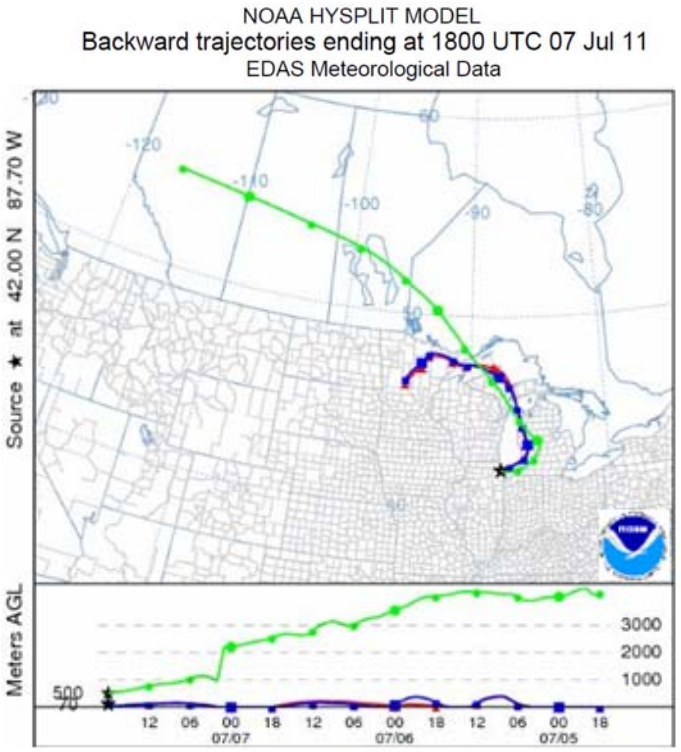

b)

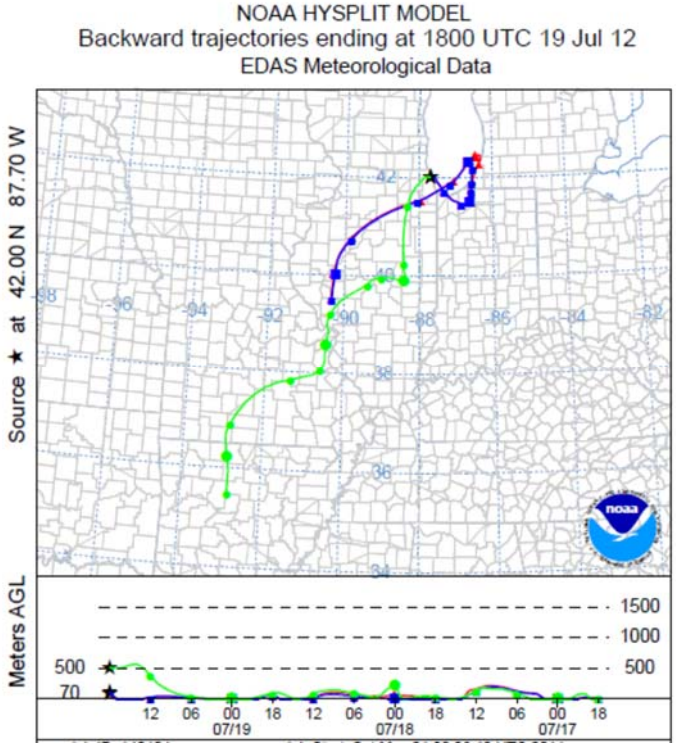

Figure 24. HYSPLIT 72-hour backward air parcel trajectories for a) July 7, 2011 and b) July 19, 2012.[88,89] Trajectories at three different heights (meters AGL), 70 (red), 100 (blue), and 500 (green) are shown.

CHAPTER VII

FUTURE PROJECT RECOMMENDATIONS FOR USING COMPUTER MODELS TO SIMULATE CHICAGO REGION POLLUTION EPISODES

Overview

The future direction of this project's focus should include the use of available computer models to simulate weather and air pollution development over the Midwest, with a specific focus on reproducing small mesoscale events like the Chicago lake breeze. Taking physical air pollution samples and completing air studies is the first step in providing pollutant data, whereas simulating air pollution and meteorology will enhance these data and place them in a broader context of pollution evolution and transport.

There are several computer models that have been developed and one in particular is considered to be the most advantageous due to its online capability. The Weather Research and Forecasting–Chemistry model (WRF–Chem) is a 3-dimensional model simulating not only pollution emissions and pollutants mixing in an air mass, but also transport of emitted pollutions as well as atmospheric processing and fate (deposition) of air pollutants along with meteorology. Both aerosols and trace gases can be simulated in the model.[90] WRF–Chem is an online or integrated model, allowing influence or interaction between processes of chemical and physical nature to affect one another during the simulation.[91] This contrasts offline models preceding WRF–Chem, which treat meteorology and chemistry as separate entities, often resulting in a loss of chemical

information due to different time scales of meteorological output and reaction time of chemical processes.[91] WRF–Chem can be utilized for several purposes including: 1) simulation of ideal or real cases to increase the understanding of trace gas and particulate matter evolution, optical properties of aerosols, and the impact on regional climate,[90] 2) simulation of the evolution of an observed air pollution episode and compare model results to field measurements taken during the period of simulation, evaluating the accuracy of model predictions,[92,93] and 3) study aerosol-cloud interaction, radiative forcing, and processing.[90]

There are four major parts in the WRF–Chem model structure including a WRF pre-processing system (WPS), a data assimilation system WRF–Var, WRF solver including chemistry options, and post-processing tools for data and visualization of model results.[94] A substantial amount of input data and parameter settings are needed. For example, in WPS, setting the (x, y) model domain (km), number of grid points, grid size, latitude and longitude center of interest, and number of vertical levels is required. Extraction and transformation of meteorological data, biogenic emissions, United States Geological Survey (USGS) land use data, anthropogenic emissions data, etc. to file formats that can be used by the model also has to be done. Post-processing and visualization of model results also requires a substantial amount of resources. Many groups that use WRF–Chem run simulations on computer clusters or collaborate with a supercomputing facility.

Test Simulation

A test-simulation using WRF–Chem was completed at the National Center for Atmospheric Research (NCAR) in Boulder, Colorado. The 10-day simulation spanned 0:00:00 July 12, 2010 through 0:00:00 July 22, 2010, coordinated universal time (UTC). The time period chosen had several observed reference days and a lake breeze day within. The goal of this simulation was to understand how well the model reproduced observed air pollution concentrations and meteorology and whether the model was able to develop a lake breeze circulation. One coarse domain, 20 km x 20 km grid size (51 x 51 grid points) with 31 vertical levels, was defined using Lambert projection with the central point of the domain at Chicago coordinates, 42.0° N, 87.7° W. The domain described the x, y area of interest while the vertical levels represent the z-axis. Nesting domains were not included in the test-simulation due to computational restraints. Nesting involves two domains in a model, one smaller than the other. For example, a nested model may have a coarse domain (20 km x 20 km) grid and a fine domain (4 km x 4 km) grid; this reduces computational requirements compared to running both domain simulations separately while producing high-resolution model results.

Initial meteorology fields and boundary conditions were obtained from the NCEP/NCAR Reanalysis dataset. Calculations of gases and aerosols produced by terrestrial systems were generated using MEGAN (Model of Emissions of Gases & Aerosols from Nature) while MOZART (Model for Ozone and Related Chemical Tracers) was used to create a file with USGS land use data within the domain. MOZART calculated initial chemical and boundary conditions within the model domain and

processed anthropogenic emissions data from the USEPA National Emissions Inventory (NEI) 2005 [4 km grid resolution emissions available at a defined latitude and longitude] for initial chemical conditions. Both MEGAN and MOZART generated files were used as input information for the model prior to the simulation period start date. MOSAIC (Model for Simulating Aerosol Interactions with Chemistry) generated information about inorganic, organic, and secondary aerosol development for the given time frame. The interval for output files generated from WRF–Chem was hourly. To make data useable, post-processing and visualization of output files is required. The post-processing of output files proved to be one of the most challenging aspects of the model as raw data must be extracted from output files using programming language. Extracted model data can be graphed, evaluating model versus observed concentrations of a pollutant. Visualization of air pollutant concentrations in domain space using Ncview software is shown in Figure 25. The example shows trace gas mixing ratios at 0700 and 1300 LT on July 13, 2010, illustrating high nitrogen oxides and low ozone in the morning and low nitrogen oxides with high ozone mixing ratios in the afternoon. The shift towards air pollution modelling is advantageous as it is less time intensive than physical sampling, ideal or real case scenarios can be completed, and national data through USEPA and state air monitoring networks can be used to evaluate model output results.

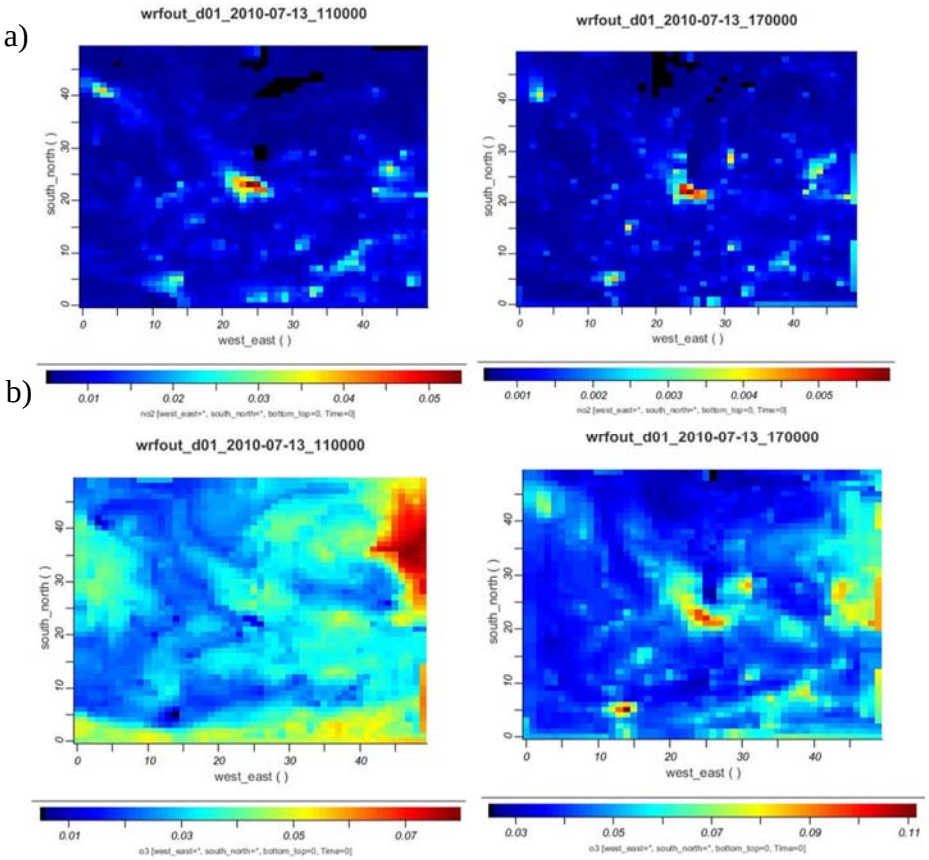

Figure 25. Example visualization of model output on July 13, 2010 for nitrogen oxide mixing ratios at 0700 LT and 1300 LT, b) ozone mixing ratios at 0700 LT and 1300 LT using Ncview.[95]

REFERENCE LIST

1. U.S. Environmental Protection Agency. History of the Clean Air Act. http://epa.gov/oar/caa/caa_history.html (Accessed January 29, 2012).

2. U.S. Environmental Protection Agency Office of Air Quality Planning and Standards. *The Plain English Guide to the Clean Air Act*; EPA-456/K-07-001; 2007, 1–27.

3. Schlesinger, R. B. The health impact of common inorganic components of fine particulate matter ($PM_{2.5}$) in ambient air: A critical review. *Inhalation Toxicol.* **2007,** *19,* 811**–**832.

4. Kampa, M.; Castanas, E. Human health effects of air pollutants. *Environ. Pollut. (Oxford U.K.)* **2008,** *151,* 362–367.

5. Balmes, J. R.; Fine, J. M.; Sheppard, D. Symptomatic bronchoconstriction after short-term inhalation of sulfur dioxide. *Am. Rev. Respir. Dis.* **1987,** *136,* 1117–1121.

6. Bascom, R.; Bromberg, P. A.; Costa, D. A.; Devlin, R.; Dockery, D. W.; Frampton, M. W.; Lambert, W.; Samet, J. M.; Speizer, F. E.; Utell, M. Health effects of outdoor air pollution. *Am. J. Respir. Crit. Care Med.* **1996,** *153,* 3**–**50.

7. Kaufman, Y. J.; Tanré, D.; Boucher, O. A satellite view of aerosols in the climate system. *Nature* **2002,** *419,* 215–223.

8. Finlayson-Pitts, B. J.; Pitts, J. N., Jr. *Chemistry of the upper and lower atmosphere;* Academic Press: New York, 2000.

9. *Climate change impacts in the United States: The third national climate assessment: U.S. global change research program;* Melillo, J. M., Richmond, T., Yohe, G. W., Eds.; U.S. Government Printing Office: Washington, DC, 2014; doi: 10.7930/J0Z31WJ2.

10. IPCC. *Climate change 2013: The physical science basis. Contribution of working group I to the fifth assessment report of the intergovernmental panel on climate change;* Stocker, T. F., Qin, D., Plattner, G. -K., Tignor, M., Allen, S. K., Boschung, J., Nauels, A., Xia, Y., Bex, V., Midgley, P. M., Eds.; Cambridge University Press: Cambridge, United Kingdom and New York, NY, USA, 2013.

11. Arimoto, R.; Duce, R. A.; Savoie, D. L.; Prospero, J. M.; Talbot, R.; Cullen, J. D.;

Tomza, U.; Lewis, N. F.; Ray, B. J. Relationships among aerosol constituents from Asia and the North Pacific during PEM-West A. *J. Geophys. Res.* **1996,** *101* (D1), 2011–2023.

12. Lee, J. H.; Hopke, P. K. Apportioning sources of $PM_{2.5}$ in St. Louis, MO using speciation trends network data. *Atmos. Environ.* **2006,** *40,* S360–S377.

13. Souza, S. R.; Vasconcellos, P. C.; Carvalho, L. R. F. Low molecular weight carboxylic acids in an urban atmosphere: Winter measurements in São Paulo City, Brazil. *Atmos. Environ.* **1999,** *33,* 2563–2574.

14. Yao, X.; Chan, C.K.; Fang, M.; Cadle, S.; Chan, T.; Mulawa, P.; He, K.; Ye, B. The water-soluble ionic composition of PM2.5 in Shanghai and Beijing, China. *Atmos. Environ.* **2002,** *36,* 4223–4234.

15. Querol, X.; Pey, J.; Minguillón, M. C.; Pérez, N.; Alastuey, A.; Viana, M.; Moreno, T.; Bernabé, R. M.; Blanco, S.; Cárdenas, B.; Vega, E.; Sosa, G.; Escalona, S.; Ruiz, H.; Artíñano, B. PM speciation and sources in Mexico during the MILAGRO-2006 campaign. *Atmos. Chem. Phys.* **2008,** *8* (1), 111–128.

16. Almeida, S. M.; Pio, C. A.; Freitas, M. C.; Reis, M. A.; Trancoso, M. A. Source apportionment of fine and course particulate matter in a sub-urban area at the Western European Coast. *Atmos. Environ.* **2005,** *39,* 3127–3138.

17. Atkinson, R. Atmospheric chemistry of VOCs and NO_x. *Atmos. Environ.* **2000,** *34,* 2063–2101.

18. Sipin, M. F.; Guazzotti, S. A.; Prather, K. A. Recent advances and some remaining challenges in analytical chemistry of the atmosphere. *Anal. Chem.* **2003,** *75,* 2929–2940.

19. Calvo, A. I.; Alves, C.; Castro, A.; Pont, V.; Vicente, A. M.; Fraile, R. Research on aerosol sources and chemical composition: Past, current and emerging issues. *Atmos. Res.* [Online] **2013,** *120–121,* 1–28. Science Direct. http://www.sciencedirect.com/science/article/pii/S0169809512003237 (accessed December 13, 2013).

20. Pöschl, U. Atmospheric aerosols: Composition, transformation, climate and health effects. *Angew. Chem., Int. Ed.* [Online] **2005,** *44,* 7520–7540. Wiley Online Library. http://onlinelibrary.wiley.com/doi/10.1002/anie.200501122/abstract (accessed December 18, 2013).

21. U.S. Environmental Protection Agency. Particulate Matter. http://www.epa.gov/air/particlepollution/ (accessed December 30, 2013).

22. U.S. Environmental Protection Agency. Our Nation's Air: Status and Trends Through 2008. http://www.epa.gov/airtrends/2010/report/fullreport.pdf (accessed December 13, 2012).

23. Du, H.; Kong, L.; Cheng, T.; Chen, J.; Yang, X.; Zhang, R.; Han, Z.; Yan, Z.; Ma, Y. Insights into ammonium particle-to-gas conversion: non-sulfate ammonium coupling with nitrate and chloride. *Aerosol Air Qual. Res.* **2010,** *10,* 589–595.

24. Matsumoto, K.; Tanaka, H. Formation and dissociation of atmospheric particulate nitrate and chloride: An approach based on phase equilibrium. *Atmos. Environ.* **1996,** *30* (4), 639–648.

25. Zheng, J.; Hu, M.; Zhang, R.; Yue, D.; Wang, Z.; Guo, S.; Li, X.; Bohn, B.; Shao, M.; He, L.; Huang, X.; Wiedensohler, A.; Zhu, T. Measurements of gaseous H_2SO_4 by AP-ID-CIMS during CAREBeijing 2008 campaign. *Atmos. Chem. Phys.* **2011,** *11,* 7755–7765.

26. Baek, B. H.; Aneja, V. P; Tong, Q. Chemical coupling between ammonia, acid gases, and fine particles. *Environ. Pollut.* **2004,** *129,* 89–98.

27. Anderson, L. D.; Faul, K. L.; Paytan, A. Phosphorus associations in aerosols: What can they tell us about P bioavailability? *Mar. Chem.* **2010,** *120,* 44–56.

28. Cecinato, A.; Amati, B.; Di Palo, V.; Marino, F.; Possanzini, M. Determination of short-chain organic acids in airborne aerosols by ion chromatography. *Chromatographia* **1999,** *50* (11/12), 670–672.

29. Grosjean, D. Organic acids in Southern California air: Ambient concentrations, mobile source emissions, in situ formation, and removal processes. *Environ. Sci. Technol.* **1989**, *23,* 1506–1514.

30. Karthikeyan, S.; Balasubramanian, R. Determination of water-soluble inorganic and organic species in atmospheric fine particulate matter. *Microchem. J.* **2006,** *82,* 49–55.

31. Kawamura, K.; Ng, L.; Kaplan, I.R. Determination of organic acids (C_1–C_{10}) in the atmosphere, motor exhausts, and engine oils. *Environ. Sci. Technol.* **1985,** *19,* 1082–1086.

32. Kroll, J. H.; Seinfeld, J. H. Chemistry of secondary organic aerosol: Formation and evolution of low-volatility organics in the atmosphere. *Atmos. Environ.* **2008,** *42,* 3593–3624.

33. City of Chicago. City of Chicago: Facts & Statistics. http://www.cityofchicago.org/city/en/about/facts.html (Accessed February 25, 2013).

34. U.S. Census Bureau. 2010 Census Interactive Population Search. http://www.census.gov/2010census/popmap/ipmtext.php?fl=17 (Accessed February 25, 2013).

35. CREATE. About CREATE, Chicago Region Environmental and Transportation Efficiency Program. http://www.createprogram.org/about.htm (accessed July 15, 2013).

36. Simcik, M. F.; Eisenreich, S. J.; Lioy, P. J. Source apportionment and source/sink relationships of PAHs in the coastal atmosphere of Chicago and Lake Michigan. *Atmos. Environ.* **1999,** *33,* 5071–5079.

37. Dye, T. S., Roberts, P. T., Korc, M. E. Observations of transport processes for ozone and ozone precursors during the 1991 Lake Michigan Ozone Study. *J. Appl. Meteorol.* **1995,** *34,* 1877–1889.

38. Fosco, T.; Schmeling, M. Determination of water-soluble atmospheric aerosols using ion chromatography. *Environ. Monit. Assess.* **2007,** *130,* 187–199.

39. Fosco, T.; Schmeling, M. Aerosol ion concentration dependence on atmospheric conditions in Chicago. *Atmos. Environ.* **2006,** *40,* 6638–6649.

40. Fosco, T. Ion Concentrations in Atmospheric Aerosols: The Influence of NO_x and Ozone Mixing Ratios, Local Meteorology, and The Lake Breeze in Chicago, IL. Ph.D. Dissertation, Loyola University Chicago, Chicago, IL, May 2006.

41. Lyons, W. A.; Cole, H. S. Photochemical oxidant transport: Mesoscale lake breeze and synoptic-scale aspects. *J. Appl. Meteorol.* **1976,** *15,* 733–743.

42. Lyons, W. A.; Olsson, L. E. Detailed mesometeorological studies of air pollution dispersion in the Chicago lake breeze. *Mon. Weather Rev.* **1973,** *101,* 387–403.

43. Lyons, W. A. The climatology and prediction of the Chicago lake breeze. *J. Appl. Meteorol.* **1972,** *11,* 1259–1270.

44. Almeida, S. M.; Pio, C. A.; Freitas, M. C.; Reis, M. A.; Trancoso, M. A. Source apportionment of atmospheric urban aerosol based on weekdays/weekend variability: Evaluation of road re-suspended dust contribution. *Atmos. Environ.* **2006,** *40,* 2058–2067.

45. Braga, C. F.; Teixeira, E. C.; Meira, L.; Wiegand, F.; Yoneama, M. L.; Dias, J. F. Elemental composition of PM_{10} and $PM_{2.5}$ in urban environment in South Brazil.

Atmos. Environ. **2005,** *39,* 1801–1815.

46. Harrison, R. M.; Smith, D. J. T.; Luhana, L. Source apportionment of atmospheric polycyclic aromatic hydrocarbons collected from an urban location in Birmingham, U.K. *Environ. Sci. Technol.* **1996,** *30,* 825–832.

47. Hsieh, L. -Y.; Chen, C. -L.; Wan, M. -W.; Tsai, C. -H.; Tsai, Y. I. Speciation and temporal characterization of dicarboxylic acids in $PM_{2.5}$ during a PM episode and a period of non-episodic pollution. *Atmos. Environ.* **2008,** *42,* 6836–6850.

48. Ravindra, K.; Stranger, M.; Van Grieken, R. Chemical characterization and multivariate analysis of atmospheric $PM_{2.5}$ particles. *J. Atmos. Chem.* **2008,** *59,* 199–218.

49. Statheropoulos, M.; Vassiliadis, N.; Pappa, A. Principal component and canonical correlation analysis for examining air pollution and meteorological data. *Atmos. Environ.* **1998,** *32,* 1087–1095.

50. Binaku, K.; O'Brien, T.; Schmeling, M.; Fosco, T. Statistical analysis of aerosol species, trace gasses, and meteorology in Chicago. *Environ. Monit. Assess.* **2013,** *185* (9), 7295–7308.

51. Hair, J. F., Jr.; Anderson, R. E.; Tatham, R. L.; Black, W. C. Canonical correlation analysis. *Multivariate data analysis with readings,* 3rd ed; Macmillan Publishing Company: New York, 1992; pp 193–222.

52. Johnson, R. A.; Wichern, D. W. Canonical correlation analysis. *Applied multivariate statistical analysis,* 4th ed.; Prentice Hall: Upper Saddle River, New Jersey, 1998; pp 587–627.

53. Manly, B. F. J. Canonical correlation analysis. *Multivariate statistical methods*: *A primer;* Chapman & Hall/CRC: New York, 2005; pp 143–161.

54. Shaw, P. J. A. Principal components analysis. *Multivariate statistics for the environmental sciences*; Oxford University Press Inc: New York, 2003; pp 92–124.

55. Wilks, D. S. Principal component (EOF) analysis. *Statistical methods in the atmospheric sciences,* 3rd ed.; Elsevier Inc.: New York, 2011; pp 519–562.

56. Google. Google Maps. maps.google.com. (accessed February 29, 2012).

57. Thermo Environmental Instruments, Inc. Introduction. *Model 49C UV Photometric O_3 Analyzer Instruction Manual;* 2000; pp 1–3.

58. Thermo Environmental Instruments, Inc. Introduction. *Model 42C Chemiluminescence NO-NO_2-NO_x Analyzer Instruction Manual;* 2001; pp 1–3.

59. U.S. Environmental Protection Agency. List of Designated Reference and Equivalent Equipment Methods. http://www.epa.gov/ttn/amtic/files/ambient/criteria/reference-equivalent-methods-list.pdf (accessed April 22, 2014).

60. Shen, Z.; Cao, J.; Arimoto, R.; Han, Z.; Zhang, R.; Han, Y.; Liu, S.; Okuda, T.; Nakao, S.; Tanaka, S. Ionic composition of TSP and $PM_{2.5}$ during dust storms and air pollution episodes at Xi'an, China. *Atmos. Environ.* **2009,** *43,* 2911–2918.

61. Wang, Y.; Zhuang, G.; Chen, S.; An, Z.; Zheng, A. Characteristics and sources of formic, acetic and oxalic acids in $PM_{2.5}$ and PM_{10} aerosols in Beijing, China. *Atmos. Res.* **2007,** *84,* 169–181.

62. Eith, C.; Kolb, M.; Rumi, A.; Seubert, A.; Viehweger, K. *Metrohm Monograph Practical Ion Chromatography: An Introduction*, 2nd ed.; Metrohm Ltd.: Herisau, Switzerland, 2009.

63. Ye, B.; Ji, X.; Yang, H.; Yao, X.; Chan, C. K.; Cadle, S. H.; Chan, T.; Mulawa, P. A. Concentration and chemical composition of $PM_{2.5}$ in Shanghai for a 1-year period. *Atmos. Environ.* **2003,** *37,* 499–510.

64. Scheff, P. A.; Wadden, R. A.; Allen, R. J. Quantitative assessment of Chicago air pollution through analysis of covariance. *Atmos. Environ.* **1984,** *18,* 1623–1631.

65. Lee, H. S.; Wadden, R. A.; Scheff, P. A. Measurements and evaluation of acid air pollutants in Chicago using an annular denuder system. *Atmos. Environ.* **1993,** *27A,* 543–553.

66. Kim B. M.; Teffera, S.; Zeldin M. D. Characterization of $PM_{2.5}$ and PM_{10} in the south coast air basin of Southern California: Part 1-spatial variations. *J. Air Waste Manage. Assoc.* **2000,** *50,* 2034–2044.

67. U.S. Energy Information Administration, 2012. State Electricity Profiles 2010. DOE/EIA0348(01)/2.

68. U.S. Energy Information Administration. State Electricity Profiles 2011. http://www.eia.gov/electricity/state/archive/sep2011.pdf (accessed May 7, 2014).

69. U.S. Energy Information Administration. State Electricity Profiles. http://www.eia.gov/electricity/state/ (accessed May 7, 2014).

70. Chebbi, A.; Carlier, P. Carboxylic acids in the troposphere occurrence, sources, and

sinks: A review. *Atmos. Environ.* **1996,** *30* (24), 4233–4249.

71. Khwaja H. A. Atmospheric concentrations of carboxylic acids and related compounds at a semiurban site. *Atmos. Environ.* **1995,** *29,* 127–139.

72. Granby, K.; Egeløv, A. H.; Nielsen, T.; Lohse, C. Carboxylic acids: Seasonal variation and relation to chemical and meteorological parameters. *J. Atmos. Chem.* **1997,** *28,* 195–207.

73. Bureau of Air, Illinois Environmental Protection Agency. *Illinois Annual Air Quality Report 2012*. http://www.epa.state.il.us/air/air-quality-report/2012/air-quality-report-2012.pdf. 2013; 1–125.

74. Bureau of Air, Illinois Environmental Protection Agency. *Illinois Annual Air Quality Report 2011*. http://www.epa.state.il.us/air/air-quality-report/2011/air-quality-report-2011.pdf. 2012; 1–112.

75. *Minitab Statistical Software*, version 16; Minitab Inc.: State College, PA, 2010.

76. Ball, W. P.; Dickerson, R. R.; Doddridge, B. G.; Stehr, J. W.; Miller, T. L.; Savoie, D. L.; Carsey, T. P. Bulk and size-segregated aerosol composition observed during INDOEX 1999: Overview of meteorology and continental impacts. *J. Geophys. Res.* **2003,** *108*(D10), 8001, doi: 10.1029/2002JD002467.

77. Rizzo, M. J.; Scheff, P. A. Fine particulate source apportionment using data from the USEPA speciation trends network in Chicago, Illinois: Comparison of two source apportionment models. *Atmos. Environ.* **2007,** *41,* 6276–6288.

78. Cooke, M. J.; Wadden, R. A. Atmospheric factors influencing daily sulfate concentrations in Chicago air. *J. Air Pollut. Control Assoc.* **1981,** *31* (11), 1197–1199.

79. U.S. Environmental Protection Agency, Office of Air and Radiation. Cross-state air pollution rule (CSAPR). http://www.epa.gov/crossstaterule/index.html (accessed July 27, 2013).

80. Yu, T. Y.; Chang, I. C. Spatiotemporal features of severe air pollution in northern Taiwan. *Environ. Sci. Pollut. Res.* **2006,** *13,* 268**–**275.

81. Zhou, F.; Guo, H.; Liu, L. Quantitative identification and source apportionment of anthropogenic heavy metals in marine sediment of Hong Kong. *Environ. Geol. (Heidelberg, Ger.)* **2007,** *53* (2), 295**–**305.

82. *SAS Statistical Software*, version 9.3; SAS Institute Inc.: Cary, NC, 2010.

83. Day, D.A.; Liu, S.; Russel, L.M.; Ziemann, P.J. Organonitrate group concentrations in submicron particles with high nitrate and organic fractions in coastal southern California. *Atmos. Environ.* **2010,** *44*, 1970–1979.

84. Garnes, L. A.; Allen, D. T. Size distribution of organonitrates in ambient aerosol collected in Houston, Texas. *Aerosol Sci. Technol.* **2002,** *36*, 983–992.

85. Liu, S.; Shilling, J. E.; Song, C.; Hiranuma, N.; Zaveri, R. A.; Russell, L. M. Hydrolysis of organonitrate functional groups in aerosol particles. *Aerosol Sci. Technol.* **2012,** *46*, 1359–1369.

86. U. S. Environmental Protection Agency. Air Emission Sources Where You Live. http://www.epa.gov/air/emissions/where.htm (accessed May 23, 2014).

87. *Google Earth*, version 7.1.2.2041; Google Inc. 2013.

88. Draxler, R. R. and Rolph, G. D. HYSPLIT (HYbrid Single-Particle Lagrangian Integrated Trajectory) Model. http://ready.arl.noaa.gov/HYSPLIT.php (accessed May 23, 2014), access via NOAA ARL READY Website, NOAA Air Resources Laboratory, Silver Spring, MD.

89. Rolph, G. D. Real-time Environmental Applications and Display sYstem (READY). http://ready.arl.noaa.gov (accessed May 23, 2014), NOAA Air Resources Laboratory, Silver Spring, MD.

90. Pacific Northwest National Laboratory. WRF-Chem. http://www.pnl.gov/atmospheric/research/wrf-chem/ (accessed November 10, 2013).

91. Grell, G. A.; Peckham, S. E.; Schmitz, R.; McKeen, S. A.; Frost, G.; Skamarock, W. C.; Eder, B. Fully coupled "online" chemistry within the WRF model. *Atmos. Environ.* **2005**, *39*, 6957–6975.

92. Geng, F.; Zhao, C.; Tang, X.; Lu, G.; Tie, X. Analysis of ozone and VOCs measured in Shanghai: A case study. *Atmos. Environ.* **2007**, *41*, 989–1001.

93. Tie, X.; Geng, F.; Peng, L.; Gao, W.; Zhao, C. Measurement and modeling of O_3 variability in Shanghai, China: Application of the WRF-Chem model. *Atmos. Environ.* **2009**, *43*, 4289–4302.

94. Peckham, S. E.; Grell, G. A.; McKeen, S. A.; Ahmadov, R.; Barth, M.; Pfister, G.; Wiedinmyer, C.; Fast, J. D.; Gustafson, W. I.; Ghan, S. J.; Zaveri, R.; Easter, R. C.; Barnard, J.; Chapman, E.; Hewson, M.; Schmitz, R.; Salzmann, M.; Beck, V.; Freitas, S. R. WRF-Chem version 3.4 user's guide. http://ruc.noaa.gov/wrf/WG11/Users_guide.pdf (accessed October 8, 2013).

95. *Ncview*, version 1.93g; David W. Pierce, http://meteora.ucsd.edu/~pierce/ncview_home_page.html, 2009.

VITA

Katrina Lyn Binaku attended Lewis University in Romeoville, Illinois where she earned a Bachelor of Science in Chemistry and Criminal Justice, with highest distinction and a Scholars Academy diploma, in May 2008. Simultaneous to undergraduate studies, from 2006 to 2008 she was a laboratory technician for Seeler Industries. Under the supervision of Quality Manager Carrie Garrett, Binaku was able to develop her skills in the laboratory and see a snapshot of what raw material and final product quality testing in the chemical industry was like. Since 2007, she has actively volunteered as a local and regional science fair judge for the Illinois Junior Academy of Science.

Binaku entered the PhD program in Chemistry at Loyola University Chicago in fall 2008. She had a departmental teaching assistantship for five years, which gave her the opportunity to aid in instructing students in general, environmental, and quantitative analysis chemistry laboratory courses. In 2011, she was awarded Teaching Assistant of the Year by the department. The Graduate School presented her with an Excellence in Graduate Student Teaching Award in April 2014. Binaku mentored many undergraduate research students including Loyola CUERP, Provost, and WISER Fellowship recipients as well as two visiting REU students. She also served as a committee member on the Chemistry Graduate Student Organization at Loyola University.

Binaku presented her research at the American Chemical Society Joliet Chapter meeting in November 2010 and also presented research posters at Loyola University's

Annual Interdisciplinary Research Symposium for Graduate Students in 2011 and 2013, earning a 1st place poster award in 2013. She gave two poster presentations at Pittcon Conference and Expo in March 2014. Several journal articles were successfully published as a result of her dissertation work under the guidance of her advisor, Dr. Martina Schmeling.

Binaku earned her Doctoral degree in Chemistry in August 2014 and is currently a Laboratory Instructor in the Department of Chemistry and Biochemistry at Loyola University Chicago.